COMPARATIVE STUDY OF MECHANICAL PROPERTIES OF 316L STAINLESS STEEL BETWEEN TRADITIONAL PRODUCTION METHODS AND SELECTIVE LASER MELTING

A thesis presented to the faculty of the Graduate School of Western Carolina University in partial fulfillment of the requirements for the degree of Master of Science in Technology.

By
Alton Dale Lackey

Advisor: Wes Stone, Ph.D.
Associate Professor, Department of Engineering & Technology

Committee:
Sudhir Kaul, Ph.D., Department of Engineering & Technology
Aaron Ball, Ed.D. Department of Engineering & Technology

April 2016

TABLE OF CONTENTS

LIST OF TABLES

LIST OF FIGURES

LIST OF EQUATIONS

ABSTRACT

COMPARATIVE STUDY OF MECHANICAL PROPERTIES OF 316L STAINLESS STEEL BETWEEN TRADITIONAL PRODUCTION METHODS AND SELECTIVE LASER MELTING

Alton Dale Lackey, M.S.T

Western Carolina University (April 2016)

Additive manufacturing, also known as 3D printing, is a technology which has recently seen expanding use, as well as expansion of the materials and methods able to be used. This thesis looks at the comparison of mechanical properties of 316L stainless steel manufactured by both traditional methods and selective laser melting found by tensile testing. The traditional method used here involved cold rolled 316L steel being machined to the desired part geometry. Selective laser melting used additive manufacturing to produce the parts from powdered 316L stainless steel, doing so in two different build orientations, flat and on edge with regards to the build plate. Solid test specimens, as well as specimens containing a circular stress concentration in the center of the parts, were manufactured and tensile tested. The tensile tests of the specimens were used to find the mechanical properties of the material; including yield strength, ultimate tensile strength (UTS), and Young's modulus of elasticity; where statistical analyses were performed to determine if the different manufacturing processes caused significant differences in the mechanical properties of the material. These analysis consisting of f-tests, to test for variance, and t-test, testing for significant difference of means. Through this study it was found that there were statistically significant differences existing between the mechanical properties of selective

laser melting, and its orientations, and cold roll forming of production of parts. Even with a statistical difference, it was found that the results were reasonably close between flat oriented SLM parts and purchased parts. So it can be concluded that, with regards to strength, SLM methods produce parts similar to traditional production methods.

CHAPTER ONE: INTRODUCTION

Problem Statement

This research focuses on the impact of using the Selective Laser Melting (SLM) process to include part features in 316L stainless steel, while comparing the effect varying part orientations and manufacturing processes has on material properties. Using both traditional methods, in this case cold roll forming, and advanced production methods, SLM, two geometries were produced for tensile testing, and the results statistically analyzed. The two geometries are that of tensile testing specimens, one with a solid geometry, and another containing a circular stress concentration. For the purposes of this research, the EOS M290 SLM system was operated using predetermined process parameters provided through EOS, including predetermined support structure geometry. The tensile testing was completed with accordance of the ASTM E8 standard test methods for tension testing of metallic materials, which in turn allowed the mechanical properties of the various production methods to be determined.

The objective of this research was to determine, through statistical analysis, if the SLM process is able to produce parts with similar mechanical properties as parts produced using traditional methods. For this experiment the SLM process, and its various build orientations, will be compared with annealed cold rolled 316L stainless steel. The research specifically looked into how each production method handles the addition of stress concentrations in tensile testing specimen, while looking in the area of part strength, in detail in yield strength. It was made certain that each production methods produced the geometries to specific dimensions, including similarly sized stress concentrations. The cold rolled specimens were purchased without prior testing, so that the specimens from each production method would receive tensile testing within

the same environment, using the same equipment. Within each mechanical properties found for the production methods, comparisons were made to match corresponding geometries during statistical analysis. Being an important mechanical property of the material, when being used in part production, the yield strength of the specimens was utilized in further statistical analysis to determine how different production methods responded when containing a stress concentration.

Hypothesis

With regards to the comparison of various production methods of tensile testing specimens, it was expected that testing results would reflect similarly from each method. Each mechanical property found; yield strength, Young's modulus of elasticity, ultimate tensile strength (UTS); could then be used in the comparison of the various production methods. These comparisons of mechanical properties comprising of the following:

- SLM Edge Solid vs. SLM Flat Solid
- SLM Edge Solid vs. Purchased Solid
- SLM Flat Solid vs. Purchased Solid
- SLM Edge with Hole vs. SLM Flat with Hole
- SLM Edge with Hole vs. Purchased with Hole
- SLM Flat with Hole vs. Purchased with Hole

These comparisons were to be used in the statistical analysis of the production methods to determine if a significant difference exists in each mechanical property. The first analysis to be completed is an analysis of variance. For this an f-test will be used in each comparison for each property. The f-tests will contain a null and alternate hypothesis to determining the result of the variance analysis. This is statistically expressed in the null hypothesis:

$$H_0: \sigma_1^2 = \sigma_2^2$$

Accepting the null hypothesis given here would show a result stating the variances of the two production methods are assumed equal. If the result states the null hypothesis is rejected, then an alternate hypothesis must be accepted. The alternate hypothesis for these f-tests would appear as follows:

$$H_a: \sigma_1^2 \neq \sigma_2^2$$

This alternate hypothesis states that the results of the analysis of variance show the two variances are assumed to be unequal. The f-tests are only to be used in analyzing the variance of the comparisons, another analysis method must be used to compare the means of the production methods.

Following the analysis of variance, a comparison of the means should be used. This is done using t-tests, which use the results of the f-tests previously ran, where the t-test will assume equal or unequal variances for the comparisons. Just as with the f-tests, a hypothesis must be created before testing, in this case the null is as follows:

$$H_0: \mu_1 = \mu_2$$

Where for t-tests, this null hypothesis, if failed to reject, states the means of the mechanical properties being compared are not significantly different from one another. If the null is rejected, then the alternate hypothesis is then accepted. This alternate hypothesis is as follows:

$$H_a: \mu_1 \neq \mu_2$$

The alternate hypothesis shown here, if the null hypothesis is rejected, states that the two means of the production methods being compared are significantly different. Again, as stated, these null and alternate hypotheses for both the f-tests and t-tests are to be applied to each comparison of production method shown.

An ANOVA allows the analysis of the differences between various group means, and thus may be used to make multiple comparisons with one method, but is otherwise similar to t-tests as it compares group means. Again for the ANOVA a hypothesis must be formed, the null hypothesis is stated as follows:

$$H_0: \mu_i = \mu_i$$

Which states that all sample means (*i*) are statistically equal to one another. As in other statistical analysis methods, an alternate hypothesis is also needed and is given here:

$$H_a: \mu_i \neq \mu_i$$

Which states that at least one sample mean is significantly different from another, thus stating the means are unequal. After performing an ANOVA, if the results do show a significant difference is present, it is possible to perform a post-hoc test. This test is used to determine where the differences occurred between groups. This test also uses the results of a test of variance, assuming either equal or unequal variances. This result determines which type of post hoc test is used, where equal variances utilize the Tukey post hoc test, and unequal variances use a Games-Howell post hoc test. The results of both these post hoc tests produce a chart showing intervals of each comparison made, where the intervals may be used to determine significance of the comparison.

Additive Manufacturing

As manufacturing processes continue to improve and develop, the demand for faster and less expensive manufacturing processes have allowed for a number of Rapid Prototyping (RP) processes to be developed. RP technology is unconstrained by the limitations of specially designed tooling and fixturing. Therefore, almost any geometry with variation in size and complexity can be produced to a high degree of accuracy (Simchi & Asgharzadeh, 2004). RP

techniques are capable of manufacturing complex 3D geometries by using Additive Manufacturing (AM). Rather than removing material from a stock until a desired geometry is met, as found in Subtractive Manufacturing (SM), material is added in specifically shaped layers to build up the geometry. Each successive layer of material is adhered to the previous layer by some form of controlled heat exposure, depending on the method used. Initially AM techniques were used to create prototypes or any low quantity amount of parts. Though currently the use of AM is not limited to prototyping or as a temporary stage in the design but rather includes many applications of the technology, including, modeling, pattern-making, tool-making, and the production of end-use parts in large quantities (Banther, 2009) (Kruth, et al., 2010).

With the EOS Parameter Sets, the system manufactures parts with standardized Part Property Profiles (PPPs) for a broad range of applications (EOS e-Manufacturing Solutions, 2014b). Each material is assigned one or more parameter sets with corresponding PPPs. These PPPs typically include the following groups of properties:

- Geometric properties such as minimum wall thickness and surface roughness
- Mechanical properties such as tensile strength, yield strength, elongation at break, modulus of elasticity and hardness, and where applicable dynamic fatigue life
- Thermal attributes such as thermal conductivity, specific heat capacity and thermal expansion coefficient

History of Additive Manufacturing

Varying methods of AM have been recorded as early as 1890, where a layering method was used to build up topographical maps. At the time, each layer was cut, shaped, and laid by hand. Though not an extremely precise method, it accomplished what was needed at the time (Bourell, Beaman, Jr., Leu, & Rosen, 2009). In 1972 another process was developed for

manufacturing maps that involved selectively exposing photo-hardening material to a heat source. Each layer of the material only harden where the heat was applied allowing for an improved, more automated, process. In 1979 the earliest description of a powder laser sintering process was proposed in a patent. Then 1981 A. J. Herbert described the development of a system that directs a UV laser beam to a photopolymer layer by means of mirror system on an x-y plotter.

Consolidation Methods

As AM technology has developed over time, the use or goals for the parts have also changed, for example different materials are demanded for various uses. This in turn then requires a new method or process depending on the material. Kruth (2007) gives examples of the most popular layered manufacturing techniques, being: photo-polymerization, Stereolithography (SLA and its derivatives), ink-jet printing (IJP), 3D printing (3DP), Fused Deposition Modelling (FDM), Selective Laser Sintering or Melting (SLS/SLM and Electron Beam Melting) (Kruth, Levy, Klocke, & Childs, 2007). Within many of these methods are specific binding mechanisms, though this study will focus on the outcome of full melting SLM manufacturing methods, specifically using the e-Manufacturing Solutions EOS M290 Metal Additive Manufacturing System, housed within The Kimmel School of Western Carolina University.

Build Strategy/Orientations of Parts

As a greater number and better performing systems using SLM are being developed, the number of available materials also increases. As stated before the SLM process is able to use various powdered materials in polymers, ceramics and metals. EOS e-Manufacturing solutions produces systems for both SLM of polymers and metals, with multiple systems for each material type. Note that each system is setup for either polymers or metals. A list of currently available

powdered metals from EOS can be found in Table 1-1**.** This research will be done using the 316L Stainless Steel made by EOS.

Subtractive Manufacturing

Subtractive manufacturing (SM), as stated, is the removal of material from a stock to produce a desired 3D geometry. SM requires the use of a computer numerical control (CNC) machine, typically found in the form of mills, lathes, grinders, or water-jet cutters. These machines have improved greatly over time, but are still limited in capability by the available tooling and methods. A significant difference between SM and AM is the process by which the material is subject to. While SM removes from already solidified stock material, AM works by solidifying loose material to the preferred shape. The loose material can usually be found in the form of powder. For the purpose of this research, test specimens were purchased from Lab

Table 1-1: EOS Metal Materials
(EOS e-Manufacturing Solutions, 2013)

EOS Metal Materials	
Composition	Trade Name
Maraging Steel	EOS MaragingSteel MS1
Stainless Steel	EOS StainlessSteel GP1
	EOS StainlessSteel CX
	EOS StainlessSteel 316L
	EOS StainlessSteel PH1
Nickel Alloy	EOS NickelAlloy IN718
	EOS NickelAlloy IN625
	EOS Nickel Alloy HX
Cobalt Chrome	EOS CobaltChrome MP1
	EOS CobaltChrome SP2
Titanium	EOS Titanium Ti64
Aluminium	EOS Aluminium AlSi10Mg

Testing Incorporated, where cold rolled 316L stainless steel was machined to the correct dimensional geometry. The process of cold rolling is performed close to normal room temperature and uses pressure to change the size of the material being processed. In the case of these parts, the material was cold rolled into bar stock which was then used in milling the parts to the desired dimensions.

Mechanical Properties

Tensile Testing

This research will focus on the comparison of mechanical properties of 316L stainless steel between two manufacturing methods, SLM and subtractive manufacturing, in this case milling. The mechanical properties of these materials will be determined by tensile testing. A tensile test, also known as tension test, is performed by pulling on a material, usually until failure. By doing this test a tensile profile will be formed in a curve showing how the material reacted to the forces being applied (Instron, n.d.). Data can then be interpreted from the tensile profile taken from the material. This experiment will be looking into; stress, strain, yield stress, ultimate tensile stress, and Young's modulus of elasticity. Stress is the internal resistance of a material to distorting effects of an external force or load. The calculation for stress can be found in Eq. 3.1, where σ equals stress, F is the force being applied, and A is the cross-sectional area of the specimen. The resulting unit for stress is MPa.

$$\sigma = F/A \qquad \textit{Equation 1-1}$$

Strain is defined as the deformation of a solid due to stress. This can be seen as the elongation during tensile testing. Strain is calculated using the equation Eq. 3.2, where ε is the unit-less measure of strain, Δl is the change in length, and l_0 is initial length.

$$\varepsilon = \Delta l / l_0 \qquad \textit{Equation 1-2}$$

Young's modulus of elasticity is a measure of stiffness of an elastic material, and is used to describe the elastic properties of objects when they are stretched or compressed. The equation for Young's modulus can be found in Eq 3.3. This elastic modulus is a ratio of stress and strain, and once known can be used to predict the elongation or compression of an object where the stress is less than the yield strength of the material, otherwise known as the elastic region. Young's modulus is represented by E and units MPa.

$$E = \sigma / \varepsilon \qquad \textit{Equation 1-3}$$

The Young's modulus is only applicable to materials when they remain in the elastic region during testing. This elastic region is the area before the yield strength of a material. The positioning of the Young's modulus can be seen in Figure 1-1. As can be seen, the Young's modulus appears parallel to the beginning part of the elastic region of the stress-strain curve, though it is offset in the strain by 0.2%. Where the Young's modulus intersects with the stress-strain curve is the yield strength of the material, or the end of the elastic region.

Also visible in the example stress-strain curve is the ultimate tensile strength (UTS). This is a value found by locating the maximum amount of stress within the stress-strain curve, as indicated in the diagram at the peak of the curve.

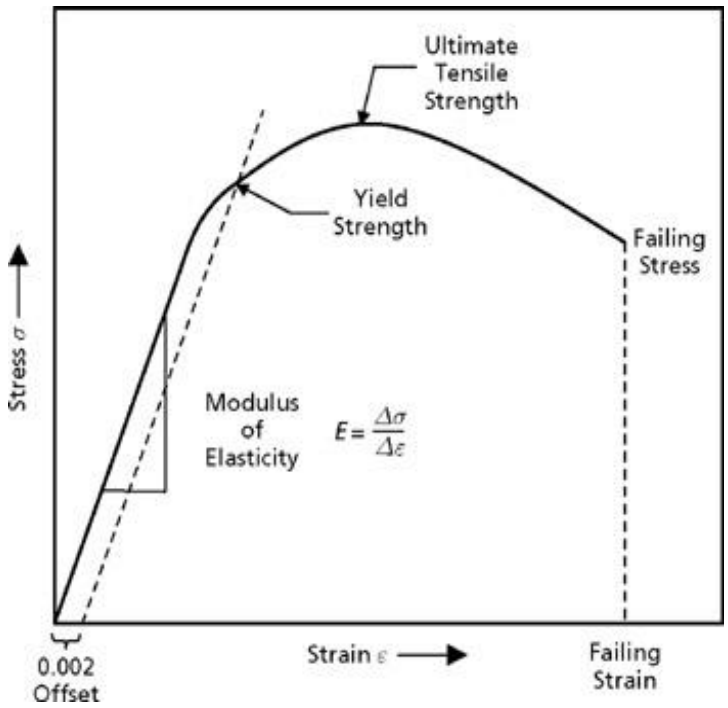

Figure 1-1: Example of Typical Stress Strain Curve (IHS Engineering 316, 2006)

Provisions of the Study

It has been stated, this study will encompass various production methods for tensile testing specimens. These production methods specifically include the SM method of machining of cold rolled bar stock of 316L stainless steel, to a dimensional geometry described by ASTM E8. The other method entails using the AM method of SLM manufacturing of 316L powdered metal, provided by EOS e-manufacturing, producing the parts to the same dimensional geometry. Within the SLM process two build orientations will be included. These two build orientations involve the part being in a flat orientation, which is parallel to the build surface, and an edge orientation, where the part is perpendicular to the build surface. For both production methods, the same 316L stainless steel was used so the results would reflect the production methods and not variations in materials. A parameter set predetermined and provided by EOS e-

manufacturing was used in each part production. These parameters included machine parameters as well as support structure design and dimensions.

The preparations of the stress concentrations vary between the different production methods. For the flat oriented SLM produced parts, no preparation or post processing of the actual stress concentrations are needed. The edge oriented SLM produced parts, support structure was needed within the stress concentration and thus was required to be removed before testing, which was done by use of a metal file. A stress concentration could not be placed in the part during the production using traditional methods. The stress concentration was placed in these parts by use of a milling machine to drill the correct size hole into the parts, which was consistently done for each traditional production part which required the stress concentration.

The tensile testing of this research was done in accordance with the ASTM E8 standard of tensile testing metals. The requirements of testing set forth by this standard were used for testing of all test specimens. The entirety of tensile testing was performed using the Instron 5960 series dual column testing system. Also the testing of parts for this research was limited to tensile testing of the parts, as the desired mechanical properties can be found from tensile testing. These mechanical properties were limited to yield strength, UTS and Young's modulus, for this study.

As AM production methods become more commonly used, it is important to know the potentiality of what the method can produce. This includes but is not limited to knowing the effects SLM production has on the mechanical properties of a material when compared to traditional methods of production, when is explored in this research. This study also investigates the comparison of the methods when including a part geometry in tensile testing specimens. Moving forward in new technologies and production methods it is necessary to know the capabilities of the methods used.

So as we see here, this research will be looking into the comparison of various manufacturing methods, with regards to mechanical properties of the parts, and will be achieved by performing the following:

- All production methods will use 316L stainless steel
- The SLM process will include two build orientations, edge and flat
- All the SLM produced and purchased parts will include two geometries, with and without the same size stress concentrations
- Tensile testing will be performed, using the same test setup for each production method
- Mechanical properties, yield strength, UTS, and Young's modulus will be extracted from the tensile testing results
- Comparisons of the production methods will be made for each mechanical property
- Statistical analyses of these comparisons within each mechanical property will be made and conclude in either a significant difference being present or absent

Following these procedure, this research will determine whether using SLM production methods to produce parts, both with and without stress concentrations, or traditional manufacturing of parts containing the same geometry will result in similar or varying mechanical properties.

DEFINITIONS

Additive Manufacturing (AM) – a process of joining materials to make objects from 3D model data, usually layer upon layer, as opposed to subtractive manufacturing methodologies.

Arbitrarily oriented minimum bounding box – *of a part*, the minimum perimeter cuboid that can span the maximum extents of the points on the surface of a 3D part calculated without any constraints on the resulting orientation of the box.

Build Platform (Build Plate) – *of a machine*, any base which provides a surface upon which the build is started and supported throughout the build process.

Build Surface – area where material is added, normally on the last deposited layer which becomes the foundation upon which the next layer is formed.

CAD – Computer-Aided Design. The use of computers for the design of real or virtual objects.

CAM – Computer-Aided Manufacturing. Typically refers to systems that use surface data to drive CNC machines, such as digitally-driven mills and lathes, to produce parts, molds, and dies.

CNC – Computer Numerical Control. Computerized control of machines for manufacturing.

Initial Build Orientation – *of a part*, is the orientation of the part as first placed in the build volume and becomes the reference for any further part reorientation.

Orthogonal Orientation Notation – *of a part's initial build orientation*, may be used when the intended build orientation for a part is such that its arbitrarily oriented minimum bounding box is aligned parallel to the X, Y, and Z axes of the build volume origin, its orientation may be described by listing which axis is parallel to the longest overall dimension of the bounding box first, followed by the axis which is parallel to the second

longest overall dimension of the bounding box second, followed by the axis which is parallel to the third longest overall dimension of the bounding box.

Rapid Prototyping (RP) – additive manufacturing of a design, often iterative, for form, fit, or functional testing, or combination thereof.

Selective Laser Melting (SLM) – a powder bed fusion process used to produce objects from powdered materials using one or more lasers to selectively fuse or melt the particles at the surface, layer by layer, in an enclosed chamber.

STL (STereoLithography) – *in additive manufacturing*, file format for 3D model data used by machines to build physical parts; STL is the de facto standard interface for additive manufacturing systems.

Stress – *in mechanics*, the force per unit area on a body that tends to cause it to change shape. Stress is a measure of the internal forces in a body between its particles. These internal forces are a reaction to the external forces applied on the body that cause it to separate, compress or slide.

Subtractive Manufacturing (SM) – making objects by removal of material (for example, milling drilling, grinding, carving, etc.) from a bulk solid to leave a desired shape, as opposed to additive manufacturing.

Ultimate Tensile Strength (UTS) – the capacity of a material or structure to withstand loads tending to elongate.

X axis – *of a machine*, shall run perpendicular to the Z axis and parallel to the front of the machine.

Y axis – *of a machine*, shall run perpendicular to the Z and X axes with positive direction defined to make a right hand set of coordinates as specified in ISO 841.

Z axis – *of a machine*, for processes employing planar layerwise addition of material, shall run normal to the layers. Shall run perpendicular to the X and Y axes with positive direction being vertical to the work area.

CHAPTER TWO: LITERATURE REVIEW

Additive Manufacturing

The research presented here discusses the effect various production methods have on material properties. Previously, several studies have been conducted in related areas. The related areas being effects of SLM manufacturing, AM processes involving 316L stainless steel, and part orientation during SLM. At this time no research has been found with regards to purposefully including part features or stress risers in the SLM process and how it effects material properties.

SLM

When looking at the detailed descriptions of the history of AM, it becomes apparent how the various techniques used individually in the past were able to come together and influence the methods used today. The selective heat exposure to materials has been used it many techniques, though in new methods the accuracy of the heat exposure has be greatly increased. The improvement of these methods also included the use of layerwise scanning of the geometry, where one layer was formed at a time. This improvement in heat exposure accuracy is due to both the advancement in technology, but also a technique which introduced the use of a laser beam controlled by a computer and directed by a set of mirrors. SLM is an AM process which uses many of these techniques, which were developed over time, in one production method.

SLM/EOS System

SLS vs. SLM, Partial vs. Full Melting

It can be said that SLS and SLM are similar methods, in that both utilize a computer controlled laser to consolidate layers of metal powder onto previously consolidated layers. The distinction between SLS and SLM is vague and does not cover all types of consolidation, though a more detailed specification of binding mechanisms can be found in Figure 2-1. Looking at these binding mechanisms allows for a better discrepancy to be made between SLS and SLM methods. Solid state sintering (SSS) is a consolidation process which occurs below the materials melting temperature. The material consolidates by forming necks between adjacent powder particles which grow larger over time. This consolidation technique is used primarily with ceramics, as the diffusion rate of atoms in SSS is slow and not feasible for process productivity (Kruth, Levy, Klocke, & Childs, 2007). Liquid phase sintering (LPS) and partial melting include a variety of binding mechanisms in which part of the powder material is melted while other parts remain solid. As some of the material is melted it quickly moves between the remaining solid material, binding the material together. The material that melts to become the binder may not be

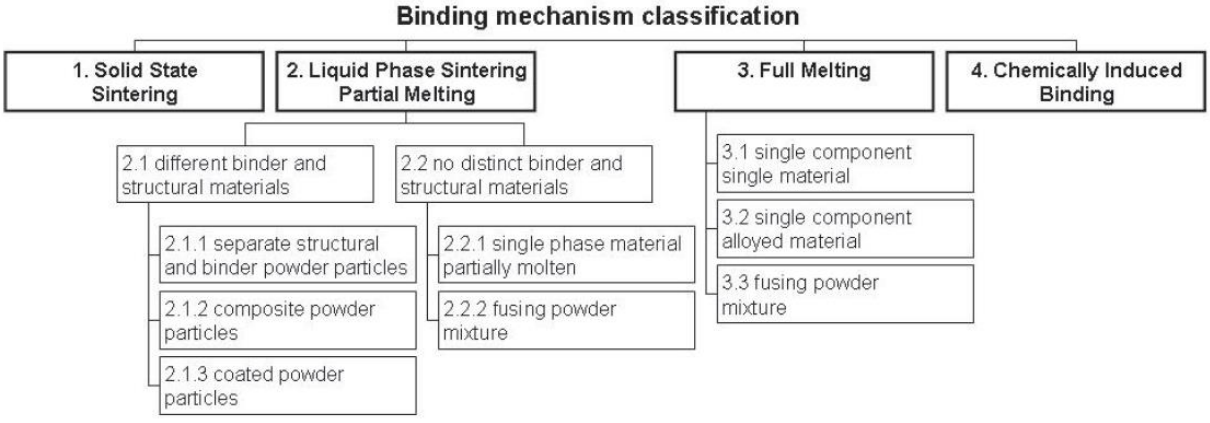

Figure 2-1: Laser-based powder consolidation mechanisms (Kruth, Levy, Klocke, & Childs, 2007)

the same as that which remains solid. For example a material containing coated particles could be used in which the coating material has a lower melting temperature which would allow it to solely react to the applied heat. Partial melting can also be used when there is no distinct binding material. In this use the SLS parameters are adjusted to only partially melt the powder particles. LPS and partial melting typically require a post process to produce a fully dense part (Kruth, Levy, Klocke, & Childs, 2007). Full melting, used in SLM, is a major consolidation mechanism often used to achieve fully dense parts without need for any post-process densification. While it has the advantage of no post-processing there are some potential drawbacks that can occur without carful process control. Balling phenomena is a possible SLM defect and can be detrimental to the forming quality of the parts. Within the balling behavior there are two possible types; an ellipsoidal balls with a dimension of 500 μm and spherical balls with dimension of about 10 μm. The ellipsoidal balls tend to cause problems with quality while the spherical balls are not as significant. Some main disadvantages caused by balling given by Li (2012) are as follows:

1. The balling phenomenon could increase the surface roughness; thus, requiring some post-process such as polishing. While trivial, this could also cause dimensional inaccuracy.
2. A large amount of pores in SLM component tend to form between many discontinuous metallic balls, which result in a lesser density and thus results in poor mechanical properties.
3. When the balling phenomenon is severe enough there is potential for the balls to hinder the movement of the recoater blade of the layering system. The result is either the part is slightly damaged or scratched, or the recoater blade is stopped completely (Li, Liu, Shi, Wang, & Jiang, 2012).

316L Stainless

The materials used in the SLM process begin as very fine powdered metal, with the powder particles ranging in sizes of 5-10 µm. Most manufacturers of SLM systems also produce metal powder mixtures that work best with their system. EOS Stainless Steel 316L is a corrosion resistant iron based alloy which has been optimized especially for processing on EOSINT M290

Table 2-1: Expected Chemical Composition of EOS 316L Stainless Steel Parts

Expected Chemical Properties of Parts			
	EOS Stainless Steel 316L		
Material Composition	Element	Min.	Max.
	Fe	Balance	
	Cr	17.00	19.00
	Ni	13.00	15.00
	Mo	2.25	3.00
	C	-	0.03
	Mn	-	2.00
	Cu	-	0.50
	P	-	0.025
	S	-	0.01
	Si	-	0.75
	N	-	0.10

Table 2-2: Expected Chemical Composition of Purchased 316L Stainless Steel Parts

Expected Chemical Properties of Parts			
	Purchased Stainless Steel 316L		
Material Composition	Element	Min.	Max.
	Fe	58.23	73.61
	Cr	16.00	18.50
	Ni	10.00	15.00
	Mo	-	3.00
	C	-	0.08
	Mn	-	2.00
	Cu	-	1.00
	P	-	0.045
	S	-	0.35
	Si	-	1.00
	N	-	0.10
	Ti	-	0.70

systems. The parts built from EOS Stainless Steel 316L can be machined, shot-peened and polished in as-built or stress relieved states if required. This research will use parts that have not been stress relieved. EOS states that the relative density of finished parts, using standard parameters, are approximately 100% or minimum 7.9 g/cm^3 (EOS E-Manufacturing Solutions, 2014a). The expected material composition can be found in Table 2-1, each element shown in percentages, while the measured chemical composition may be found in the appendix. According to EOS (2014a) this chemical composition is within limits of ASTM F138 "Standard Specification for Wrought 18Cr-14Ni-2.5Mo Stainless Steel Bar and Wire for Surgical Implants" (EOS E-Manufacturing Solutions, 2014a). Also the expected chemical composition of the purchased parts can be found in Table 2-2.

Material Specifics

Kamath (2014) discusses various manufacturing strategies for achieving greater density in 316L stainless steel parts. The strategies investigated here were changing of the scanning parameters of the machine. These parameters included laser power; scaling from 150 to 400W; and adjusting the laser scan speeds. It was found that with a given laser power increasing the scan speeds could result in insufficient melting and a lower part density. As well as when at high laser powers, the density is higher over a wider range of scan speeds, unlike at lower laser powers. Kamath's experiment showed that when using optimized parameter settings on a machine, it is possible to produce small parts with >99% relative density using SLM (Kamath, El-dasher, Gallegos, King, & Sisto, 2014). When a process uses properly generated process parameters, the balling phenomenon is easily avoided. Along with the possibility of balling, residual stresses in AM produced parts can be a significant setback. According to Mercelis

(2006) residual stresses in parts are not always disadvantageous, sometimes the stresses are induced so that a part contains a certain quality. However, residual stresses are primarily unwanted as they result in a deformation of the intended dimensions. Mercelis (2006) explains the two mechanisms which introduce residual stress as follows:

> The first mechanism introducing residual stress is called the temperature gradient mechanism (TGM, Figure 2-2**)**. It results from the large thermal gradients that occur around the laser spot. Owing to the rapid heating of the upper surface by the laser beam and the rather slow heat conduction, a steep temperature gradient develops. Since the expansion of the heated top layer is restricted by the underlying material, elastic compressive strains are induced. When the material's yield strength is reached, the top layer will be plastically compressed. In absence of mechanical constraints, a counter bending away from the laser beam would be perceived. During cooling the plastically compressed upper layers start shrinking and a bending angle towards the laser beam develops. This mechanism is also present in SLS and SLM, where the underlying layers inhibit the expansion of the heated top layers. It is important to notice that this mechanism does not require the material to be molten.
>
> A second mechanism that induces residual stresses is the cool-down phase of the molten top layers (in SLM). The latter tend to shrink due to the thermal contraction. This deformation is again inhibited by the underlying material, thus introducing tensile stress in the added top layer and compressive stress below (Mercelis & Kruth, 2006).

Other research investigating optimal process parameters discusses residual stresses in parts when using varying process parameters. The research of Mercelis (2006) involves 316L stainless steel to determine how residual stresses are affected by changes in the SLM building

process. The results stated that a reduction of residual stresses is possible by heating the build plate as it reduces the temperature gradients during building. It is also discussed that it is possible to reduce the stress levels by applying a heat treatment to the part using the laser, by multiple scans, though no drastic reductions could be obtained in their investigation. A major conclusion was a distinction between parts left on the build plate and parts what were removed. Mercelis (2006) states that parts which remain attached to the build plate contain high amounts of stress levels. While parts which are removed from the plate contain lower stress levels, but those parts suffer from deformation during the part removal (Mercelis & Kruth, 2006).

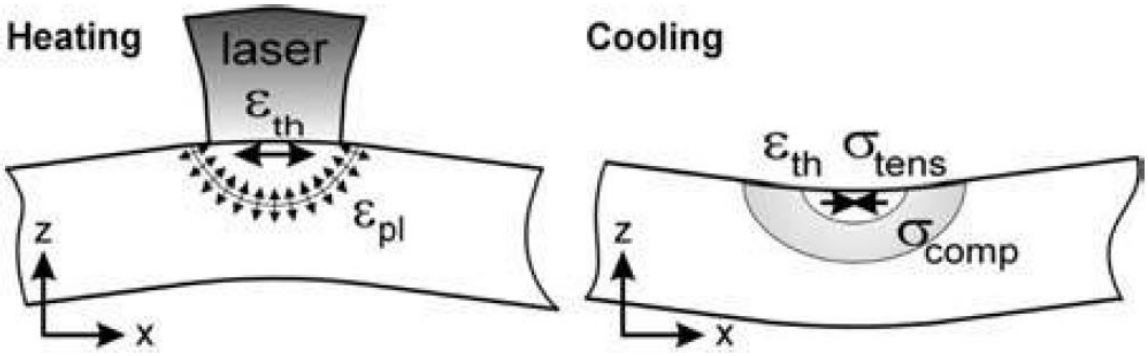

Figure 2-2: TGM inducing residual stress
(Mercelis & Kruth, 2006)

For the EOS metal systems there are three different Parameter Sets (PS), each are meant to achieve a different attribute, and are as follows:

- Speed – (30 – 60 µm layer thickness) – higher productivity, good surface quality. The Speed PS represents a good compromise between building speed and surface quality. The building time is shorter compared to the Performance PS.
- Performance – (30 – 40 µm layer thickness) – good surface quality. This parameter set is ideally suited when the focus is good surface quality. Compared to the Surface PS, it

offers a higher productivity due to thicker powder layers which helps to reduce production costs.

- Surface – (20 µm layer thickness) – fine details, high surface quality. Compared to the above parameter sets, the Surface PS is built with the lowest layer thickness. Therefore, it is the perfect choice for parts that require fine and high detail resolution and best surface quality (EOS e-Manufacturing Solutions, 2013b).

The experimentation with the EOS M290 included the prearranged Performance parameter set, which will provide the best all-around performance. Most process details of the parameter sets provided by EOS are not known, such as the laser power, scan speed, etc. Though some technical data are given such as; each powder layer has a thickness of 20 µm, the typical achievable part accuracy in small parts is approximately ± 20-50 µm, as well as expected surface roughness of as-manufactured parts being R. 13 ± 5 µm; R. 80 ± 20 µm (EOS E-Manufacturing Solutions, 2014a).

Microstructure and Grain Structure from SLM Process

Microstructure of a material can be described as, "The arrangement of phases and defects within a material (Materials and Minerals Science Course C: Microstructure)." Microstructures are generally generated when a material undergoes a phase transformation brought about by change in temperature and/or pressure. An example being the cooling of a melt pool during a SLM process. Solidification of a crystal from a melt occurs through a process of nucleation and growth. Below the melting temperature, small clusters of atoms in the melt come together through random chance to form a small crystalline particle (a nucleus). The nucleus forms a template onto which other atoms can attach. Each nucleus grows into an individual grain of the crystal. When adjacent grains impinge they form grain boundaries. Since individual nuclei form

in different orientations, there is no orientational relationship between adjacent grains (Materials and Minerals Science Course C: Microstructure). These grains and grain boundaries make up the microstructure of a material. During the process of SLM a melt pool is formed in the powdered material as the laser passes over, and as this melt pool cools the microstructure forms. While the microstructure is forming, the melt pool is also adhering to the previously melted layer of the part. This fresh melt pool's grains interact with that of the previous layer which cause the two layers to bond. In theory, each time these layers bonded together the microstructure should remain uniform, but this is not the case. A 'phase' is taken to be any part of a material with a distinct crystal structure and/or chemical composition. Different phases in a material are separated from one another by distinct boundaries (Materials and Minerals Science Course C: Microstructure). It can then be described that each melt pool caused by the laser can be seen as a phase. As SLM is a layered method, and the microstructure for all layers are not uniform, the distinction between the layers can be seen using microscopy. Figure 2-3 allows the various melt

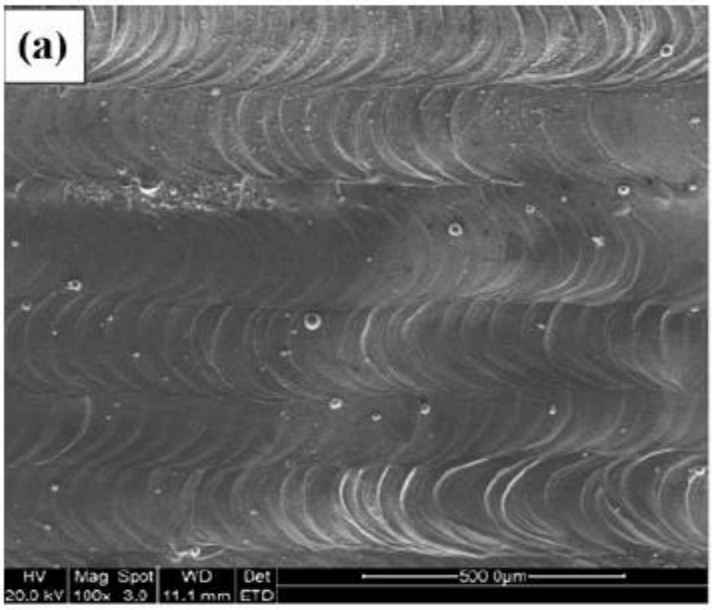

Figure 2-3: Balling characteristics when oxygen=0.1%
(Li, Liu, Shi, Wang, & Jiang, 2012)

pools formed during the SLM process to be seen, each running parallel and overlapping with one another.

Effects of Various Orientations

Along with parameter settings, the orientation in which a part is built can be adjusted to provide different results. When describing the orientation of a SLM manufactured part it is necessary to have a coordinate system or terminology in which to describe the orientation. ASTM standard 52921 provides the standard for identifying the various 3D orientations for parts. This coordinate system uses the X, Y, and Z axes of the build volume origin, where the parts orientation is described by listing which axis is parallel to the longest overall dimension of the

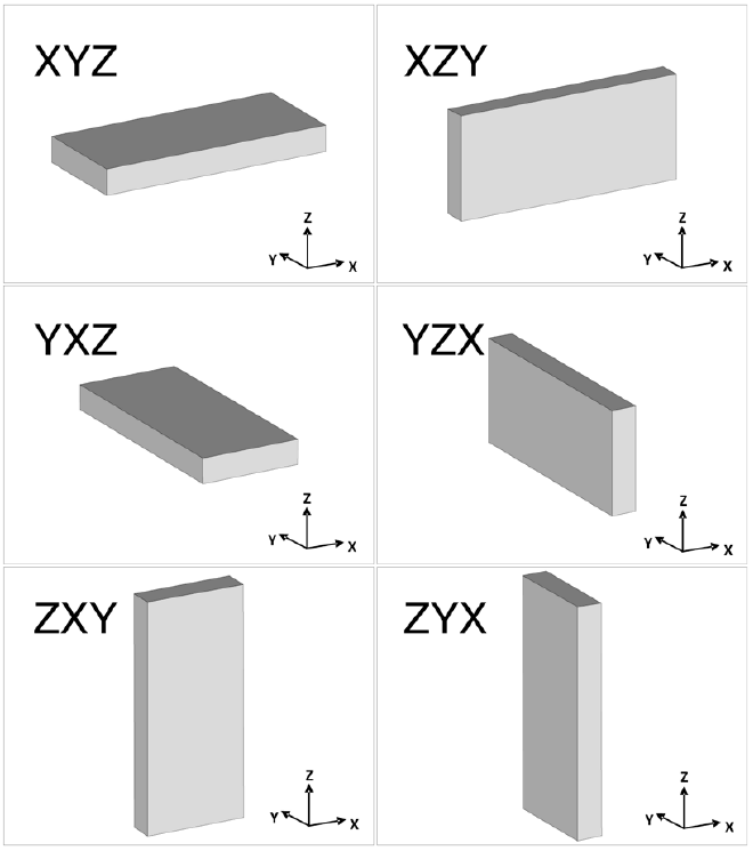

Figure 2-4: Orthogonal Orientation Notation (ASTM ISO / ASTM52921-13,, 2013)

part first, followed by the axes parallel with the second longest dimension, followed by the axis which is parallel to the third longest overall dimension. This will allow part orientations to be described by XYZ notations as shown in Figure 2-4. Orthogonal orientation notation may be abbreviated where symmetry allows, thus when using flat tensile test coupons bilateral symmetry can be applied allowing the notation to be shortened to ZX, or XY as shown in Figure 2-5.

Simonelli (2014) looked at what effect build orientation had on SLM created parts in Ti-6Al-4V. The experiment looked at three orientations of tensile coupons, these being ZX (vertical), XY (flat), and XZ (edge). The flat orientation of these parts showed significant curling during the SLM process. Some specimens were curled enough to be discarded, while others were machined into flat parts. The results from the tensile testing showed the elastic modulus did not vary with the change in the build orientation. The flat oriented tensile bars gave the lowest elongation at failure. This result was attributed to the curling of the parts, thus preventing an even powder deposition when forming layers. Simonelli stated that the edge oriented bars

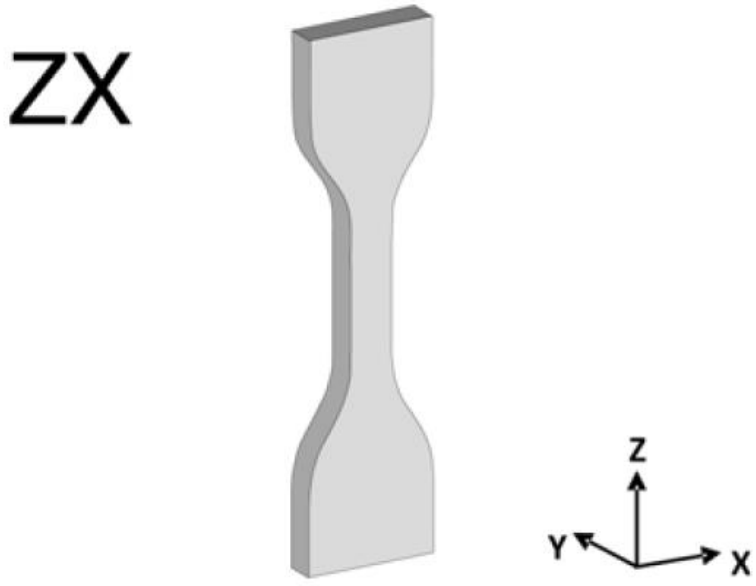

Figure 2-5: Example of Symmetry Abbreviation of Orthogonal Orientation Notation (ASTM ISO / ASTM52921-13,, 2013)

produced the best tensile properties and the greatest elongation at fracture (Simonelli, Yse, & Tuck, 2014).

Tolosa (2010) conducted an experiment to see the effects on AM created parts with various build orientations and angles. These parts used AISI 316L stainless steel. The various orientations were displayed as case A, B, and C; where case A samples were manufactured in the XY orientation; case B were built in the XZ orientation; case C in the ZX orientation; and case D was built in the ZX with various angles with respect to the build plate. Within each class different groups of parts were built with different angles rotating about the Z axis. It should also be noted that to avoid the use of supports from the samples to the build plate, the samples were built with prismatic geometry and then machined to size after the AM process completed. Tensile tests were performed on both the SLM manufactured specimens and parts created with traditional manufacturing, in this case rolled steel machined to size. When Tolosa compared the results of the various cases for orientation, for strength the best option is the case A (XY) orientation. While case C provides the best ductility values (Tolosa, Garciandía, Zubiri, Zapirain, & Esnaola, 2010).

Much research on SLM capabilities involve Ti-6Al-4V and 316L stainless steel, Mertens (2014) states it is because of the materials use in biomedical and aeronautical applications. Mertens performed an experiment which involved both these materials. The goal of this experimentation was to see how the SLM process effected mechanical properties of the two materials, with different build orientations seen in Figure 2-6. Uniaxial tensile tests were performed to samples of both materials in accordance with the ISO 6892-1 B 25: 2009 standard. An optical micrograph of 316L showed semi-circular shapes perpendicular to the building direction, which corresponded with individual melt pools. Though two different types of

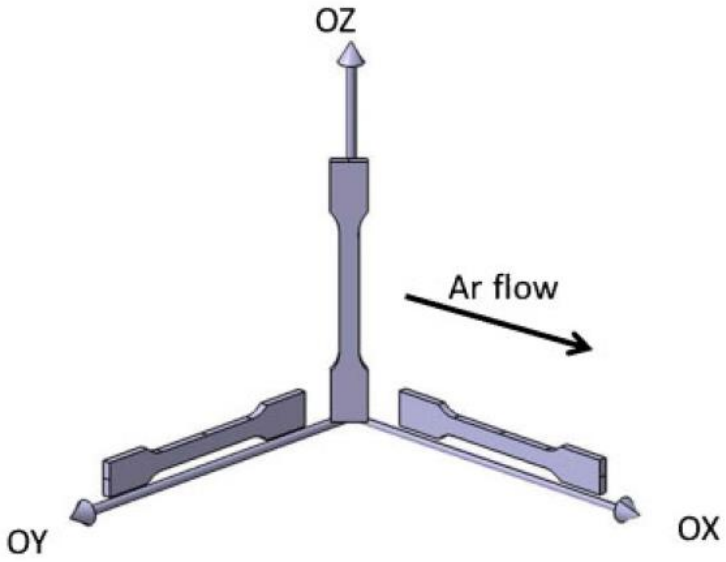

Figure 2-6: Representation of various orientations of tensile samples with respect to building direction (oz) (Mertens, et al., 2014)

porosities could be observed. Of these were spherical pores formed by gas bubbles between melt pools, and larger more elongated shapes localized between melt pools of two successive layers. These larger defects were scarce in the OY and OX orientations, however a greater number were found in the OZ orientation. These elongated shapes can be attributed to unmelted powder or insufficient remelting of the previous layer of material. After tensile testing it was found that the OX and OY orientations had similar material properties as well as a typical ductile fracture behavior. Though the OZ orientation specimens produced much lower strength results as well as much smaller elongation during testing. The reduced material properties for the OZ orientation can be attributed to the defects caused by lack of melting. Mertens concluded by comparing the two materials to each other. Fro0m this it was determined that Ti-6Al-4V is more susceptible to the build-up of internal stresses than 316L. Though material defects as a result of the SLM process appear more often in the 316L stainless, this was found to correspond with the difference in thermal conductivity of the two materials (Mertens, et al., 2014).

EOS Machine Specifics

With the SLM process many experiments and evaluations have been formed using a wide variety of different brands of machines and processes. Through this investigation only a few research studies were conducted using EOS SLM systems. Most of the research briefly discuss the M290 system's capabilities or use it to determine possibilities with AM processes. Bhavar (2014) reviews the present capabilities and challenges of AM systems. This review also compares various types of systems such as SLM, SLS, and EBM, to discover advantages, disadvantages, as well as differences in capabilities and materials. Within the discussion is also included a variety of systems available on the market including different EOS systems, but specifically the comparison contains the EOS M290 SLM system. The author primarily discusses the possibilities and applications possible, and some challenges with AM, and further compares specifically of the SLM and EBM systems. These two systems have a major difference in the laser type they use, but also in how the powder bed is heated during building. SLM systems heat the build plate to a wanted temperature and let the heat travel through the part being built, where EBM preheats the actual powder layer about to be scanned. Also the heating temperatures are vastly different, where the EOS M290 system heats the plate to 85°C and the EBM system heats the powder layer to around 700-900°C. Also the supports needed for EBM are needed for head conduction rather than part support. EBM systems have a higher build rate compared to the SLM, but also inferior dimensional and surface finish qualities. EBM systems also build within a vacuum, which is necessary for the quality of the electron beam, as well as reducing thermal gradients and possible oxidation of the parts like titanium alloys. Even with EBM systems having these advantages SLM is still more popular. Bhavar attributes this popularity to EBM

systems having higher machine cost, low accuracy and small build volumes (Bhavar, et al., 2014).

The EOS M290 system can also be found in the work of Krantz (2015) where a model was built to discover the viability of full scale production using AM versus traditional manufacturing, including milling and die casting. While creating the cost estimation model it was discovered that as needed accuracy in a part increased, the price for milling also increased and was not a linear change. This resulted in a step away from exact prices and towards price-spans. This work did result in a working mathematical model for each process, but was not used to specify which process at the time which method was more cost efficient (Krantz & Sjöö, 2015).

Again using the EOS M290 system Poyraz (2015) performs an investigation of block support structures of overhanging geometry parallel to the XY plane during the building process. The first part of the experimentation investigated the impact of the support dimensions, such as hatch distance of a block. However, the second set of experiments focused mainly on the effects of part to support contact in the way of teeth dimensions. The two experiments were controlled by dimensional inspection and light optical microscopy. Each experiment was performed using Inconel 625, and constant process parameters to avoid introducing different variables. The results of change in hatch distance showed when the hatch distance was increased the overhanging geometry was more distorted and at the max, one mm, distance the separation between the part and support structure was most significant. Thus keeping a smaller hatch distance will cause the part to distort less as it is better connected to the support structure. For the change in tooth dimensions it was found both the top length and Z offset value reductions influence the distortion results. However, it was also observed that when the top length; the length of the tooth touching

the part; increases, the impact of the Z offset; the height of the tooth; value decreases. In a final conclusion Poyraz states that with regard to part distortion and overhang geometry lifting, hatch distance has a more significant effect when changed. This experiment found that using lower hatch distance is useful for maintaining less distortion of parts, and the best results were achieved with a 0.5mm hatch distance (Poyraz, Yasa, Akbulut, Orhangül, & Pilatin, 2015).

Tensile Properties/Test

Stress Risers

When discussing stress concentrations concerning AM processes, it usually pertains to uncontrolled or unwanted features that form during the building process are historically the primary factors. This can vary from a part detaching and curling during the build, to portions of the powder layer not completely melting and creating larger than normal porosity defects. At the time of this research no testing has been found in the area of purposefully forming a stress concentration, such as a hole, in a part created by SLM meant for tensile testing to determine mechanical properties.

Research has been done in the area of tensile testing specimens which contain a stress concentration in the form of a circular hole. Most of this research has been in the area of mathematical models and estimating how the specimen will react during testing. There was little information found on testing materials with this type of stress concentration and the research performed using metals was done using large sheet type specimens that were multi-axially loaded. An example of the desired tensile specimen geometry may be seen in Figure 2-7. As stated, there has been no research found using this specimen geometry within metals.

Figure 2-7: Tensile specimen containing a circular hole stress concentration

Standard for Tensile Testing Metals

ASTM E8/E8M – 13a is the standard for test methods for tensile testing of metallic materials, and will drive the tensile testing performed in this experimentation. The specific size and geometry for the test specimen may be found in Figure 3-1. This test will be using rectangular tension test specimens. The following are sections necessary for set-up processes and predetermining test settings pertaining to this experiment.

Zeroing of the Testing Machine: The testing machine shall be set up in such a manner that zero force indication signifies a state of zero force on the specimen. Any force (or preload) imparted by the gripping of the specimen must be indicated by the force measuring system unless the preload is physically removed prior to testing. Artificial methods of removing the preload on the specimen, such as tearing it out by a zero adjust pot or removing it mathematically by software, are prohibited because these would affect the accuracy of the test results.

Gripping of the Test Specimen: For specimens with reduced sections, gripping of the specimen shall be restricted to the grip section, because gripping in the reduced section or in the fillet can significantly affect test results.

Speed of Testing: Speed of testing may be defined in terms of (*a*) rate of straining of the specimen, (*b*) rate of stressing of the specimen, (*c*) crosshead speed, (*d*) the elapsed time for completing part or all of the test, or (*e*) free-running crosshead speed.

Crosshead Speed: the allowable limits for crosshead speed, during a test, may be specified in mm/min in this case. Many testing machines are equipped with pacing or indicating devices for the measurement and control of the crosshead speed during a test, but in the absence of such devices the average crosshead speed can be experimentally determined by using suitable length-measuring and timing devices.

It is from this standard that the testing procedures and tensile specimen geometry have been determined.

CHAPTER THREE: METHODOLOGY

The methodology of this research covers each step that was taken in preparation of the parts for each production method, and the tensile testing and data recording of each part from each production method.

Preliminary Procedures

All test specimens used in this experiment have been created to the size and shape recommended by the ASTM E8 standard test methods for tension testing of metallic materials. The chart containing the recommended sizing can be found in Figure 3-1. The specimens use the measurements of the sheet type, 12.5 mm wide selection. Along with these measurements a

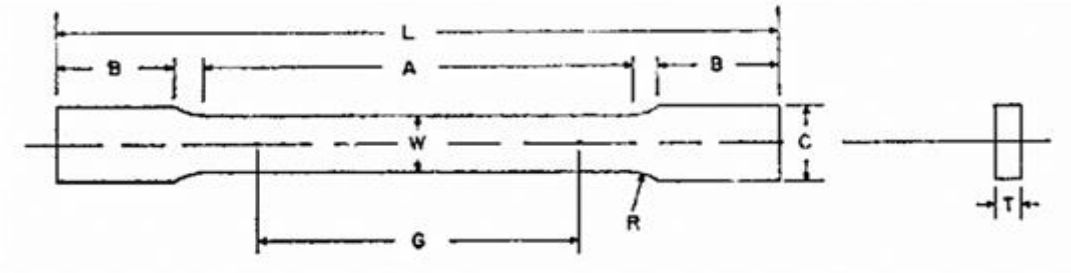

	Dimensions
	Standard Specimens
	Sheet-Type, 12.5 mm [0.500 in.] Wide
	mm [in.]
G - Gauge Length	50.0 ± 0.1 [2.000 ± 0.005]
W - Width	12.5 ± 0.2 [0.500 ± 0.010]
T - Thickness	Thickness of Material
R - Radius of fillet, min	12.5 [0.500]
L - Overall length, min	200 [8]
A - Length of reduced dection, min	57 [2.25]
B - Length of grip section, min	50 [2]
C - Width of grip section, approximate	20 [0.750]

Figure 3-1: Rectangular Tension Test Specimens (ASTM E8 / E8M-15a, 2015)

thickness of 3.175 mm was used. Both methods of part manufacturing will be aiming for these measurements. All actual measurements of parts were taken and recorded for later use. The machined specimens were purchased from Lab Testing Inc., who manufacture and test various specimens. The specimens were purchased in an untested state so that the machined and AM specimens were tested using the same equipment in the same conditions.

SLM Preparation

Part position and Support Structure

The part was first designed using Pro Engineer, using the dimensions determined by the standard. Both geometries, with and without the stress concentration were modeled. These 3D models were then converted to STL files to be used with other software. These STL files were then transferred to Magics, which is a popular software used by many AM processes. This software was then used to generate the 3D model in a space where support structure could then be formed. Magics generates support structure on parts where it believes it will be needed during the SLM process. On many parts it is formed on the underside or overhanging geometries to ensure the part is fully supported during processing, to prevent the parts from curling or dipping which could result in a failed build. It is then possible to remove areas of suggested support structure or to add more if necessary. This allows for any unwanted or unnecessary support to be removed, which is primarily done to avoid the need for more post processing.

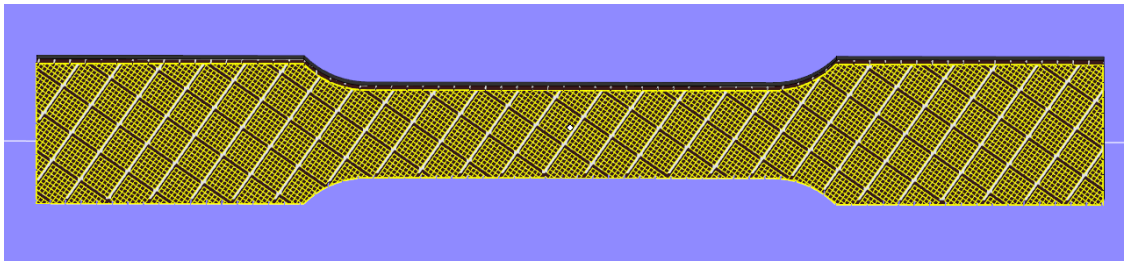

Figure 3-2: Flat oriented specimen showing support structure

Support structure was created for each geometry, as each had various requirements. All geometries used block support, except the stress concentration in the edge orientation, which used gusset supports. For the flat specimens, the solid geometry required support material beneath the entire part, shown in Figure 3-2. Whereas for the part containing the stress concentration, no support structure was created where the hole exists, as seen in Figure 3-3. The differences in necessary support structure may also be seen in the differing support structures for parts built on edge. For example in the edge oriented test specimen instead of removing unnecessary support structure, more was needed to be used within the stress concentration. Along with the support structure needed directly below the part, it is seen in Figure 3-4 that when the stress concentration is being formed in this orientation it is necessary to support it, as the top half of the arc acts as an overhanging geometry. If the support structure was not being used in the stress concentration the resulting shape would not resemble what was wanted. This is because, as overhanging material is being scanned it has a tendency to curl upwards due to heat and residual

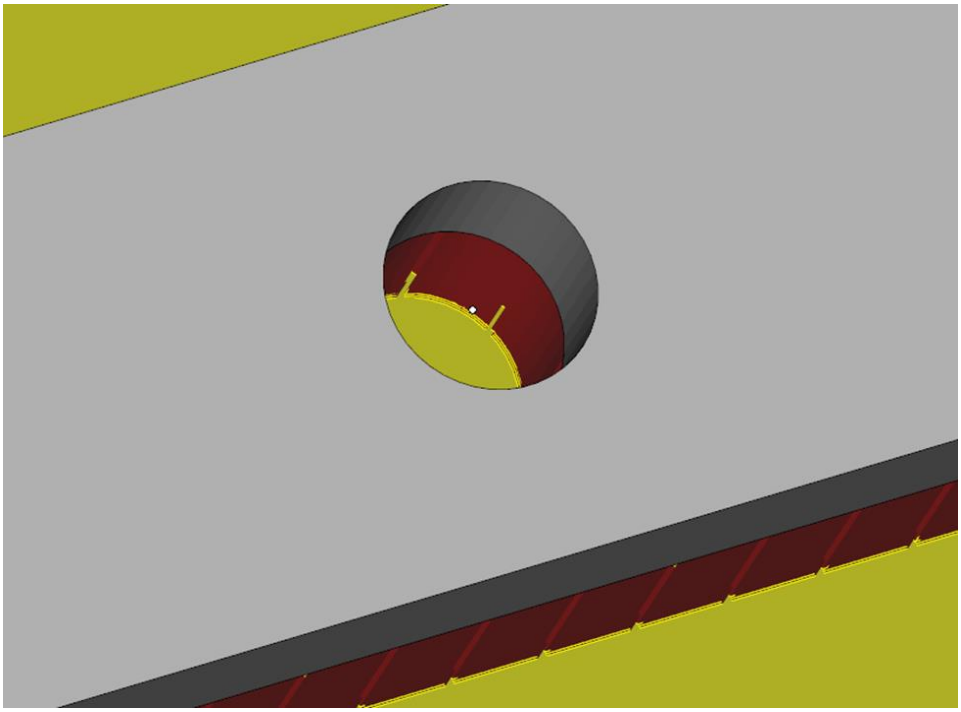

Figure 3-3: Flat test specimen with stress concentration and support structure

stresses. When this layer curls, the next layer is scanned at this raised position, and thus causing a change to the desired shape. As a result of this, the stress concentration more resembled a tear drop shape rather than a circular hole. An example of this may be seen in Figure 3-5.

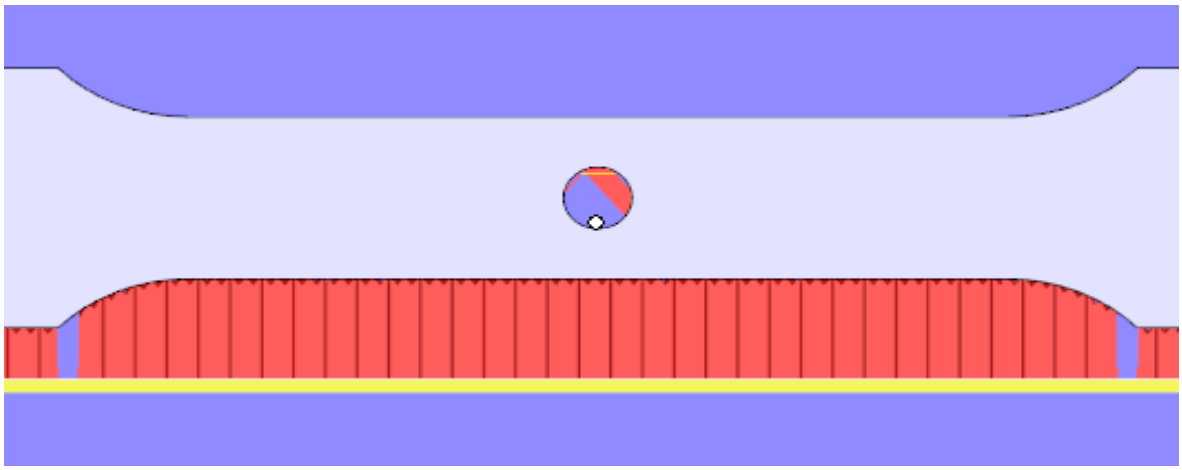

Figure 3-4: Edge oriented test specimen showing supported stress concentration

Once the specimens and their respective support structure was generated, the parts were moved to EOSPRINT, where the layout of the build plate was designed. In EOSPRINT it is possible to visually position the desired parts within the build volume. This is done to be sure the parts fit but also to optimally position the parts for processing. The need for positioning of the parts depends on the part geometry, as well as preventing possibilities of failure during the build.

Figure 3-5: Edge oriented test specimen build without stress concentration supports

When creating the build plate for these testing specimens care was taken to avoid possible issues with part positioning. Some of these being staggering the parts with relation to the recoating blade seen in Figure 3-6. There could be a greater chance of the blade catching the edge of the parts if they were all aligned square with the blade. Another part positioning which was taken into consideration was the part angle with respect to the edges of the build plate. Parts were rotated to angles around 10°. This was again done to avoid having square contact with the recoating blade. These precautions were again taken as there is a possibility the recoater blade will catch on edges flat with the blade. Both of these position adjustments can be seen in Figure 3-6. Once the support structures have been generated, and the layout of the build plate has been created, the file is then transferred to the M290. Within the transfer process the build is broken down into layers and sent to the machine in this format.

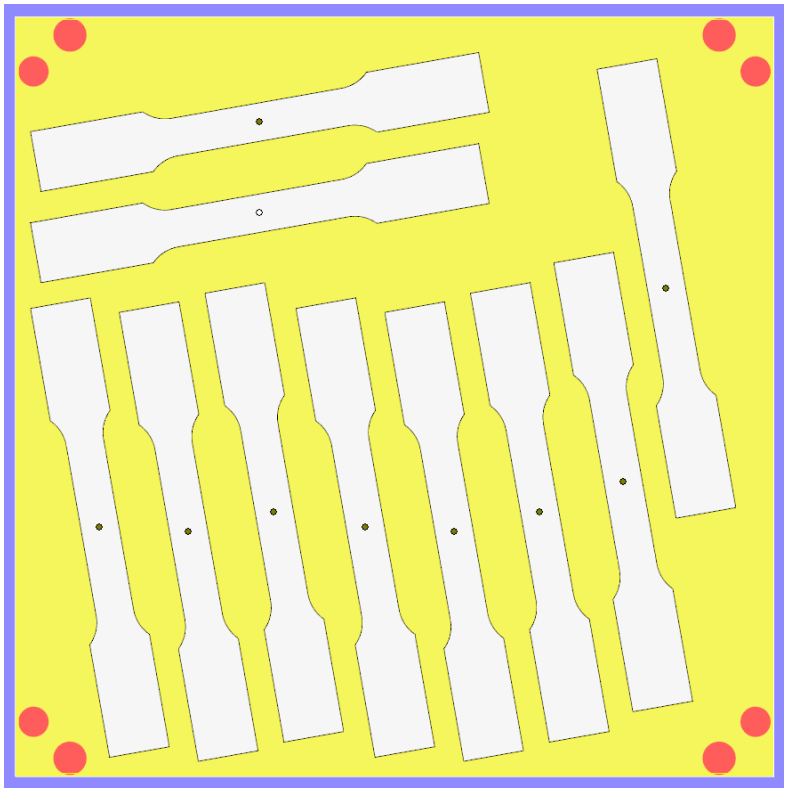

Figure 3-6: Build Plat Layout

Machine preparation

Once the code was transferred to the machine, the machine itself need to be prepared for operation. There are a set of steps that must be taken before a build may be started. The first step is loading the build plate into the machine, once seated in place the build plate is heated to a required temperature. The M290 requires the build plate be at 80°C before the build may be started. Once the plate reaches the required temperature the bolts are put in place and tightened, keeping the plate in place during the building process. Now that the plate is in place, the first layer must be made. This is done by first leveling the plate in both the X and Y directions with respect to the recoater blade. This is done by sliding spacer gages between the recoater blade and the build plate. It is first done with the recoater blade in the left half of the build plate, adjusting the plate to be level for the front and back halves of the plate. The recoater blade is then moved to the right half of the plate and adjusted so that the left and right halves of the build plate are level. This leveling is then checked by manually placing the first layer, by moving the recoater blade across the build plate while spreading a layer of the powdered metal to be sure the resulting layer is evenly spread. This layer does not have to be an exact thickness, as it is being created by hand, but is usually between 20-40µm thick.

After a layer of acceptable thickness has been made, and the plate is confirmed to be level with the recoater blade, the rest of the machine preparation must be made. Once the build volume door has been completely closed, the build volume's atmospheric requirements must be met. These are steps that are done at the same time. Both the build volume and the machines filtration system must be purged by an argon or nitrogen atmosphere to reach a certain oxygen percentage. An argon atmosphere is needed to use the 316L stainless steel material. The required oxygen percentage in the build volume and filtration system are 0.1% and 1.0% respectively.

Once this step is complete, the machine has been fully prepared for operation. The loaded build plate code is started and the machine builds the parts. The actual building of the parts varies depending mostly upon the geometries being created, ranging anywhere from 8 hours to 120 hours for particularly large builds. It is a rule of thumb that the taller the part the longer the build will be, but it can be presumed that the more volume required to create, the longer the build will take to complete.

Preparation of Printed Pieces

After the machine has finished scanning the final layer of the build and has finished, the parts must be removed from the build volume. As the machine scans each layer of the part, and lays a new layer of powder, the entire build plate area is covered. This continues through the entire process, and as a result the parts are encased in the excess powdered metal, seen in Figure 3-7. This powder must then be transferred and sieved to be used again. Once the entirety of the powder has been removed and the parts have been vacuumed of powder, the bolts are removed and the plate can be taken out. When the build plate exits the building chamber, the part is fully manufactured, though there are still several steps needed before the part is usable. To begin the post processing, the parts must first be removed from the build plate. This can be accomplished many ways, a wire EDM can be used for this instance, though in this case a horizontal band saw will be used. Another reason that support structure is used in most manufactured parts is to assist in the removal of the part. This support structure not only creates the teeth geometry for easier removal, but also gives material between the build plate and the part itself for a cutting device. Because of this, neither the part nor the build plate are damaged during the part removal. For the

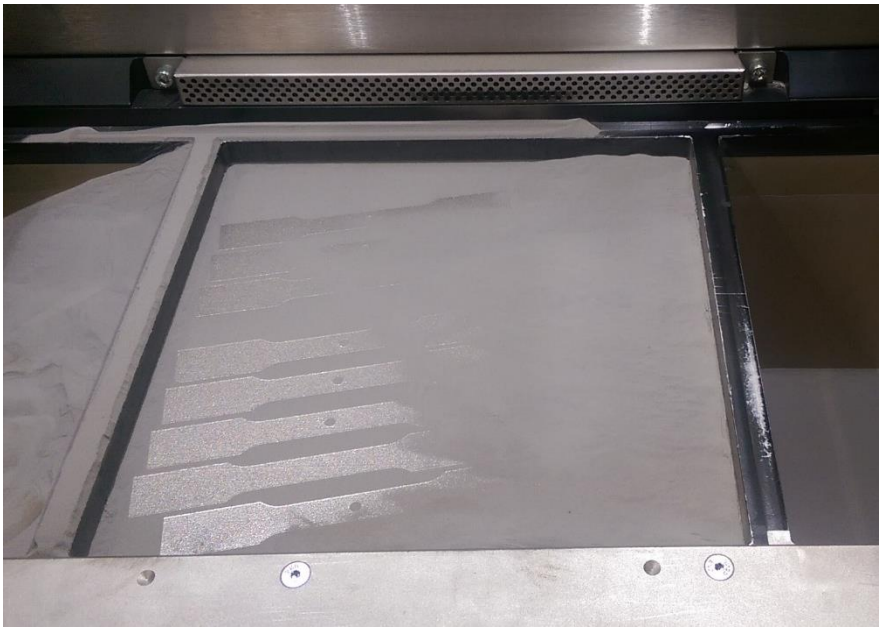

Figure 3-7: Finished SLM parts encased in excess powdered metal

parts used here a band saw is used to remove the parts from the plate. Care must be taken here as to not damage the plate with the blade, but the blade needs to be close enough to the plate as to not cut into any parts but rather only the support structure. After being removed from the plate each part must have the support structure removed.

This part of post processing can change methods based on the geometry and where the supports are being removed. There are a variety of methods used for removing support structure, such as a CNC mill or lathe, grinding/sanding station, or removal by hand. Because the nature of the process of SLM is based on increased temperature of the material, raising the temperature during post processing was avoided where possible during this experimentation. This meant that any tooling was circumvented and a simpler process was used. Each of the individual specimens had their support structure removed by hand, using a hammer and chisel. This was made easier due to the teeth of the support structure at the base of the specimen. These teeth may be seen in Figure 3-8, where the bottom "dashed" area is the support structure. The chisel was aligned with the teeth of the support structure when struck by the hammer. As the teeth and support structure

Figure 3-8: Support Material Tooth Structure

was hatched and not a fully dense part, it gave way easier than the part itself would have, allowing the chisel to follow the edge of the part only removing the support structure. This allowed for easy separation from the part. Because of the method used to remove support structure, the specimens were left with a rough surface finish where the support structure was removed. These surfaces were filed, using a metal file, to remove the roughness which could have possibly been remaining tooth and support structure. This method was used for each geometry to remove the support structure spanning from the part to the build plate. As shown in Figure 3-4, the edge oriented SLM specimen containing the circular stress concentration required gusset support structure to properly form the circular shape. This support structure was also removed though a different approach was used. Instead of using a tool to cut out the support material, a small circular metal file was used to remove the support material. As gusset supports are made up of a fin like geometry there was not much material to remove. The holes were filed out until the correct corresponding size was achieved. After the removal of support structure the parts were able to be tested.

Along with the SLM manufactured specimens, traditionally manufactured parts were also tested. In this case, the specimens were created from milling of 316L stainless steel stock. The specimens were purchased and manufactured from Laboratory Testing Inc. These purchased specimens were machined to the same size as the SLM manufactured pieces, again dictated by the ASTM E8 standard. As parts were manufactured using SLM which contained circular stress concentrations, a number of milled specimens also required the stress concentration to be created. This was accomplished after receiving the parts by drilling a hole by way of a CNC machine. A CNC code was created so the position of the hole was repeatable with use of a fixture to hold the test specimens. This fixture, seen in Figure 3-9, was also created using CNC code. The fixture has an inset area which is large enough for a test specimen to be seated in. The machined area, meant to hold the test specimen, was designed so that the gage length of the part could be held in a position and one end of the part was fixed flush, thus keeping the center of the gage length in a repeatable position during the CNC drilling. Two other smaller parts were machined, and with the use of four bolts, were used to keep the test specimen flat within the machining fixture. Using this fixture allowed for each purchased specimen to be held and machined in repeatable locations on the center of the gage length. For the drilling, process a 3/16” drill bit, made for use in stainless steel, was used.

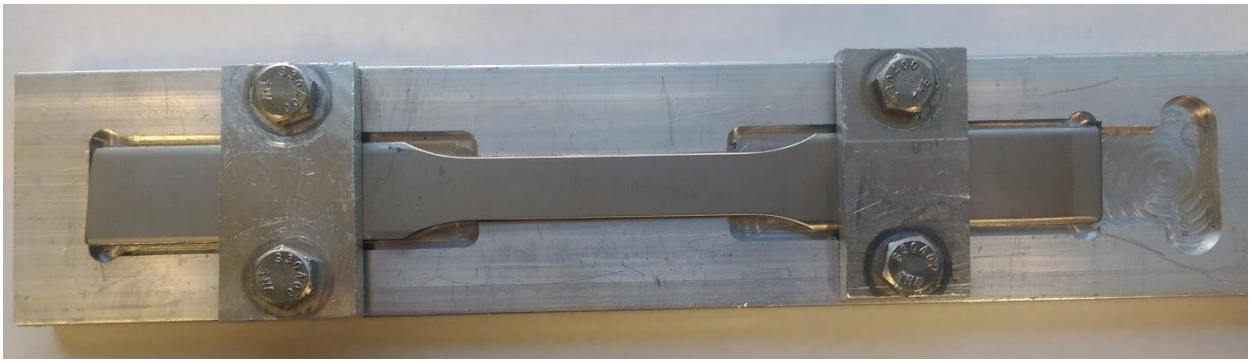

Figure 3-9: Fixture for repeatability of drilling in specimens

Experimental Procedures

Tensile Testing

Before the specimens were tensile tested, the exact dimensions of the cross-section were measured. This was done by micrometers and recorded prior to testing. The measurements also included the diameter of the holes for both the SLM and traditionally manufactured specimens. The testing set-up followed the ASTM E8 standard for metal tensile testing, and used an Instron Testing Machine® (hereafter referred to as Instron), housed at Western Carolina University. The testing set-up can be seen in Figure 3-10, which includes two vertically aligned pneumatic clamps which fixture the specimen in place for testing. Connected to the body of the test specimen is the extensometer, which is used by the Instron machine for accurate extension measurements during testing. When testing specimens containing the circular stress concentrations, the contact points of the extensometer were placed above and below the hole. The Instron testing machine works by having one stationary clamp, the bottom in this case, and one moving clamp, the upper, also known as the crosshead. This allows the machine to control the movement and speed by moving only one clamp. The testing is performed by having the upper clamp move at the speed dictated in the testing method. All tests were performed using the same crosshead speed of 10mm/min. Per ASTM Standard E8 the machine was exercised or warmed up before testing following a prolonged period of machine inactivity, this is done to minimize errors that may result from transient conditions within the machine. When placing the specimen into the clamps it is necessary to keep the specimen vertical and parallel with the testing direction as to give more accurate results. Loading the specimen into the clamps is done one clamp at a time, beginning with the bottom clamp. This is done because it is the top clamp that is allowed to move and this movement is necessary in the loading of the specimens. The

Figure 3-10: Instron Part Test Set-up

nature of the clamps, is to close moving towards the opposite clamp, because of this precautions were taken during the closing of the crosshead clamp. It is during the closing of the upper clamp that the position of the clamp should be manually adjusted to reduce the amount of compressive force on the specimen. This is done in accordance with ASTM Standard E8 which requires momentary (dynamic) forces due to gripping to not exceed 20% of the material's nominal yield strength and that static preloads not exceed 10% of the material's nominal yield strength. After a specimen has been successfully loaded and before the test begins, the gage length of the clamps is reset, though the preload is remains, as described by ASTM E8. The testing method built using Bluehill included two events during testing. One signaled for the removal of the extensometer, which was activated by a decrease of 5% from maximum strain on the specimen. The test was paused at this event and was manually resumed after removing the extensometer, to prevent the extensometer from being on the part during failure. The final event was at the failure of the specimen and was dictated by the strain dropping 60% from the maximum. The test method in

Bluehill was organized so that at the end of a test the program produced an excel spreadsheet containing all the information gathered from the test. This information included the following: time (s), strain (mm/mm), tensile stress (MPa), extension (mm), and load (N). The extensometer was used during testing to collect accurate extension data, which was used to calculate the strain produced in the Excel sheet. These spreadsheets allow the collected data to analyzed and compared.

CHAPTER FOUR: RESULTS

After the completion of testing, the excel files created by BlueHill were exported to begin analysis of the data. The Microsoft Excel® (hereafter referred to as Excel) sheet produced from the software included data and values collected during the testing. This collected data comprised of the following: time (s), tensile strain (MPa), extension (mm), and load (N). This data was then used to determine the following values: calculated yield strength (MPa), extensometer yield strength (MPa), UTS (MPa), and extensometer Young's modulus (GPa).

As the Instron provided data recorded from the machine at intervals of time, the calculated values were found using intervals matching those of time. Doing this step produced data for each of the intervals for each of the calculated values. This data could then be further used to display the results. When evaluating tensile testing, the mechanical properties can be found by analyzing the stress-strain curve of the part. The stress-strain curve displays the amount of stress within the part during testing, where stress (σ) is in the y-axis, and strain (ε) is along the x-axis. An example of a stress-strain diagram using the data from Purchased Solid Part 1-1 can be seen in Figure 4-1. From this diagram, and the associated data, it is possible to extract the wanted mechanical properties. Also seen on the stress-strain diagram, running parallel to the first portion of the diagram is a 0.2% offset of the Young's Modulus of Elasticity. For this research there are two types stress-strain graphs produced, one using the calculated strain, while the other uses the actual strain given by the extensometer. Both graphs contain similar shapes and produce the same types of mechanical properties.

The mechanical properties were found for each tested specimen, and the means were determined for each of the mechanical properties, as well as dimensional measurements of the

parts. These collected means of mechanical properties are displayed by each category of parts (e.g. SLM Edge Hole, Purchased Solid, etc.) and is shown in Table 4-1. The raw data displaying these values for each part that was tested may be found in Appendix A.

The data was then used to produce boxplots to visually show a comparison of the part groups when looking at each mechanical property. An example of the boxplots can be found in Figure 4-2. This boxplot displays the results for the calculated yield strength of each part type. A boxplot was created for each of the mechanical properties and each of these, as well as the data the plots use, may be found in APPENDIX E.

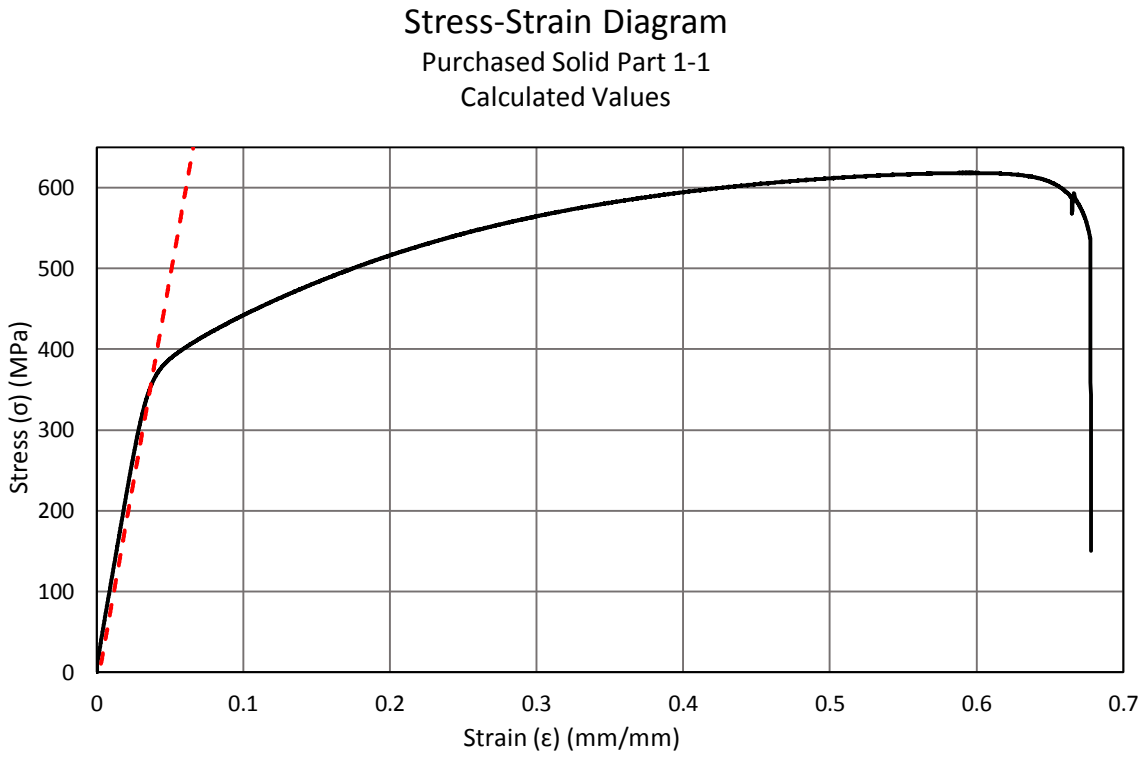

Figure 4-1: Example of Stress-Strain Diagram using data from Purchased Solid Part 1-1

Table 4-1: Collected Means of mechanical properties of specimen groups

	Collected Means							
	Thickness	Width	Hole Dia.	Area	Calculated Yield Strength	Ext. Yield Strength	UTS	Ext. Young's Modulus
	mm	mm	mm	mm^2	MPa	MPa	MPa	GPa
SLM Edge Solid	3.29	12.77		42.06	472		576	177
SLM Edge With Hole	3.29	12.70	4.75	26.17	379		615	238
SLM Flat Solid	3.37	12.56		42.35	473	463	567	178
SLM Flat With Hole	3.29	12.54	4.67	25.90	553	509	629	256
Purchased Solid	2.98	12.84		38.27	357	350	618	212
Purchased With Hole	2.98	12.83	4.75	24.13	429	395	666	242

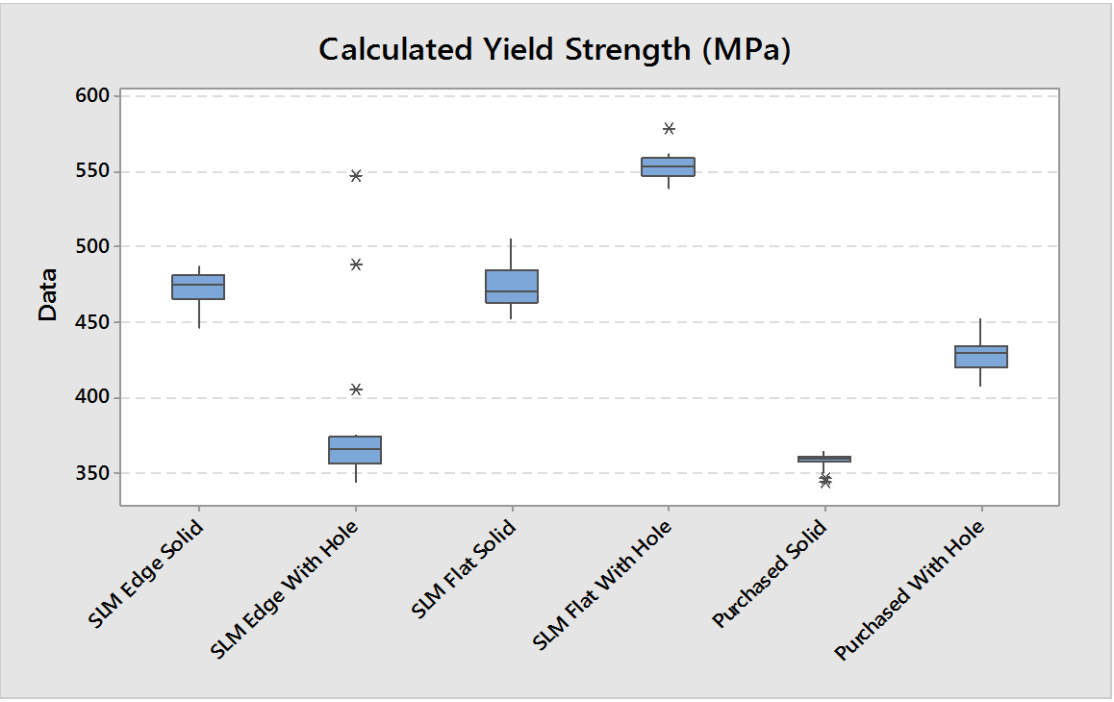

Figure 4-2: Boxplot of Calculated Yield Strength

Using the collected part data, six comparisons were made between part categories as follows:

- SLM Edge Solid vs. SLM Flat Solid
- SLM Edge Solid vs. Purchased Solid
- SLM Flat Solid vs. Purchased Solid
- SLM Edge with Hole vs. SLM Flat with Hole
- SLM Edge with Hole vs. Purchased with Hole
- SLM Flat with Hole vs. Purchased with Hole

For these comparisons, it was needed to know if the two methods had equal or unequal variances between them, thus the f-tests were completed to determine equal or unequal variances. An f-test was done for each comparison for each mechanical property, each of which is displayed in APPENDIX B. Summary tables showing the results of the f-tests may also be seen in Table 4-2.

Table 4-2: F-Test Summary Results Table

	F-Test Summary Results Table			
	Calculated Yield Strength	Extensometer Young's Modulus	UTS	Extensometer Yield Strength
SLM Edge Solid vs. SLM Flat Solid	Equal Variance	Unequal Variance	Equal Variance	
SLM Edge Solid vs. Purchased Solid	Unequal Variance	Equal Variance	Unequal Variance	
SLM Flat Solid vs. Purchased Solid	Unequal Variance	Equal Variance	Unequal Variance	Unequal Variance
SLM Edge Hole vs. SLM Flat Hole	Unequal Variance	Equal Variance	Unequal Variance	
SLM Edge Hole vs. Purchased Hole	Unequal Variance	Equal Variance	Unequal Variance	
SLM Flat Hole vs. Purchased Hole	Equal Variance	Unequal Variance	Equal Variance	Equal Variance

Now knowing if each comparison contained equal or unequal variances, t-tests of the data comparisons could be conducted, assuming either equal or unequal variance for the t-test. A t-test was done for each comparison of parts for each mechanical property. Each individual test results may be seen in APPENDIX C. A summary table showing the t-test results can be found in Table 4-3.

Table 4-3: T-Test Results Summary Table

	T-Test for Statistical Significance Summary Table			
	Calculated Yield Strength	Extensometer Young's Modulus	UTS	Extensometer Yield Strength
SLM Edge Solid vs. SLM Flat Solid	$\mu1 = \mu2$	$\mu1 = \mu2$	$\mu1 \neq \mu2$	
SLM Edge Solid vs. Purchased Solid	$\mu1 \neq \mu2$	$\mu1 = \mu2$	$\mu1 \neq \mu2$	
SLM Flat Solid vs. Purchased Solid	$\mu1 \neq \mu2$	$\mu1 = \mu2$	$\mu1 \neq \mu2$	$\mu1 \neq \mu2$
SLM Edge Hole vs. SLM Flat Hole	$\mu1 \neq \mu2$	$\mu1 = \mu2$	$\mu1 \neq \mu2$	
SLM Edge Hole vs. Purchased Hole	$\mu1 \neq \mu2$	$\mu1 = \mu2$	$\mu1 \neq \mu2$	
SLM Flat Hole vs. Purchased Hole	$\mu1 \neq \mu2$	$\mu1 = \mu2$	$\mu1 \neq \mu2$	$\mu1 \neq \mu2$

After completion of the t-tests the comparison of SLM flat parts and purchased parts were investigated further, this included narrowing the focus to the extensometer based Yield Strength comparison of the parts. The reasoning for this decision is discussed in Chapter 5. The further analysis of these comparisons used both Excel and Minitab capabilities.

Prior to testing the data, it was necessary to know if each group of data contained a normal distribution, and so a normal probability plot was produced for both SLM flat parts and purchased parts for extensometer yield strength, using Minitab. An example normal probability

plot can be seen in Figure 4-3. The normal probability plots for all data may be seen in APPENDIX F.

In Matlab, four columns were made for each part category, SLM flat and purchased parts, with and without circular stress concentration. The extensometer yield strength data for each category was then placed in each corresponding column. These four columns were then reduced to two columns, by placing the data in one column, labeled MPa, and the part categories of those data were placed in the adjacent column allowing each data point to be labeled by its category. Though reduced to two columns, the different part categories remained grouped together. A general linear model (GLM) was then ran on the data in the two columns. The residual plots produced from the GLM can be seen in Figure 4-4, while the text output, containing the analysis of variance, can be found in APPENDIX G.

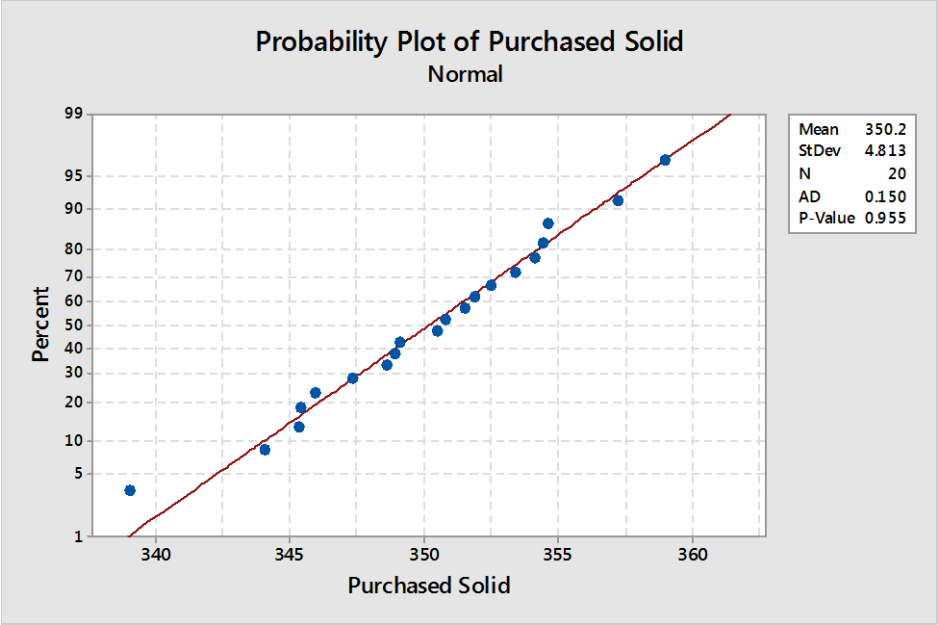

Figure 4-3: Normal Probability Plot of Extensometer Yield Strength for Purchased Solid Parts

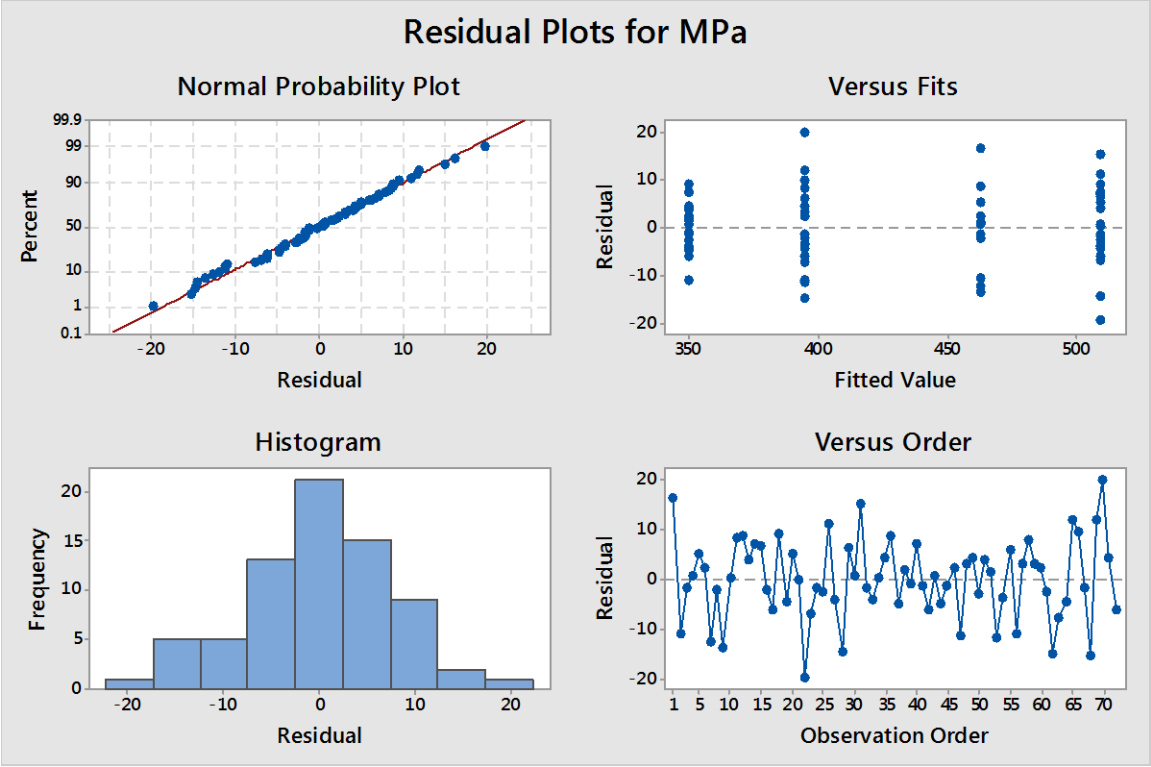

Figure 4-4: Residual Plots created by the GLM in Minitab

The extensometer yield strength data of the four part categories was then used to perform a One Way ANOVA in Minitab. The ANOVA was ran assuming unequal variance, as the results from the GLM show. This ANOVA produced a variety of plots including boxplot of MPa, individual value plot of MPa vs. Categories, and interval plot of MPa vs. Categories. Each of these plots can be found in APPENDIX G. After completing the ANOVA, a post hoc analysis was done using a Games-Howell post-hoc analysis. The Games-Howell test is ran when assuming unequal variance in the means of the groups. The test was ran on the data within the four categories using Minitab, and resulted in a plot of each comparison made between the groups. The results from the Games-Howell test may be found in Figure 4-5. Where each interval represents the comparisons made in the test. As stated by Minitab, if an interval does not contain zero, the corresponding means are significantly different.

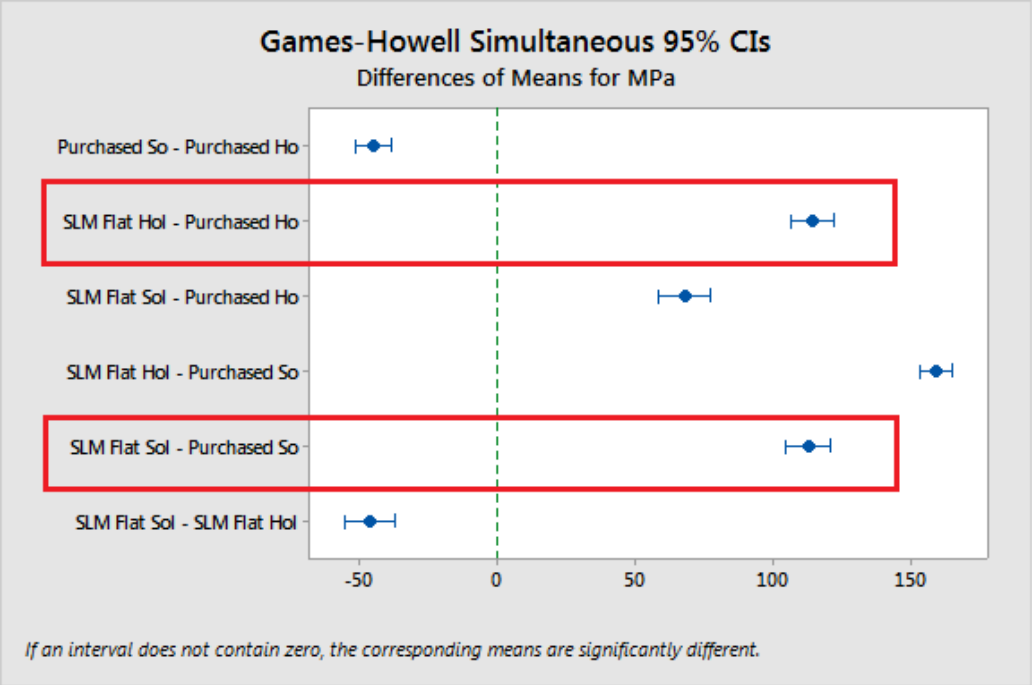

Figure 4-5: Games-Howell Test Results Chart

Once the analyses were completed using Minitab, the data was transferred, kept in the four columns, to Excel. The method used here looks at the differences of differences of the part categories, such that the change in extensometer yield strength from SLM Flat Solid to SLM Flat with Hole is compared with the change of extensometer yield strength between Purchased Solid and Purchased with Hole. The data was sorted, within each column, in descending order as seen in Table 4-4. This table shows that SLM flat solid contains less data than the other categories, this lack of data was a result of testing complications when using the extensometer. The differences between SLM Flat Solid and SLM Flat with Hole, as well as Purchased Solid and Purchased with Hole were calculated and placed into two columns, labeled Δ SLM Flat, Δ Purchased respectively, are also shown in Table 4-4. Using these two columns an f-test was used to test the variances of the two groups, which was followed by a t-test on the two columns of differences. The t-test assumed equal or unequal variance, based on the result of the f-test. These two tests may be seen in Table 4-5, and Table 4-6.

The four columns of extensometer yield strength data was then used in a Monte Carlo Method. This method found the means and standard deviation for each part category, shown in Table 4-7, then using those values to manufacture data using Excel. The differences were found, similarly as before between the solid and with hole variations of each part type, in two separate columns. An f-test was done on these two columns, the resulting equal or unequal variance then used to perform a t-test of the data. The results of the f-test and t-test may be found in Table 4-8 and Table 4-9 respectively.

Table 4-4: Ordered Extensometer Yield Strength Data and Calculated Part Difference

Extensometer Yield Strength Data				Calculated Part Difference	
SLM Flat Solid (MPa)	SLM Flat Hole (MPa)	Purchased Solid (MPa)	Purchased Hole (MPa)	Δ SLM Flat (MPa)	Δ Purchased (MPa)
479	524	359	415	45	56
471	520	357	407	49	50
471	518	355	407	47	52
468	516	354	405	48	50
465	516	354	403	51	49
464	515	353	401	52	48
463	514	352	399	51	47
461	513	352	398	52	46
461	510	352	398	49	47
452	509	351	397	57	46
450	508	351	393	57	43
449	507	349	393	58	43
	507	349	391		42
	506	349	390		42
	505	347	389		41
	505	346	387		41
	503	345	384		38
	502	345	383		38
	495	344	380		36
	489	339	380		41

Table 4-5: f-Test Comparing Calculated Part Differences

F-Test Two-Sample for Variances

	Δ SLM Flat	*Δ Purchased*
Mean	51.24634133	44.77050541
Variance	17.87281294	25.60406063
Observations	12	20
df	11	19
F	0.698046032	
P(F<=f) one-tail	0.274391269	
F Critical one-tail	0.376211386	

Table 4-6: t-Test Comparing Calculated Part Differences

t-Test: Two-Sample Assuming Equal Variances

	Δ SLM Flat	*Δ Purchased*
Mean	51.24634	44.77051
Variance	17.87281	25.60406
Observations	12	20
Pooled Variance	22.76927	
Hypothesized Mean Difference	0	
df	30	
t Stat	3.716652	
P(T<=t) one-tail	0.000413	
t Critical one-tail	1.697261	
P(T<=t) two-tail	0.000827	
t Critical two-tail	2.042272	

Table 4-7: Mean and Standard Deviation used for Monte Carlo Method

	SLM Flat Solid	SLM Flat Hole	Purchased Solid	Purchased Hole
Mean	462.9440	509.1334	350.2080	394.9785
Standard Deviation	9.0774	8.3895	4.8133	9.6141

Table 4-8: f-Test Comparing Part Differences using Monte Carlo Method

F-Test Two-Sample for Variances - Ext Yield Strength		
	ΔSLM Flat	Δ Purchased
Mean	46.108	45.185
Variance	152.405	116.965
Observations	10000.000	10000.000
df	9999.000	9999.000
F	1.303	
alpha	0.050	
p-value	0.000	
f-crit	1.040	
Significant Difference	yes	
Variance of parts	Unequal	

Table 4-9: t-Test Comparing Part Differences using Monte Carlo Method

t-Test: Two-Sample Assuming Unequal Variances		
	ΔSLM Flat	*Δ Purchased*
Mean	46.10794592	45.18469101
Variance	152.4050532	116.9653616
Observations	10000	10000
Hypothesized Mean Difference	0	
df	19658	
t Stat	5.625312819	
P(T<=t) one-tail	9.38459E-09	
t Critical one-tail	1.644931145	
P(T<=t) two-tail	1.87692E-08	
t Critical two-tail	1.960084669	

CHAPTER FIVE: ANALYSIS AND CONCLUSIONS

Analysis of Findings for Tensile Testing Comparison Experiment

Expected Results

There are many different results that were found during this research, most arising from the comparison of part categories for various mechanical properties. Before performing the testing, expected results of the tests were formed. The expected results of the tests performed on the results data can be expressed by the comparison of each part category within a mechanical property.

When looking at the Young's modulus of materials, it is understood that this mechanical property is a measurement of how the material reacts to tensile testing, when still in the elastic region of testing. Because this value is based on the material itself and not the geometry of the parts being tested, all measured results should be similar. For this research, the expected results for Young's modulus was that each manufacturing method, as well as each geometry, will result in a statistically similar results.

The other mechanical properties; calculated yield strength, UTS, and extensometer yield strength; do involve the cross-sectional area of the parts in their calculation. Because of this the expected results of these mechanical properties may be condensed into part categories with a stress concentration and without the stress concentration. For the parts without the stress concentration, or solid parts, all three mechanical properties here will have the same expected result. For calculated yield strength, the expected result is that SLM flat solid, SLM edge solid, and Purchased solid will result in statistically similar values. The expected results of calculated yield strength for SLM flat with hole, SLM edge with hole, and Purchased with hole, are that the

values are statistically similar. As the parts with the stress concentration are similar and the parts without the concentration are similar, it should be known that the parts with and without stress concentration are expected to be statistically different from one another. As states before, the three mechanical properties; calculated yield strength, UTS, and extensometer yield strength; have the same expected results for the t-tests, testing for statistically significant difference.

The last of the expected results is from the comparison of the differences of part categories, where the difference was found for both; SLM flat solid, SLM flat hole, and Purchased Solid, and Purchased hole; and then those differences were compared to one another using a t-Test. The expected result here was that the differences would be statistically significantly different. And that the SLM flat parts would show a larger improvement in extensometer yield strength, when creating parts with a stress concentration, than the Purchased parts.

Stress-Strain Graph

As stated before, the stress-strain diagram shows the amount of stress within the part during testing. In both sets of graphs produced, the stress remains constant, as it is calculated by force divided by cross-sectional area for both. Though in the first set of graphs created, the strain is calculated. The calculation for strain is shown in Eq. 1.2. This calculation included data produced by the Instron machine measuring the extension of the grips. This is not entirely accurate for the extension of the gauge length since it also includes the interactions of the grips to the part. During testing it is possible that the part slips while in the grips, or that the part within the grips has a significant extension, outside of the gage length. These are variables that can affect the measurement of Δl within the machine. This means that the calculated strain, while still able to be used for comparisons, is not the most accurate strain that can be obtained. The

calculated strain will be used in the preliminary stages of the data analysis, where the strain collected by the extensometer will be used throughout the entire analysis.

The stress-strain diagrams were created using excel for both plotting the data as well as calculating the data used. The first step taken was to import the necessary data from the file BlueHill created into a new excel sheet. This data was the time, extension, and load collected during the testing. Next the measurements of the parts, taken prior to testing, were used to find the cross-sectional area of each part. This is data which is needed to begin calculating what is needed for the stress-strain diagram.

Once the data was transferred into an Excel sheet, the first calculated column was produced, which was the strain. In Excel, in the top cell of a column labeled strain, an equation 1.2 was applied, using the gage length and extension. This equation was applied to the entire column, relative to the amount of extension data. After calculating the strain data, the stress column was formed. This column used equation 1.1, using both the load and cross-sectional area to calculate stress. Once both the stress and strain columns have been calculated, the stress – strain diagram of the part may be created. Using the chart tools in Excel, an X Y scatter plot was chosen, using strain in the X axis and stress in the Y.

Mechanical Properties Determined from Stress-Strain Graph

After completing the stress-strain graph and calculations it requires, it is possible to begin finding the mechanical properties. The first property found from this graph, was the Young's modulus. The Young's modulus is calculated by finding the slope of the graph in beginning of the elastic region of the part. This was done using the slope command in Excel, and in doing so produced the value used for Young's modulus.

Following the calculation of the Young's modulus of a part, the yield strength is found. This is done by creating a new column for a second calculated stress. In this column an equation was formed which would create a linear equation using the known slope of the Young's modulus of the part, and the known stress, to create a line, parallel to the Young's modulus, but offset in the positive X axis by 0.2%. In doing so, a line is created on the stress-strain graph which runs parallel in the elastic region, but intersects with the stress-strain curve. This intersection point is known as the yield strength of the part. The stress at the intersection is calculated, and that value is used as the yield strength of that part. As stated prior there are two types of graphs created in this research, one with calculated strain and another with measured strain, thus two types of yield strength are found. When using the calculated strain, these calculations will produce the calculated yield strength, and thus when using extensometer measured strain, extensometer yield strength is found.

The ultimate tensile strength (UTS) signifies the maximum amount of stress a part may withstand while being tensile tested. As such, this is found by locating the maximum amount strain found during testing. This was done in Excel by using the Maximum equation, which locates the maximum value of a given data selection, in this case being the stress of the parts.

Material Composition

The expected material composition of each production method, provided by the material producers, are shown in Table 2-1 and Table 2-2. These expected compositions contain a range for a majority of the elements found in the compositions. To measure the actual composition of the materials, an X-MET 5100 X-ray fluorescence (XRF) analyzer from Oxford Instruments was used. The XRF system utilizes x-rays, and their measureable reaction to materials to identify which, and how much of each elements are currently in the specimen. This XRF device was used

on both SLM produced and purchased parts. The results from this device may be seen in Table 5-1 and Table 5-2. As can be seen in these two tables, there is variation in the amounts of some of the elements between the two compositions, notably the amount of Iron (Fe), and Chromium (Cr). A large variation in these elements could have an effect the strength or behavior of parts.

Table 5-1: Measured Material Composition of EOS 316L Stainless Steel

Measured Material Composition of Parts			
	EOS Stainless Steel 316L		
Material Composition	Element	Conc.	Limit
	Fe	61.81%	-
	Cr	18.25%	18.00-20.00%
	Ni	14.42%	11.00-15.00%
	Mo	3.02%	3.00-4.00%
	Mn	1.27%	0.00-2.00%
	Cu	0.02%	0.00-0.35%
	S	0.00%	-
	Si	0.00%	0.00-1.00%
	Ti	0.03%	-
	V	0.00%	-
	Co	0.19%	-
	Nb	0.01%	-
	W	0.00%	-

Statistical Analysis of Results

Boxplots of Each Mechanical Property

The analysis of results will begin by discussing the boxplots of each mechanical property. Then leading into the f-Test and t-Tests ran comparing part types within each mechanical property. This section will conclude with the in depth investigation of the comparison of SLM flat parts and Purchased parts, within the area of extensometer yield strength.

Using Minitab boxplots were created where each contained the information of a single mechanical property, such as calculated yield strength, UTS, etc. Each mechanical property

boxplot contained all applicable data of each part category. As stated these boxplots can be found in APPENDIX E.

The UTS boxplot, seen in APPENDIX E, shows the six part categories and displays their data along the same Y axis. First looking at the sizes of the box and whiskers describing the data, for the solid part categories the SLM flat solid and Purchased solid have smaller boxes, meaning the sample population are tightly grouped, while the SLM edge solid parts have a taller box showing that the results are further spread apart. Also important to note is the difference in box positions for the solid parts. The SLM edge solid and SLM flat solid boxes are in similar positions in the Y axis, while the Purchased solid box is comparatively higher. This signifies that the purchased solid parts have a higher UTS than both the SLM categories. Moving to the part categories with stress concentrations, the boxplot shows similar results to the solid parts. Again the SLM flat with hole and the Purchased with hole have similarly sized boxplots, while the

Table 5-2: Measured Material Composition of Purchased 316L Stainless Steel

Measured Chemical Properties of Parts			
	Purchased Stainless Steel 316L		
Material Composition	Element	Conc.	Limit
	Fe	67.38%	-
	Cr	16.78%	16.00-18.00%
	Ni	10.11%	10.00-14.00%
	Mo	1.97%	2.00-3.00%
	Mn	1.74%	0.00-2.00%
	Cu	0.42%	-
	S	0.00%	-
	Si	0.00%	0.00-1.00%
	Ti	0.00%	0.00-0.20%
	V	0.12%	-
	Co	0.65%	-
	Nb	0.02%	-
	W	0.00%	-

SLM edge with hole has a much taller box. This indicates that the UTS results for SLM edge with hole are spread out, much more than the SLM flat with hole, Purchased with hole, and even SLM edge solid. Here again it can be seen that the Purchased with hole box contains larger results than that of the SLM categories. When comparing the boxplots of the solid parts to those of the stress concentration parts, it is visible that all categories containing stress concentrations have greater spacing within their boxes. The cause of this increase in variability here is attributed to the stress concentration included in the parts, along with the SLM process and the actual drilling of the holes causing some variation, the major decrease in cross-sectional area is likely to play a large role.

The Young's modulus boxplots for the various part categories can be seen in APPENDIX E. Here the solid part categories appear to show similarities between one another, though there are some significant differences between each. Looking at the box and whisker plot for SLM edge solid, the box and whiskers for this part type are small and indicate a tight grouping of the results. But this does include one outlier above its upper limit. SLM flat solid on the other hand has no outliers, but does have a box which is skewed below the median of the parts. While the Purchased solid has both a skew from the median as well as outliers. The skew is above the median and is quite significant when compared to SLM edge solid. Also apparent here are three large outliers outside the upper limit of the whiskers. As this mechanical property was reliant upon the extensometer, it is possible that the outliers were caused by a slipping of the extensometer during testing while in the elastic region. The category of parts with stress concentrations show a much uniform display of the Young's modulus of the parts. It can been seen that the medians of SLM edge with hole, SLM flat with hole, and Purchased with hole all appear to be close to one another, as well as the boxes do not signify any large skew of the data.

Also worth noting is the lack of outliers in these part categories. When looking at the Young's modulus boxplot overall it is apparent that all the results are closely related, especially when looking at parts with and without a stress concentration. This agrees with the notion that the Young's modulus should be similar across all parts, as it is related to the material and not necessarily the geometry.

Looking at the calculated yield strength boxplots, shown in APPENDIX E, it can be see how the different part categories compare. When comparing the part categories with and without the stress concentration, it is obvious that a difference should be apparent. In the case of SLM flat and Purchased parts it is seen that there is an increase in the calculated yield strength when going from solid parts to those with stress concentrations. This is because the stress calculations for the parts with the stress concentration include a smaller cross-sectional area and thus the stress will result in a higher value. This shows true for both the SLM flat and purchased parts, but in the case of SLM edge parts it is the opposite. As can be seen in this figure, the calculated yield strength, looking from SLM edge solid to SLM edge hole, decreases rather than increases. From this it can be inferred that the SLM edge hole is not a suitable comparison to the other part categories when including a stress concentration.

Comparison F-Tests and T-Tests

This section discusses the comparisons formed between the part categories and the techniques used for said comparisons. Forming these comparisons included limiting them to comparing with a like category in terms of having a stress concentration, so only solid parts are compared to other solid parts and the same for parts with stress concentrations. For the comparisons, the data was assumed to have a normal distribution. The comparison testing included both f-tests and t-tests.

The comparisons began with f-tests, in order to determine equal or unequal variance between the categories, which is then used in running t-tests of the comparisons. All f-tests may be found in APPENDIX B, while a summary table can be seen in Table 4-2. The f-tests used were two-tailed tests. When performing f-tests, a null hypothesis (H_0) and alternate hypothesis (H_a) are made and used to state the result of the test. In the case of this research the null and alternate hypothesis are as follows:

$$H_0: \sigma_1^2 = \sigma_2^2$$

$$H_a: \sigma_1^2 \neq \sigma_2^2$$

Where H_0 is a stated assumption that there is no difference in the variances of the two groups, and H_a states that there is a statistical difference between the variances. This null and alternate hypothesis were assumed for all f-testing done in this research. The results of the f-test were found and used in assuming equal or unequal variance in the t-tests of the same data.

The t-tests used the same comparisons found in the f-tests previously performed, and are two-tailed tests. As stated before, the t-tests assumed equal or unequal variance which was determined by the f-tests. The t-test was used to determine if the two sets of data are significantly different from one another. T-tests use a null and alternate hypothesis such as that used in the f-tests and is presented as follows:

$$H_0: \sigma_1^2 = \sigma_2^2$$

$$H_a: \sigma_1^2 \neq \sigma_2^2$$

Where H_0 is a stated assumption that there is no difference in the means of the two groups, and H_a states that there is a statistical difference between the means. This null and alternate hypothesis were assumed for all of the t-tests performed in this research.

First looking at the results of the hypothesis testing when making comparisons based on Young's modulus, it can be seen in Table 4-3, that each comparison made resulted in the two sets of data failing to reject the null hypothesis, and not being significantly different. This supports the expected results of this mechanical property. This implies that the two production methods used in the comparisons, result in the material having statistically similar Young's modulus.

The UTS results, found in Table 4-3, do not reflect the same outcome as for the Young's modulus. Instead here it can be seen that each comparison of UTS results in rejecting the null hypothesis and stating that all of the comparisons made are significantly different from one another. Looking at the specific means of these comparisons, it becomes evident that the purchased parts resulted in a higher UTS. In comparisons including both SLM flat and SLM edge, the results vary. For the solid parts SLM edge has a higher UTS, while the parts containing hole result with SLM flat parts having a higher UTS. But when looking at all comparisons containing purchased parts, the purchased parts have the higher mean of UTS. From this it is possible to state that Purchased parts, both with and without stress concentrations result in a significantly different and higher UTS mean.

The results from the calculated yield strength are similar to the UTS results though with one difference. In Table 4-3 the hypothesis testing results show that all but one comparison resulted in rejecting the null hypothesis. The SLM edge solid and SLM flat solid was the only comparison resulting in failing to reject the null hypothesis and thus deemed not significantly different. When looking at the specific means of the calculated yield strength within the comparisons which rejected the null hypothesis, there is again one part category which stands out when being compared. The SLM flat parts result in a higher calculated yield strength in the comparisons which reject the null hypothesis.

From looking at the performances of the part categories in the various mechanical properties it cannot directly be determined a part type which out performs the others. Though with these results it can be found that in terms of strength properties, SML edge parts performed poorly. A goal of this testing was to find which part production resulted in the best performance when including a stress concentration. This assessment is not based entirely on the t-tests performed, but also include the results of the boxplots of the data. When looking at the calculated yield strength boxplot, it is shown that the SLM edge parts containing stress concentrations resulted in lower values, when the values should have rose. It is with this knowledge that the SLM flat and purchased parts were selected for additional statistical analysis. This choice is supported by the work of A. Mertens, which states that from the point of view of strength, the best option is the building strategy using flat oriented test specimens (Mertens, et al., 2014).

Additional Statistical Analysis

The additional statistical analysis discussed in this section pursues the comparison of SLM flat and purchased parts, in regards to performance with and without stress concentrations. The analysis has also been narrowed to look at only the calculated yield strength of the parts. The additional analysis included the use of both Minitab and Excel, as well as use of the Monte Carlo method.

This analysis began by running each part type; SLM flat solid, SLM flat with hole, Purchased solid, Purchased with hole; through a normal probability plot to test the sample for normality. These plots may be seen in APPENDIX F. These plots were created in Minitab, by the use of a normality test, found under the graph tab. A probability plot allows for the normality of a set of data to be tested. The null hypothesis states that the data is normally distributed, whereas the alternate hypothesis states the data is not normally distributed. This hypothesis is

tested by using the P-value produced by the probability plot. As seen in the probability plots produced for our part categories, each P-value is above α of 0.05, stating that each collection of data is normally distributed.

Following the probability plots produced, other evaluations of the data were ran using Minitab. First a General Linear Model (GLM) was ran to determine the analysis of variance, which resulted in rejecting the null hypothesis and assuming unequal variance. Within the results of the GLM, found in APPENDIX G, there are some produced values worth noting. These values are located under the coefficients section of the results and are identified as Variance Inflation Factor (VIF), which measures how much the variance of the estimated regression coefficients are inflated as compared to when the predictor variables are not linearly related. Minitab suggests the following guidelines when interpreting the VIF:

VIF	Status of Predictors
VIF=1	Not correlated
1<VIF<5	Moderately correlated
VIF>5 to 10	Highly correlated

As seen in the results, when using Purchased solid results as the constant term, the resulting VIF for Purchased with hole, SLM flat solid, and SLM flat with hole, are 1.44, 1.33, and 1.44 respectively. These results state that the various part categories are moderately correlated. A One-Way ANOVA was then performed on the data to determine if the means of two groups differ within each comparison. Using the analysis of variance results from the GLM, the One-Way ANOVA was ran assuming unequal variance. When using an unequal variance assumption, the One-way ANOVA uses a Welch's Test (unequal variance T-Test) to determine statistically significant difference between groups. The results of the One-Way ANOVA, found in

APPENDIX G, show the Welch's Test to have a P-value less than $\alpha=0.05$, in which the null hypothesis is rejected, stating that the four part categories are statistically significantly different. When performing post-hoc analyses, the type of analysis should correspond with the assumed variance of the data. For example when it is assumed equal variance, the Tukey test may be used, though in this case the variance is assumed unequal. Because of this assumption the Games-Howell post-hoc analysis was used. As can be seen in Figure 4-5, the Games-Howell analysis results in group comparisons represented by intervals on the chart. As stated by Minitab, if an interval does not contain zero, the corresponding means are significantly different. This post-hoc test does include all data and makes all available comparisons, which in doing so created some comparisons which are not necessary. For this research the group comparisons which will be investigated here are as follows:

- SLM Flat with Hole vs. Purchased with Hole
- SLM Flat Solid vs. Purchased Solid

In the results chart of the test, these two comparisons are represented by two boxes. As can been seen from the results chart, neither comparison contained zero in its interval, thus both comparisons result in the means of extensometer yield strength being statistically significantly different.

The four part categories being further analyzed; SLM flat solid, SLM flat with hole, purchased solid, Purchased with hole; were then transferred to Excel, where other methods would be used to test for significant difference. The following testing methods were used to determine if a significant difference existed in the differences of each production method, caused by including a stress concentration. In others words, the comparison is being used to determine if a production method is able to handle stress concentrations better than the other.

Once the data was organized in each column, a sort function was used to order each column of data in descending order, as can be seen in Table 4-4. The data is not paired data and allows for it to be reordered without significant consequence. Using this ordered data, differences were calculated in adjacent columns, labeled ΔSLM Flat and ΔPurchased. The values of these columns were found by subtracting the results of solid parts from the results of stress concentration parts, for each production method. Once the differences were calculated in the respective columns, as shown in Table 4-4, an f-test and subsequent t-test were performed using the Excel data analysis tools. Table 4-5 shows the results of the f-test, where the P-value is greater than the alpha of $\alpha=0.05$, meaning it fails to reject the null hypothesis. This results in assuming equal variances of the comparison. This assumption was then used in performing the T-test, as seen in Table 4-6. The t-test shows a result in which the P-value is less than the alpha. This causes the null hypothesis to be rejected, meaning the two means of part differences are statistically significantly different. Even with a significant difference, when looking at the actual means of the differences, ΔSLM Flat=51.25 MPa and ΔPurchased=44.77, it can be seen while statistically the difference is significant, the means are still relatively close to one another. This does not change the significant difference, but should be included when discussing these results.

The final method included here involves the use of the Monte Carlo method. This method is used to allow for a comparison for small samples under realistic data conditions by producing simulated data with constrictions created by the actual data. In this case, the mean and standard deviation of each part category was taken, seen in Table 4-7. This data was then used in Excel's data analysis package, under random number generation, where the various requirements of the data was entered. This included number of random numbers desired, distribution type, and parameters based on the distribution type selected. For this method the number of random

numbers was set at 10,000. The type of distribution was selected as normal, based on the probability plots created earlier. The required parameters for this distribution type was the mean and standard deviation desired for the generated values. This number generation was used for each part type, each type using its own mean and standard deviation taken from the original data. After generating this new data, the differences of part types were once again calculated between; SLM flat solid and SLM flat with hole, purchased solid and Purchased with hole. After calculating these differences, an f-test was performed on the two columns of difference data. The result of the f-test may be seen in Table 4-8, where the result shows an unequal variance is to be assumed for the comparison. Using this knowledge, a t-test based on these results was ran, shown in Table 4-9. The results of the t-test show that the two-tail P-value = 1.877E-08, much less when compared to the alpha of α=0.05. This result means that the null hypothesis is rejected and the two means of differences are statistically significantly difference. Again it is important to look at the actual means of the data, ΔSLM Flat=46.16 and ΔPurchased=45.18. Here is another situation where the means are significantly different, but the actual means are still realistically close to one another.

Looking at the results from the statistical methods, shown in Table 4-6 and Table 4-9, it can be seen that the variances of the groups vary between each analysis. The variances of the groups are greater when using the Monte Carlo method, than the ordered data method. This may be associated with the data being randomly generated in the Monte Carlo method, whereas the other uses the actual data, which contains a less amount of samples. Also, the group with the greater variance changes when looking from one method to the next. This adjustment of which group contains the higher variance is attributed to the amount of specimen samples seen in each category. In the ordered data method, the number of differences which can be calculated is

limited by the amount of data provided, where it is seen that the ΔFlat contains less samples than ΔPurchased. Then seen in the Monte Carlo method, both of the calculated differences contain the same number of samples, as the values were generated using Excel.

After completing the further analysis of the SLM flat and Purchased parts data, when looking at the results from the various methods used to analyze the data, it can be determined that the different methods support each finding of the comparisons. The comparisons of differences between solid and with hole parts, repeatedly produced similar results of significant difference. Though as stated, when discussing these differences, the actual means should be included in the discussion.

Conclusions

The goal of this research was to determine if there was a significant difference in performance of mechanical properties between different production methods, when including a stress concentration. The two methods selected were traditional manufacturing, by using a milling machine, and AM, by using the EOS M290 Selective Laser Melting system. Other research was investigated to establish a better understanding of both the SM and AM processes and capabilities. Through this research, the behavior, history and inner workings of the SLM process and powder consolidation were discussed, as well as advantages and disadvantages the technology has. In order to test the mechanical capabilities of these two methods, tensile testing specimens were produced and tested on an Instron Universal Testing Machine. Two geometries were used in this research, solid specimens as well as those containing a circular stress concentration. Data was collected during testing by the Instron and its extensometer. This data was then used to determine a few main mechanical properties of the material, including yield strength, UTS, and Young's modulus.

After establishing the mechanical properties for each part type and geometry, statistical processing was used to determine the significance of these findings. This began with comparisons of parts containing like geometries within each mechanical property by using f-tests and t-tests to determine significance.

After determining that the SLM edge parts provided the worst performance of the production methods, it was decided to further investigate the performances of the SLM flat and Purchased parts. Here the research looked at how well a production process performed when containing a stress concentration compared to solid specimens. Various statistical methods were used to determine the comparison of differences for the different processes. Each of these methods returned with the same result, stating that there was a significant difference of the differences in production methods. It should be noted that while the conclusion is true, caution should be taken when using the data, as the actual means of the differences calculated are realistically close to one another, while being significantly different.

In conclusion, this research used statistical methods to compare various productions methods to determine if a significant difference exists between methods with regards to the resulting mechanical properties. It was found that while no one process was deemed a better production method than the others, SLM was confirmed as a useful and realistic production method with regards to part strength and part strength when including part geometry using the process.

With regards to SLM processes, there are many directions that future research has the potential to go. With expanding on the research done here some areas to investigate in the future would be changing machine parameters to see how mechanical properties are affected. Also testing performance using various different materials would be possible, as well as determining

the affect heat treating has on specimens. In expanding outwards from this research, part dimension analysis with regards to position on the plate, as well as part dimension repeatability capabilities could be investigated. This is a technology which is beginning to see expanded use in part production, and contains the potential for many more research opportunities in the future.

REFERENCES

ASTM E8 / E8M-15a. (2015). Standard Test Methods for Tension Testing of Metallic Materials. West Conshohocken, PA: ASTM International. Retrieved from www.astm.org

ASTM ISO / ASTM52921-13,. (2013). Stanard Terminology for Additive Manufacturing-Coordinate Systems and Test Methodologies,. West Conshohocken, PA: ASTM International. Retrieved from www.astm.org

Banther, B. R. (2009). A Regression Analysis on Rapid Prototyping Fits and Tolerances for Fused Deposition Modeling. *Master's Thesis, Western Carolina University*.

Bhavar, V., Kattire, P., Patil, V., Khot, S., Gujar, K., & Singh, R. (2014). A Review on Powder Bed Fusion Technology of Metal Additive Manufacturing. *Materials Science & Technology 2014*.

Bourell, D. L., Beaman, Jr., J. J., Leu, M. C., & Rosen, D. W. (2009). A Brief History of Additive Manufacturing and the 2009 Roadmap for Additive Manufacturing: Looking Back and Looking Ahead. *Workshop On Rapid Technologies*, 5-11.

EOS e-Manufacturing Solutions. (2013). *EOS: e-Manufacturing Solutions.* Retrieved from www.eos.info: http://www.hessen-nanotech.de/mm/mm001/3D_Additive_Manufacturing_Schultheiss_EOS.pdf

EOS e-Manufacturing Solutions. (2013b). *Whitepaper.* Retrieved from www.eos.info: https://scrivito-public-cdn.s3-eu-west-1.amazonaws.com/eos/public/7e99ba072eca9ad8/294354957693f78ddb4787d3959e7057/ppm_whitepaper.pdf

EOS E-Manufacturing Solutions. (2014a, February). *EOS 316L Stainless Steel Material Data Sheet.* Retrieved from http://www.eos.info: https://scrivito-public.s3-eu-west-1.amazonaws.com/eos/public/77d285f20ed6ae89/c5b1a52d8738143eea09c8a0d7bcc023/EOSStainlessSteel316L.pdf

EOS e-Manufacturing Solutions. (2014b). *Metal Solutions.* Retrieved from www.eos.info: https://scrivito-public-cdn.s3-eu-west-1.amazonaws.com/eos/public/413c861f2843b377/93ef12304097fd70c866344575a4af31/EOS_System-DataSheet-EOS-M290.pdf

IHS Engineering 316. (2006). *Appendix C: Mechanical and Environmental Properties*. Retrieved from www.globalspec.com: http://www.globalspec.com/reference/37452/203279/appendix-c-mechanical-and-environmental-properties

Instron. (n.d.). *Tensile Testing*. Retrieved from www.instron.com: http://www.instron.com/en-us/our-company/library/test-types/tensile-test?region=North%20America

Kamath, C., El-dasher, B., Gallegos, G. F., King, W. E., & Sisto, A. (2014). Density of additively-manufactured, 316L SS parts using laser powder-bed fusion at powers up to 400 W. *International Journal of Advanced Manufacturing Technology*.

Krantz, A., & Sjöö, F. (2015). Additive manufacturing - Viability in full scale production (A model for cost comprison with traditional manufacturing). *Masters Thesis*.

Kruth, J. P., Badrossamay, M., Yasa, E., Deckers, J., Thijs, L., & Van Humbeek, J. (2010). Part and material properties in selective laser melting of metals. *16th International Symposium on Electromachining*.

Kruth, J. P., Levy, G., Klocke, F., & Childs, T. (2007). Consolidation phenomena in laser and powder-bed based layered manufacturing. *Annals of the CIRP*.

Li, R., Liu, J., Shi, Y., Wang, L., & Jiang, W. (2012). Balling behavior of stainless steel and nickel powder during selective laser melting process. *International Journal of Advanced Manufacturing Technology*.

Materials and Minerals Science Course C: Microstructure. (n.d.). Retrieved from www.inference.phy.cam.ac.uk: http://www.inference.phy.cam.ac.uk/prlw1/minp/CourseC/CP1.pdf

Mercelis, P., & Kruth, J.-P. (2006). Residual Stresses in Selective Laser Sintering and Selective Laser Melting. *Emerald insight*, 254-265.

Mertens, A., Reginster, S., Paydas, H., Contrepois, Q., Dormal, T., Lemaire, O., & Lecomte-Beckers, J. (2014). Mechanical properties of alloy Ti-6Al 4V and of stainless steel 316L processed by selective laser melting: influence of out-of-equilibrium microstructures. *Institute of Materials, Minerals and Mining*.

Poyraz, Ö., Yasa, E., Akbulut, G., Orhangül, A., & Pilatin, S. (2015). INVESTIGATION OF SUPPORT STRUCTURES FOR DIRECT METAL LASER SINTERING (DMLS) OF IN625 PARTS. *Solid Freeform Fabrication Symposium* .

Simchi, A., & Asgharzadeh, H. (2004, November). Densification and microstructural evaluation during laser sintering of M2 high speed steel powder. *Materials Science and Technology, 20*, 1462-1468.

Simonelli, M., Yse, Y. Y., & Tuck, C. (2014). Effect of the build orientation on the mechanical properties and fracture modes of SLM Ti-Al-4V. *Materials Science & Engineering: A*.

Tolosa, I., Garciandía, F., Zubiri, F., Zapirain, F., & Esnaola, A. (2010). Study of mechanical properties of AISI 316 stainless steel processed by "selective laser melting", following different manufacturing strategies. *International Journal of Advanced Manufacturing Technology*.

APPENDIX A: PART SUMMARY TABLES

	Thickness	Width	Hole Dia.	Area	Gage Length	Calculated Yield Strength	Ext. Yield Strength	UTS	Ext. Young's Modulus
	mm	mm	mm	mm2	mm	MPa	MPa	MPa	GPa
SL M Edge Solid 1-1	3.3	12.87		42.47	50	486		571	167
SL M Edge Solid 1-2	3.3	12.85		42.41	50	469		573	152
SL M Edge Solid 1-3	3.3	12.9		42.57	50	480		572	185
SL M Edge Solid 1-4	3.3	12.82		42.31	50	487		575	152
SL M Edge Solid 1-5	3.31	13.06		43.23	50	466		562	164
SL M Edge Solid 1-6	3.29	13		42.77	50	481		569	163
SL M Edge Solid 1-7	3.32	12.82		42.56	50	481		570	160
SL M Edge Solid 1-8	3.28	12.97		42.54	50	480		571	161
SL M Edge Solid 1-9	3.3	12.8		42.24	50	487		575	163
SL M Edge Solid 2-1	3.27	12.67		41.43	50	460		582	183
SL M Edge Solid 2-2	3.3	12.68		41.84	50	479		580	176
SL M Edge Solid 2-3	3.28	12.66		41.52	50	476		585	190
SL M Edge Solid 2-4	3.28	12.65		41.49	50	464		584	208
SL M Edge Solid 2-5	3.29	12.66		41.65	50	473		581	257
SL M Edge Solid 2-6	3.29	12.66		41.65	50	472		582	171
SL M Edge Solid 2-7	3.28	12.65		41.49	50	477		583	176
SL M Edge Solid 2-8	3.3	12.64		41.71	50	446		579	207
SL M Edge Solid 2-9	3.29	12.69		41.75	50	473		580	161
SL M Edge Solid 2-10	3.3	12.69		41.88	50	448		575	181
SL M Edge Solid 3-1	3.3	12.65		41.75	50	460		575	156

	Thickness	Width	Hole Dia.	Area	Gage Length	Calculated Yield Strength	Ext. Yield Strength	UTS	Ext. Young's Modulus
	mm	mm	mm	mm2	mm	MPa	MPa	MPa	GPa
SLM Edge Hole 1-1	3.3	12.87	4.7	26.96	50	351	N/A	605	191
SLM Edge Hole 1-2	3.31	12.86	4.75	26.84	50	359	N/A	602	234
SLM Edge Hole 1-3	3.31	12.89	4.77	26.88	50	487	N/A	600	213
SLM Edge Hole 1-4	3.3	12.79	4.74	26.57	50	547	N/A	611	233
SLM Edge Hole 1-5	3.29	12.81	4.77	26.45	50	355	N/A	612	238
SLM Edge Hole 1-6	3.3	12.83	4.67	26.93	50	351	N/A	606	272
SLM Edge Hole 1-7	3.3	12.8	4.74	26.60	50	355	N/A	612	266
SLM Edge Hole 1-8	3.32	12.88	4.45	27.99	50	344	N/A	573	230
SLM Edge Hole 1-9	3.29	12.82	4.76	26.52	50	357	N/A	610	223
SLM Edge Hole 1-10	3.3	12.84	4.77	26.63	50	356	N/A	610	224
SLM Edge Hole 2-1	3.24	12.55	4.74	25.30	50	369	N/A	631	263
SLM Edge Hole 2-2	3.25	12.57	4.78	25.32	50	365	N/A	629	251
SLM Edge Hole 2-3	3.28	12.57	4.76	25.62	50	366	N/A	625	263
SLM Edge Hole 2-4	3.29	12.56	4.78	25.60	50	363	N/A	623	266
SLM Edge Hole 2-5	3.29	12.58	4.77	25.69	50	368	N/A	623	183
SLM Edge Hole 2-6	3.27	12.57	4.8	25.41	50	374	N/A	624	251
SLM Edge Hole 2-7	3.27	12.61	4.78	25.60	50	405	N/A	623	243
SLM Edge Hole 2-8	3.29	12.55	4.85	25.33	50	375	N/A	626	250
SLM Edge Hole 2-9	3.27	12.57	4.77	25.51	50	368	N/A	623	261
SLM Edge Hole 2-10	3.28	12.57	4.76	25.62	50	368	N/A	626	211

	Thickness	Width	Hole Dia.	Area	Gage Length	Calculated Yield Strength	Ext. Yield Strength	UTS	Ext. Young's Modulus
	mm	mm	mm	mm^2	mm	MPa	MPa	MPa	GPa
SLM Solid Flat 1-1	3.39	12.56		42.58	50	484	N/A	562	220
SLM Solid Flat 1-2	3.37	12.57		42.36	50	468	N/A	568	195
SLM Solid Flat 1-3	3.36	12.60		42.34	50	471	N/A	570	198
SLM Solid Flat 1-4	3.38	12.61		42.62	50	473	N/A	565	188
SLM Solid Flat 1-5	3.37	12.62		42.53	50	464	N/A	567	127
SLM Solid Flat 1-6	3.38	12.60		42.59	50	456	N/A	565	N/A
SLM Solid Flat 1-7	3.42	12.60		43.09	50	475	N/A	562	146
SLM Solid Flat 1-8	3.37	12.57		42.36	50	483	N/A	566	157
SLM Solid Flat 2-1	3.39	12.54		42.51	50	500	N/A	567	N/A
SLM Solid Flat 2-2	3.35	12.55		42.04	50	481	N/A	574	N/A
SLM Solid Flat 2-3	3.35	12.59		42.18	50	452	N/A	570	N/A
SLM Solid Flat 2-4	3.40	12.57		42.74	50	504	N/A	567	N/A
SLM Solid Flat 2-5	3.32	12.56		41.70	50	486	N/A	576	N/A
SLM Solid Flat 2-6	3.35	12.57		42.11	50	468	N/A	574	N/A
SLM Solid Flat 2-7	3.37	12.56		42.33	50	467	N/A	567	N/A
SLM Solid Flat 2-8	3.35	12.55		42.04	50	466	N/A	570	N/A
SLM Solid Flat 2-9	3.35	12.57		42.11	50	462	N/A	569	N/A
SLM Solid Flat 2-10	3.32	12.58		41.77	50	505	N/A	577	N/A
SLM Solid Flat 3-1	3.39	12.56		42.58	50	456	479	569	190
SLM Solid Flat 3-2	3.39	12.59		42.68	50	459	452	565	145
SLM Solid Flat 4-1	3.36	12.54		42.13	50	472	461	568	182
SLM Solid Flat 4-2	3.36	12.55		42.17	50	484	464	569	173
SLM Solid Flat 4-3	3.38	12.53		42.35	50	469	468	564	204
SLM Solid Flat 4-4	3.37	12.53		42.23	50	477	465	565	185
SLM Solid Flat 4-5	3.43	12.51		42.91	50	455	450	555	171
SLM Solid Flat 4-6	3.35	12.53		41.98	50	469	461	568	190
SLM Solid Flat 4-7	3.47	12.53		43.48	50	476	449	550	181
SLM Solid Flat 4-8	3.35	12.53		41.98	50	466	463	568	165
SLM Solid Flat 4-9	3.34	12.54		41.88	50	466	471	572	181
SLM Solid Flat 4-10	3.36	12.54		42.13	50	479	471	567	192

	Thickness	Width	Hole Dia.	Area	Gage Length	Calculated Yield Strength	Ext. Yield Strength	UTS	Ext. Young's Modulus
	mm	mm	mm	mm2	mm	MPa	MPa	MPa	GPa
SLM Flat with Hole 1-1	3.28	12.53	4.69	25.72	50	560	513	636	229
SLM Flat with Hole 1-2	3.34	12.53	4.96	25.28	50	560	516	639	243
SLM Flat with Hole 1-3	3.27	12.57	4.65	25.90	50	559	516	628	252
SLM Flat with Hole 1-4	3.29	12.56	4.66	25.99	50	548	507	627	223
SLM Flat with Hole 1-5	3.28	12.51	4.67	25.72	50	549	503	632	235
SLM Flat with Hole 1-6	3.27	12.54	4.66	25.77	50	551	518	631	249
SLM Flat with Hole 1-7	3.33	12.54	4.64	26.31	50	542	505	618	229
SLM Flat with Hole 1-8	3.27	12.53	4.65	25.77	50	558	514	632	241
SLM Flat with Hole 2-1	3.29	12.52	4.65	25.89	50	551	509	632	210
SLM Flat with Hole 2-2	3.26	12.54	4.64	25.75	50	555	489	621	248
SLM Flat with Hole 2-3	3.32	12.52	4.61	26.26	50	545	502	622	241
SLM Flat with Hole 2-4	3.31	12.56	4.64	26.22	50	552	508	627	255
SLM Flat with Hole 2-5	3.25	12.51	4.69	25.42	50	562	506	634	242
SLM Flat with Hole 2-6	3.22	12.52	4.62	25.44	50	578	520	644	261
SLM Flat with Hole 2-7	3.31	12.52	4.63	26.12	50	545	505	627	275
SLM Flat with Hole 2-8	3.30	12.57	4.68	26.04	50	547	495	623	504
SLM Flat with Hole 2-9	3.28	12.57	4.65	25.98	50	553	515	634	247
SLM Flat with Hole 2-10	3.29	12.54	4.66	25.93	50	555	510	631	220
SLM Flat with Hole 2-11	3.29	12.53	4.66	25.89	50	556	524	633	284
SLM Flat with Hole 3-1	3.35	12.60	4.64	26.67	50	538	507	613	228

	Thickness	Width	Hole Dia.	Area	Gage Length	Calculated Yield Strength	Ext. Yield Strength	UTS	Ext. Young's Modulus
	mm	mm	mm	mm2	mm	MPa	MPa	MPa	GPa
Purchased Solid 1-1	2.97	12.81		38.05	50	353	346	618	159
Purchased Solid 1-2	3.02	12.83		38.75	50	358	351	612	168
Purchased Solid 1-3	2.99	12.83		38.36	50	360	354	620	171
Purchased Solid 1-4	2.98	12.84		38.26	50	359	359	620	200
Purchased Solid 1-5	2.97	12.85		38.16	50	356	345	619	137
Purchased Solid 1-6	2.98	12.86		38.32	50	358	352	615	604
Purchased Solid 1-7	2.98	12.82		38.20	50	359	349	619	165
Purchased Solid 1-8	3.00	12.83		38.49	50	358	357	614	437
Purchased Solid 1-9	2.99	12.82		38.33	50	360	349	617	156
Purchased Solid 1-10	2.99	12.80		38.27	50	350	344	617	150
Purchased Solid 1-11	2.96	12.86		38.07	50	363	351	620	146
Purchased Solid 1-12	2.98	12.85		38.29	50	358	345	617	155
Purchased Solid 1-13	2.96	12.85		38.04	50	357	349	619	210
Purchased Solid 1-14	2.99	12.83		38.36	50	360	352	618	172
Purchased Solid 1-15	2.98	12.87		38.35	50	343	339	615	330
Purchased Solid 1-16	2.98	12.84		38.26	50	361	353	622	216
Purchased Solid 1-17	3.00	12.84		38.52	50	364	355	617	164
Purchased Solid 1-18	2.97	12.85		38.16	50	346	347	617	160
Purchased Solid 1-19	2.97	12.86		38.19	50	363	354	621	167
Purchased Solid 1-20	2.95	12.84		37.88	50	363	352	621	161

	Thickness	Width	Hole Dia.	Area	Gage Length	Calculated Yield Strength	Ext. Yield Strength	UTS	Ext. Young's Modulus
	mm	mm	mm	mm2	mm	MPa	MPa	MPa	GPa
Purchased Holes 1-1	2.99	12.81	4.75	24.10	50	408	383	661	212
Purchased Holes 1-2	2.96	12.82	4.73	23.95	50	426	391	668	223
Purchased Holes 1-3	3.02	12.83	4.74	24.43	50	438	401	666	257
Purchased Holes 1-4	2.98	12.83	4.75	24.08	50	431	384	667	229
Purchased Holes 1-5	2.99	12.86	4.73	24.31	50	427	398	661	253
Purchased Holes 1-6	2.99	12.85	4.78	24.13	50	426	403	672	230
Purchased Holes 1-7	2.99	12.82	4.75	24.13	50	430	398	672	250
Purchased Holes 1-8	2.99	12.81	4.75	24.10	50	420	397	672	228
Purchased Holes 1-9	2.98	12.83	4.74	24.11	50	431	393	659	240
Purchased Holes 1-10	2.98	12.80	4.73	24.05	50	419	380	663	223
Purchased Holes 1-11	2.99	12.82	4.76	24.10	50	418	387	663	247
Purchased Holes 1-12	2.98	12.81	4.74	24.05	50	431	390	669	282
Purchased Holes 1-13	3.01	12.87	4.76	24.41	50	451	407	666	227
Purchased Holes 1-14	2.97	12.85	4.73	24.12	50	434	405	664	239
Purchased Holes 1-15	2.96	12.84	4.74	23.98	50	425	393	668	227
Purchased Holes 1-16	3.00	12.84	4.74	24.30	50	418	380	660	244
Purchased Holes 1-17	2.94	12.86	4.76	23.81	50	448	407	666	234
Purchased Holes 1-18	2.99	12.84	4.78	24.10	50	450	415	673	286
Purchased Holes 1-19	2.98	12.86	4.74	24.20	50	434	399	667	253
Purchased Holes 1-20	3.00	12.83	4.76	24.21	50	420	389	656	252

APPENDIX B: ANALYSIS OF VARIANCE USING F-TEST

F-Tests for Calculated Yield Strength

F-Test Two-Sample for Variances - Calculated Yield Strength

	SLM Flat Solid	Purchased Solid
Mean	473.169	357.442
Variance	184.606	23.168
Observations	30.000	20.000
df	29.000	19.000
F	7.968	
alpha	0.050	
p-value	0.000	
f-crit	2.402	
Significant Difference	yes	
Variance of parts	Unequal	

F-Test Two-Sample for Variances - Calculated Yield Strength

	SLM Flat Hole	Purchased Hole
Mean	553.279	429.242
Variance	75.582	127.085
Observations	20.000	20.000
df	19.000	19.000
F	0.595	
alpha	0.050	
p-value	1.734	
f-crit	2.526	
Significant Difference	no	
Variance of parts	Equal	

F-Test Two-Sample for Variances - Calculated Yield Strength

	SLM Edge Solid	SLM Flat Solid
Mean	472.358	473.169
Variance	140.277	184.606
Observations	20.000	30.000
df	19.000	29.000
F	0.760	
alpha	0.050	
p-value	1.461	
f-crit	2.231	
Significant Difference	no	
Variance of parts	Equal	

F-Test Two-Sample for Variances - Calculated Yield Strength

	SLM Edge Solid	Purchased Solid
Mean	472.358	357.442
Variance	140.277	23.168
Observations	20.000	20.000
df	19.000	19.000
F	6.055	
alpha	0.050	
p-value	0.000	
f-crit	2.526	
Significant Difference	yes	
Variance of parts	Unequal	

F-Test Two-Sample for Variances - Calculated Yield Strength

	SLM Edge Hole	SLM Flat Hole
Mean	379.166	553.279
Variance	2475.933	75.582
Observations	20.000	20.000
df	19.000	19.000
F	32.758	
alpha	0.050	
p-value	0.000	
f-crit	2.526	
Significant Difference	yes	
Variance of parts	Unequal	

F-Test Two-Sample for Variances - Calculated Yield Strength

	SLM Edge Hole	Purchased Hole
Mean	379.166	429.242
Variance	2475.933	127.085
Observations	20.000	20.000
df	19.000	19.000
F	19.483	
alpha	0.050	
p-value	0.000	
f-crit	2.526	
Significant Difference	yes	
Variance of parts	Unequal	

F-Tests for Extensometer Yield Strength

F-Test Two-Sample for Variances - Ext Yield Strength		
	SLM Flat Solid	Purchased Solid
Mean	462.944	350.208
Variance	82.398	23.168
Observations	12.000	20.000
df	11.000	19.000
F	3.557	
alpha	0.050	
p-value	0.015	
f-crit	2.765	
Significant Difference	yes	
Variance of parts	Unequal	

F-Test Two-Sample for Variances - Ext Yield Strength		
	SLM Flat Hole	Purchased Hole
Mean	509.133	394.978
Variance	70.384	92.430
Observations	20.000	20.000
df	19.000	19.000
F	0.761	
alpha	0.050	
p-value	1.442	
f-crit	2.526	
Significant Difference	no	
Variance of parts	Equal	

F-Tests for UTS

F-Test Two-Sample for Variances - UTS		
	SLM Flat Solid	Purchased Solid
Mean	567.123	618.004
Variance	29.475	6.900
Observations	30.000	20.000
df	29.000	19.000
F	4.272	
alpha	0.050	
p-value	0.002	
f-crit	2.402	
Significant Difference	yes	
Variance of parts	Unequal	

F-Test Two-Sample for Variances - UTS		
	SLM Flat Hole	Purchased Hole
Mean	629.130	665.618
Variance	55.370	22.918
Observations	20.000	20.000
df	19.000	19.000
F	2.416	
alpha	0.050	
p-value	0.062	
f-crit	2.526	
Significant Difference	no	
Variance of parts	Equal	

F-Test Two-Sample for Variances - UTS		
	SLM Edge Solid	SLM Flat Solid
Mean	576.044	567.123
Variance	29.475	82.398
Observations	20.000	30.000
df	19.000	29.000
F	0.358	
alpha	0.050	
p-value	1.978	
f-crit	2.231	
Significant Difference	no	

Variance of parts	Equal

F-Test Two-Sample for Variances - UTS

	SLM Edge Solid	Purchased Solid
Mean	576.044	618.004
Variance	36.347	6.900
Observations	20.000	20.000
df	19.000	19.000
F	5.268	
alpha	0.050	
p-value	0.001	
f-crit	2.526	
Significant Difference	yes	
Variance of parts	Unequal	

F-Test Two-Sample for Variances - UTS

	SLM Edge Hole	SLM Flat Hole
Mean	614.747	629.130
Variance	188.680	55.370
Observations	20.000	20.000
df	19.000	19.000
F	3.408	
alpha	0.050	
p-value	0.010	
f-crit	2.526	
Significant Difference	yes	
Variance of parts	Unequal	

F-Test Two-Sample for Variances - UTS

	SLM Edge Hole	Purchased Hole
Mean	614.747	665.618
Variance	188.680	22.918
Observations	20.000	20.000
df	19.000	19.000
F	8.233	
alpha	0.050	
p-value	0.000	
f-crit	2.526	
Significant Difference	yes	
Variance of parts	Unequal	

F-Tests for Extensometer Young's Modulus

F-Test Two-Sample for Variances - Ext Young's Modulus		
	SLM Flat Solid	Purchased Solid
Mean	178.457	211.513
Variance	508.824	13597.473
Observations	19.000	20.000
df	18.000	19.000
F	0.037	
alpha	0.050	
p-value	2.000	
f-crit	2.546	
Significant Difference	no	
Variance of parts	Equal	

F-Test Two-Sample for Variances - Ext Young's Modulus		
	SLM Flat Hole	Purchased Hole
Mean	255.794	241.882
Variance	3719.159	360.204
Observations	20.000	20.000
df	19.000	19.000
F	10.325	
alpha	0.050	
p-value	4.535E-06	
f-crit	2.526	
Significant Difference	yes	
Variance of parts	Unequal	

F-Test Two-Sample for Variances - Ext Young's Modulus		
	SLM Edge Solid	SLM Flat Solid
Mean	176.671	178.457
Variance	618.583	29.475
Observations	20.000	19.000
df	19.000	18.000
F	20.986	
alpha	0.050	
p-value	2.587E-08	
f-crit	2.576	
Significant Difference	yes	
Variance of parts	Unequal	

F-Test Two-Sample for Variances - Ext Young's Modulus

	SLM Edge Solid	Purchased Solid
Mean	176.671	211.513
Variance	618.583	13597.473
Observations	20.000	20.000
df	19.000	19.000
F	0.045	
alpha	0.050	
p-value	2.000E+00	
f-crit	2.526	
Significant Difference	no	
Variance of parts	Equal	

F-Test Two-Sample for Variances - Ext Young's Modulus

	SLM Edge Hole	SLM Flat Hole
Mean	238.392	255.794
Variance	638.986	3719.159
Observations	20.000	20.000
df	19.000	19.000
F	0.172	
alpha	0.050	
p-value	2.000E+00	
f-crit	2.526	
Significant Difference	no	
Variance of parts	Equal	

F-Test Two-Sample for Variances - Ext Young's Modulus

	SLM Edge Hole	Purchased Hole
Mean	238.392	241.882
Variance	638.986	360.204
Observations	20.000	20.000
df	19.000	19.000
F	1.774	
alpha	0.050	
p-value	2.207E-01	
f-crit	2.526	
Significant Difference	no	
Variance of parts	Equal	

APPENDIX C: COMPARISON OF SAMPLE MEANS USING T-TEST

T-Tests for Calculated Yield Strength

t-Test: Two-Sample Assuming Unequal Variances

Calculated Yield Strength

	Variable 1	*Variable 2*
	SLM Flat Solid	Purchased Solid
Mean	473.1687525	357.4424229
Variance	184.6060944	30.74816785
Observations	30	20
Hypothesized Mean Difference	0	
df	41	
t Stat	41.7294182	
P(T<=t) one-tail	1.63466E-35	
t Critical one-tail	1.682878002	
P(T<=t) two-tail	3.26932E-35	
t Critical two-tail	2.01954097	

t-Test: Two-Sample Assuming Equal Variances

Calculated Yield Strength

	Variable 1	*Variable 2*
	SLM Flat Hole	Purchased Hole
Mean	553.2785115	429.2418809
Variance	75.58152148	127.0849376
Observations	20	20
Pooled Variance	101.3332295	
Hypothesized Mean Difference	0	
df	38	
t Stat	38.96494059	
P(T<=t) one-tail	1.512E-32	
t Critical one-tail	1.68595446	
P(T<=t) two-tail	3.02399E-32	
t Critical two-tail	2.024394164	

t-Test: Two-Sample Assuming Equal Variances

Calculated Yield Strength

	Variable 1	*Variable 2*
	SLM Edge Solid	SLM Flat Solid
Mean	472.3581675	473.1687525
Variance	140.2771544	184.6060944
Observations	20	30
Pooled Variance	167.0592223	
Hypothesized Mean Difference	0	
df	48	
t Stat	0.217247089	
P(T<=t) one-tail	0.414468302	
t Critical one-tail	1.677224196	
P(T<=t) two-tail	0.828936603	
t Critical two-tail	2.010634758	

t-Test: Two-Sample Assuming Unequal Variances

Calculated Yield Strength

	Variable 1	*Variable 2*
	SLM Edge Solid	Purchased Solid
Mean	472.3581675	357.4424229
Variance	140.2771544	30.74816785
Observations	20	20
Hypothesized Mean Difference	0	
df	27	
t Stat	39.29744585	
P(T<=t) one-tail	1.14462E-25	
t Critical one-tail	1.703288446	
P(T<=t) two-tail	2.28925E-25	
t Critical two-tail	2.051830516	

t-Test: Two-Sample Assuming Unequal Variances

Calculated Yield Strength

	Variable 1	*Variable 2*
	SLM Edge Hole	SLM Flat Hole
Mean	379.1663031	553.2785115
Variance	2475.932655	75.58152148
Observations	20	20
Hypothesized Mean Difference	0	
df	20	
t Stat	15.41506034	
P(T<=t) one-tail	7.26615E-13	
t Critical one-tail	1.724718243	
P(T<=t) two-tail	1.45323E-12	
t Critical two-tail	2.085963447	

t-Test: Two-Sample Assuming Unequal Variances

Calculated Yield Strength

	Variable 1	*Variable 2*
	SLM Edge Hole	Purchased Hole
Mean	379.1663031	429.2418809
Variance	2475.932655	127.0849376
Observations	20	20
Hypothesized Mean Difference	0	
df	21	
t Stat	4.389372268	
P(T<=t) one-tail	0.000128045	
t Critical one-tail	1.720742903	
P(T<=t) two-tail	0.00025609	
t Critical two-tail	2.079613845	

T-Tests for Extensometer Yield Strength

t-Test: Two-Sample Assuming Unequal Variances

Extensometer Yield Strength

	SLM Flat Solid	Purchased Solid
Mean	462.944	350.208
Variance	82.398	23.168
Observations	12.000	20.000
Hypothesized Mean Difference	0.000	
df	15.000	
t Stat	39.796	
P(T<=t) one-tail	0.000	
t Critical one-tail	1.753	
P(T<=t) two-tail	0.000	
t Critical two-tail	2.131	

t-Test: Two-Sample Assuming Equal Variances

Extensometer Yield Strength

	SLM Flat Hole	Purchased Hole
Mean	509.133	394.978
Variance	70.384	92.430
Observations	20.000	20.000
Pooled Variance	81.407	
Hypothesized Mean Difference	0.000	
df	38.000	
t Stat	40.010	
P(T<=t) one-tail	0.000	
t Critical one-tail	1.686	
P(T<=t) two-tail	0.000	
t Critical two-tail	2.024	

T-Tests for UTS

t-Test: Two-Sample Assuming Unequal Variances

UTS

	SLM Flat Solid	Purchased Solid
Mean	567.123	618.004
Variance	29.475	6.900
Observations	30.000	20.000
Hypothesized Mean Difference	0.000	
df	45.000	
t Stat	44.161	
P(T<=t) one-tail	0.000	
t Critical one-tail	1.679	
P(T<=t) two-tail	0.000	
t Critical two-tail	2.014	

t-Test: Two-Sample Assuming Equal Variances

UTS

	SLM Flat Hole	Purchased Hole
Mean	629.130	665.618
Variance	55.370	22.918
Observations	20.000	20.000
Pooled Variance	39.144	
Hypothesized Mean Difference	0.000	
df	38.000	
t Stat	18.442	
P(T<=t) one-tail	0.000	
t Critical one-tail	1.686	
P(T<=t) two-tail	0.000	
t Critical two-tail	2.024	

t-Test: Two-Sample Assuming Equal Variances

UTS

	Variable 1	*Variable 2*
	SLM Edge Solid	SLM Flat Solid
Mean	576.0436704	567.1225478
Variance	36.34722473	29.47536116
Observations	20	30
Pooled Variance	32.19547382	
Hypothesized Mean Difference	0	
df	48	
t Stat	5.446439951	
P(T<=t) one-tail	8.67912E-07	
t Critical one-tail	1.677224196	
P(T<=t) two-tail	1.73582E-06	
t Critical two-tail	2.010634758	

t-Test: Two-Sample Assuming Unequal Variances

UTS

	Variable 1	*Variable 2*
	SLM Edge Solid	Purchased Solid
Mean	576.0436704	618.0040612
Variance	36.34722473	6.900102399
Observations	20	20
Hypothesized Mean Difference	0	
df	26	
t Stat	28.53480353	
P(T<=t) one-tail	1.8751E-21	
t Critical one-tail	1.70561792	
P(T<=t) two-tail	3.75019E-21	
t Critical two-tail	2.055529439	

t-Test: Two-Sample Assuming Unequal Variances

UTS

	Variable 1	*Variable 2*
	SLM Edge Hole	SLM Flat Hole
Mean	614.7468489	629.1299998
Variance	188.6797806	55.37045215
Observations	20	20
Hypothesized Mean Difference	0	
df	29	
t Stat	4.117460315	
P(T<=t) one-tail	0.000145277	
t Critical one-tail	1.699127027	
P(T<=t) two-tail	0.000290554	
t Critical two-tail	2.045229642	

t-Test: Two-Sample Assuming Unequal Variances

UTS

	Variable 1	*Variable 2*
	SLM Edge Hole	Purchased Hole
Mean	614.7468489	665.6177024
Variance	188.6797806	22.9183615
Observations	20	20
Hypothesized Mean Difference	0	
df	24	
t Stat	15.63968844	
P(T<=t) one-tail	2.17895E-14	
t Critical one-tail	1.71088208	
P(T<=t) two-tail	4.3579E-14	
t Critical two-tail	2.063898562	

T-Tests for Extensometer Young's Modulus

t-Test: Two-Sample Assuming Equal Variances

Extensometer Young's Modulus

	SLM Flat Solid	Purchased Solid
Mean	178.457	211.513
Variance	508.824	13597.473
Observations	19.000	20.000
Pooled Variance	7230.022	
Hypothesized Mean Difference	0.000	
df	37.000	
t Stat	1.213	
P(T<=t) one-tail	0.116	
t Critical one-tail	1.687	
P(T<=t) two-tail	0.233	
t Critical two-tail	2.026	

t-Test: Two-Sample Assuming Unequal Variances

Extensometer Young's Modulus

	SLM Flat Hole	Purchased Hole
Mean	255.794	241.882
Variance	3719.159	360.204
Observations	20.000	20.000
Hypothesized Mean Difference	0.000	
df	23.000	
t Stat	0.974	
P(T<=t) one-tail	0.170	
t Critical one-tail	1.714	
P(T<=t) two-tail	0.340	
t Critical two-tail	2.069	

t-Test: Two-Sample Assuming Unequal Variances

Extensometer Young's Modulus

	Variable 1	*Variable 2*
	SLM Edge Solid	SLM Flat Solid
Mean	176.6705656	178.4572843
Variance	618.5833306	508.8243538
Observations	20	19
Hypothesized Mean Difference	0	
df	37	
t Stat	0.235197617	
P(T<=t) one-tail	0.407676125	
t Critical one-tail	1.68709362	
P(T<=t) two-tail	0.815352249	
t Critical two-tail	2.026192463	

t-Test: Two-Sample Assuming Equal Variances

Extensometer Young's Modulus

	Variable 1	*Variable 2*
	SLM Edge Solid	Purchased Solid
Mean	176.6705656	211.5129809
Variance	618.5833306	13597.47308
Observations	20	20
Pooled Variance	7108.028207	
Hypothesized Mean Difference	0	
df	38	
t Stat	1.306873891	
P(T<=t) one-tail	0.099554676	
t Critical one-tail	1.68595446	
P(T<=t) two-tail	0.199109352	
t Critical two-tail	2.024394164	

t-Test: Two-Sample Assuming Equal Variances

Extensometer Young's Modulus

	Variable 1	*Variable 2*
	SLM Edge Hole	SLM Flat Hole
Mean	238.3924399	255.7943176
Variance	638.9855281	3719.159402
Observations	20	20
Pooled Variance	2179.072465	
Hypothesized Mean Difference	0	
df	38	
t Stat	1.178854691	
P(T<=t) one-tail	0.122892483	
t Critical one-tail	1.68595446	
P(T<=t) two-tail	0.245784966	
t Critical two-tail	2.024394164	

t-Test: Two-Sample Assuming Equal Variances

Extensometer Young's Modulus

	Variable 1	*Variable 2*
	SLM Edge Hole	Purchased Hole
Mean	238.3924399	241.8823804
Variance	638.9855281	360.2036481
Observations	20	20
Pooled Variance	499.5945881	
Hypothesized Mean Difference	0	
df	38	
t Stat	0.49375233	
P(T<=t) one-tail	0.312161522	
t Critical one-tail	1.68595446	
P(T<=t) two-tail	0.624323043	
t Critical two-tail	2.024394164	

APPENDIX D: STRESS – STRAIN GRAPHS

Stress – Strain Graphs of SLM Edge Parts

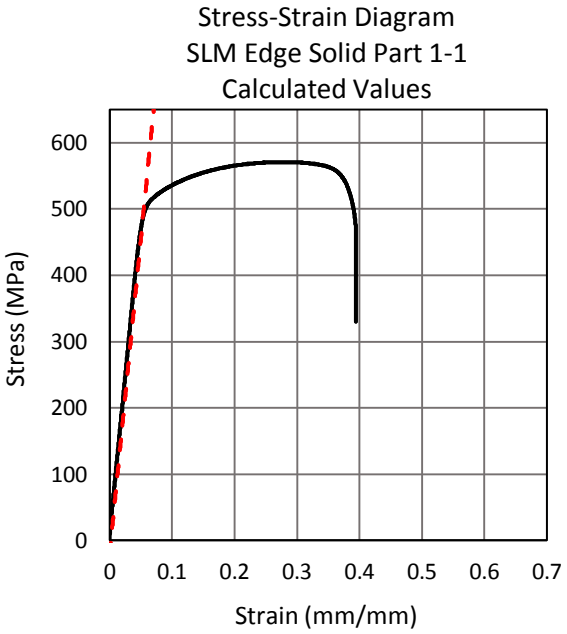

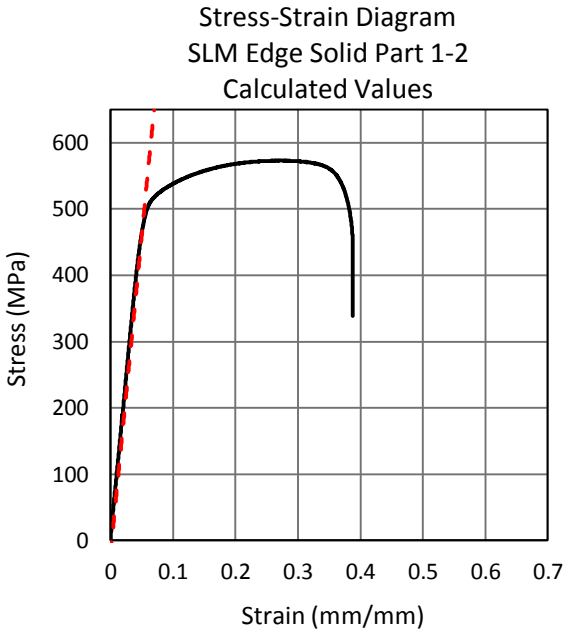

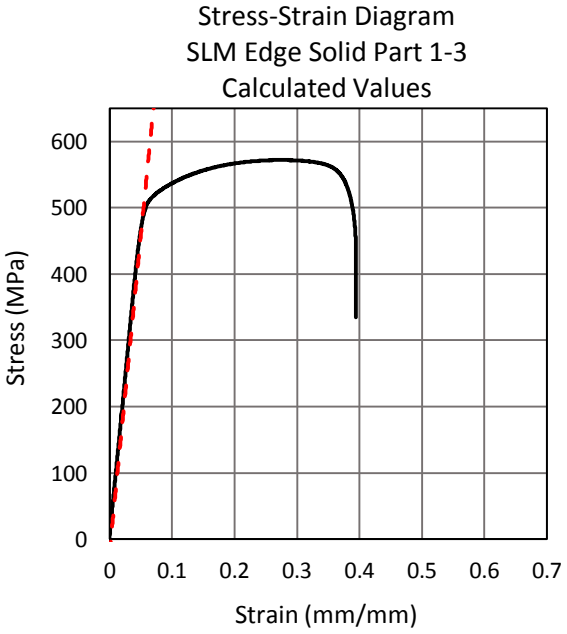

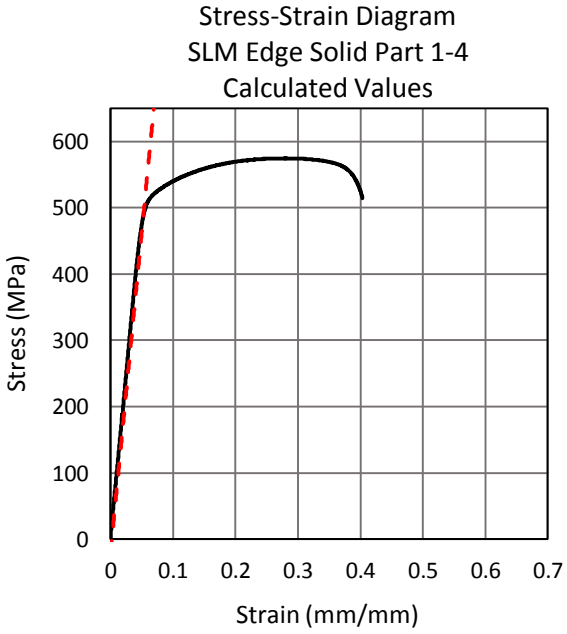

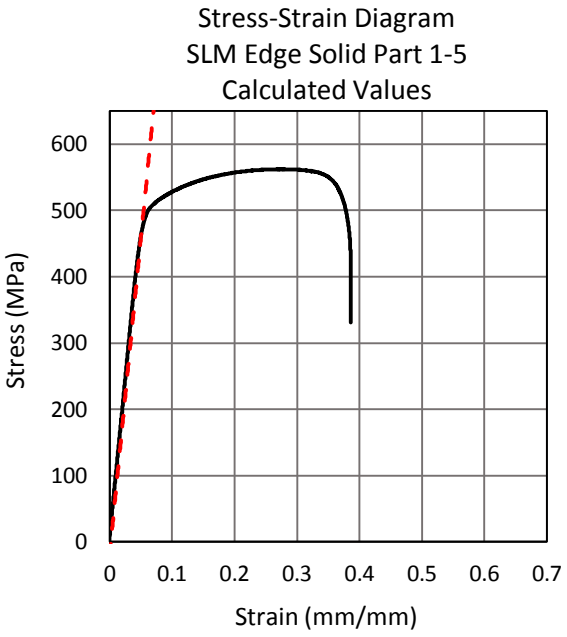
Stress-Strain Diagram
SLM Edge Solid Part 1-5
Calculated Values
Stress (MPa)
0
100
200
300
400
500
600
0
0.1
0.2
0.3
0.4
0.5
0.6
0.7
Strain (mm/mm)

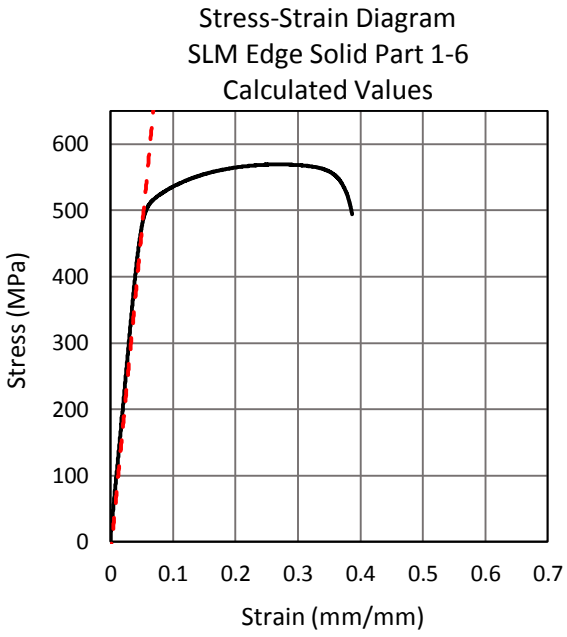
Stress-Strain Diagram
SLM Edge Solid Part 1-6
Calculated Values
Stress (MPa)
0
100
200
300
400
500
600
0
0.1
0.2
0.3
0.4
0.5
0.6
0.7
Strain (mm/mm)

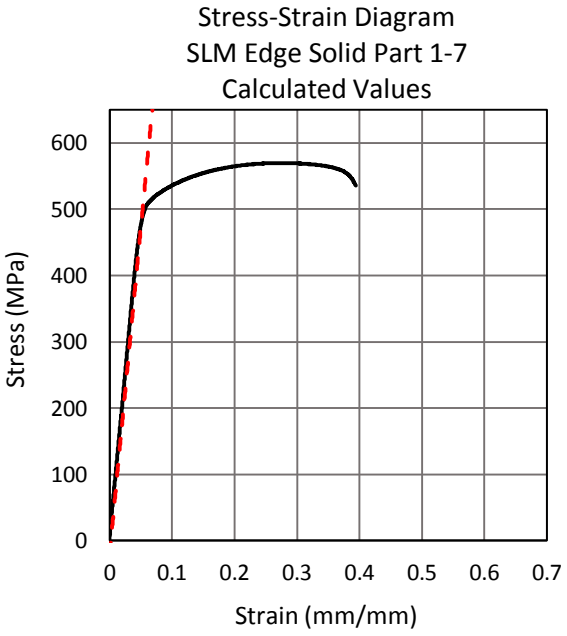
Stress-Strain Diagram
SLM Edge Solid Part 1-7
Calculated Values
Stress (MPa)
0
100
200
300
400
500
600
0
0.1
0.2
0.3
0.4
0.5
0.6
0.7
Strain (mm/mm)

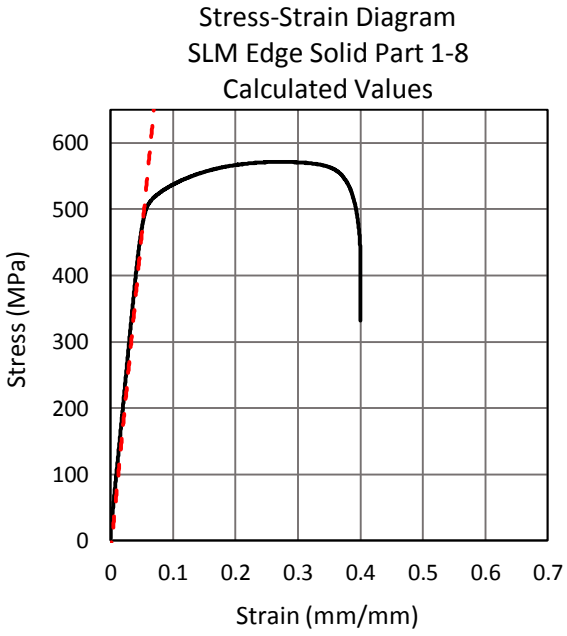
Stress-Strain Diagram
SLM Edge Solid Part 1-8
Calculated Values
Stress (MPa)
0
100
200
300
400
500
600
0
0.1
0.2
0.3
0.4
0.5
0.6
0.7
Strain (mm/mm)

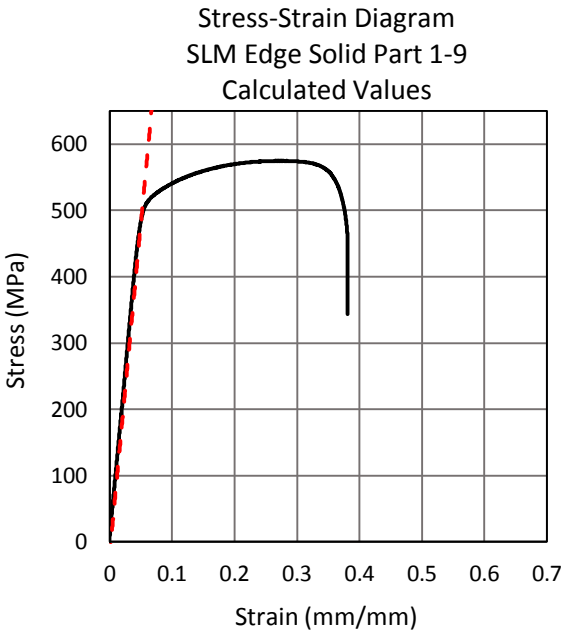
Stress-Strain Diagram
SLM Edge Solid Part 1-9
Calculated Values
Stress (MPa)
0
100
200
300
400
500
600
0
0.1
0.2
0.3
0.4
0.5
0.6
0.7
Strain (mm/mm)

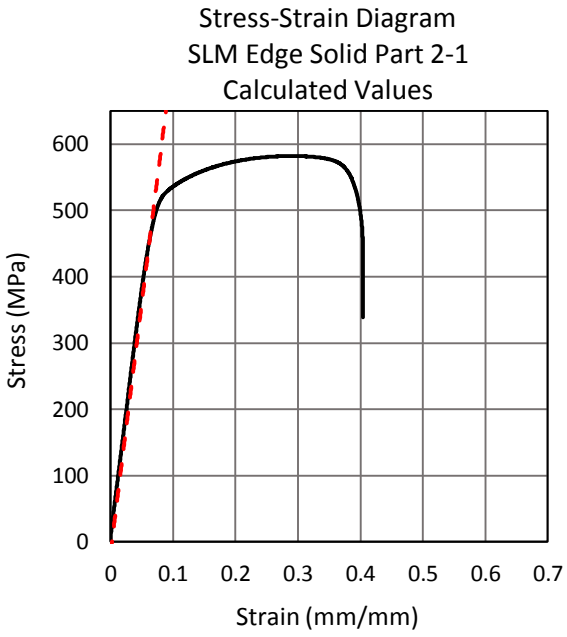
Stress-Strain Diagram
SLM Edge Solid Part 2-1
Calculated Values
Stress (MPa)
0
100
200
300
400
500
600
0
0.1
0.2
0.3
0.4
0.5
0.6
0.7
Strain (mm/mm)

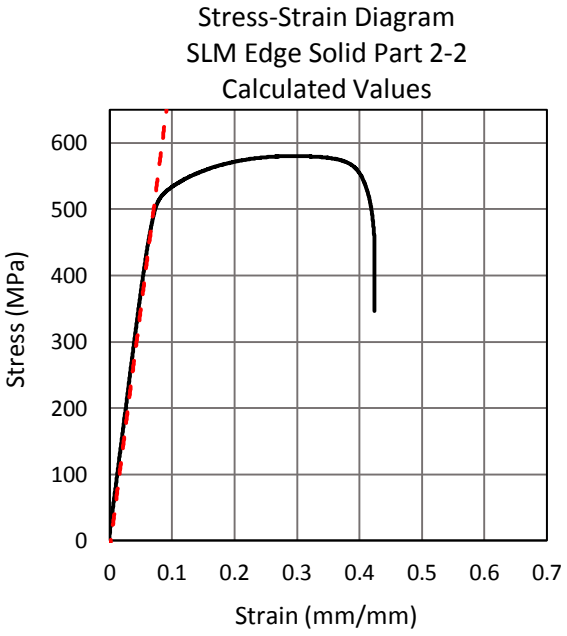
Stress-Strain Diagram
SLM Edge Solid Part 2-2
Calculated Values
Stress (MPa)
0
100
200
300
400
500
600
0
0.1
0.2
0.3
0.4
0.5
0.6
0.7
Strain (mm/mm)

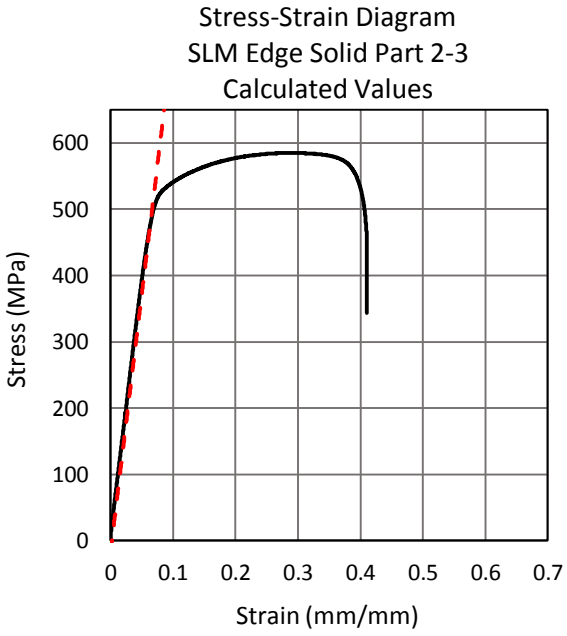
Stress-Strain Diagram
SLM Edge Solid Part 2-3
Calculated Values
Stress (MPa)
0
100
200
300
400
500
600
0
0.1
0.2
0.3
0.4
0.5
0.6
0.7
Strain (mm/mm)

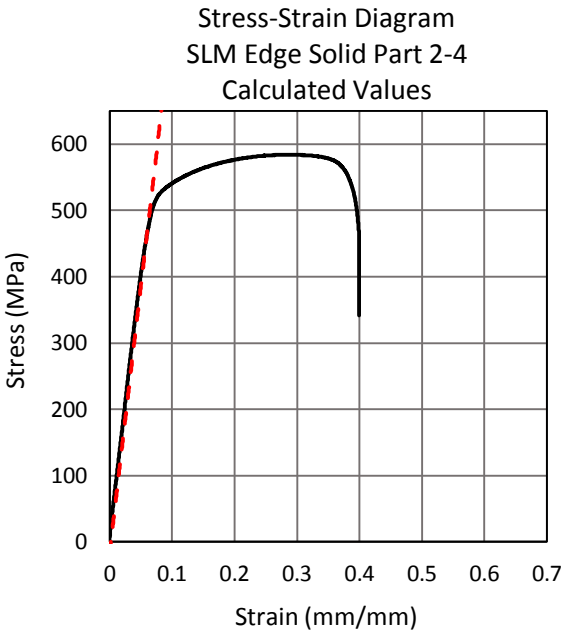
Stress-Strain Diagram
SLM Edge Solid Part 2-4
Calculated Values
Stress (MPa)
0
100
200
300
400
500
600
0
0.1
0.2
0.3
0.4
0.5
0.6
0.7
Strain (mm/mm)

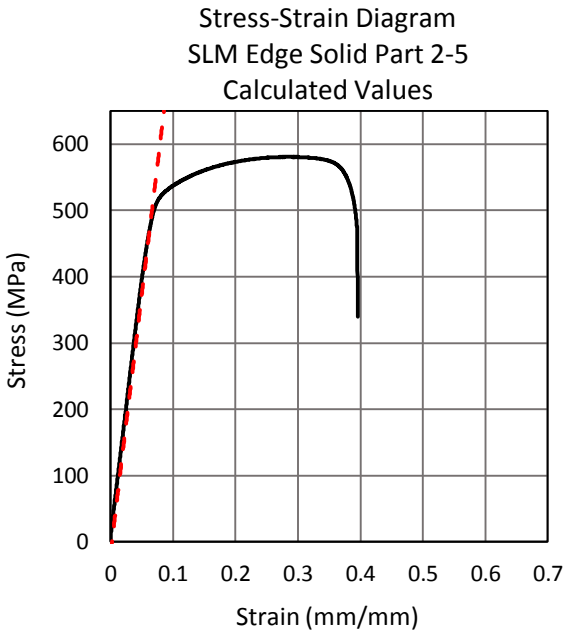
Stress-Strain Diagram
SLM Edge Solid Part 2-5
Calculated Values
Stress (MPa)
0
100
200
300
400
500
600
0
0.1
0.2
0.3
0.4
0.5
0.6
0.7
Strain (mm/mm)

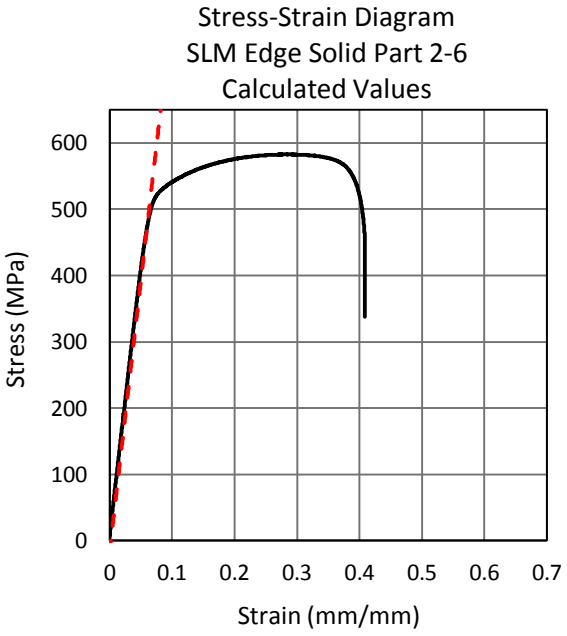
Stress-Strain Diagram
SLM Edge Solid Part 2-6
Calculated Values
Stress (MPa)
0
100
200
300
400
500
600
0
0.1
0.2
0.3
0.4
0.5
0.6
0.7
Strain (mm/mm)

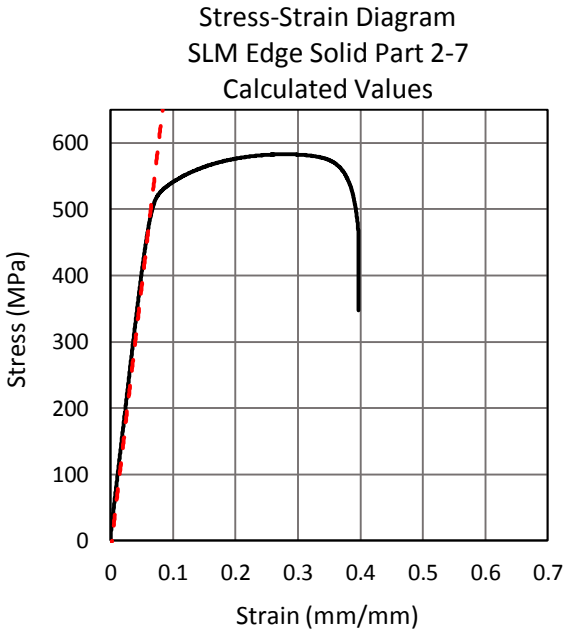
Stress-Strain Diagram
SLM Edge Solid Part 2-7
Calculated Values
Stress (MPa)
0
100
200
300
400
500
600
0
0.1
0.2
0.3
0.4
0.5
0.6
0.7
Strain (mm/mm)

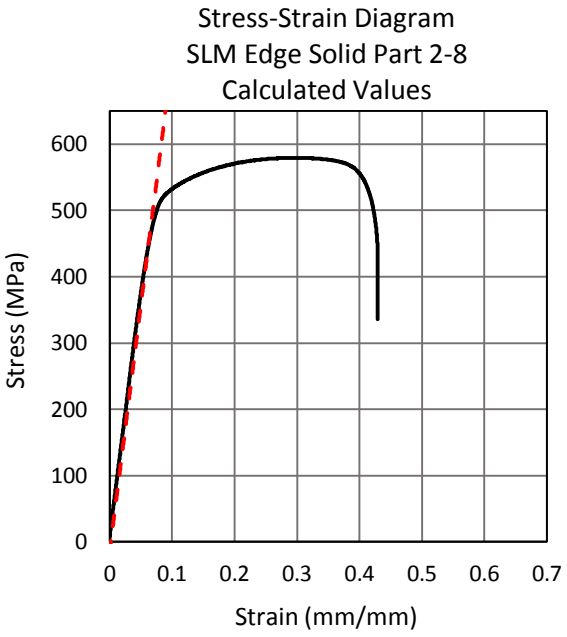
Stress-Strain Diagram
SLM Edge Solid Part 2-8
Calculated Values
Stress (MPa)
0
100
200
300
400
500
600
0
0.1
0.2
0.3
0.4
0.5
0.6
0.7
Strain (mm/mm)

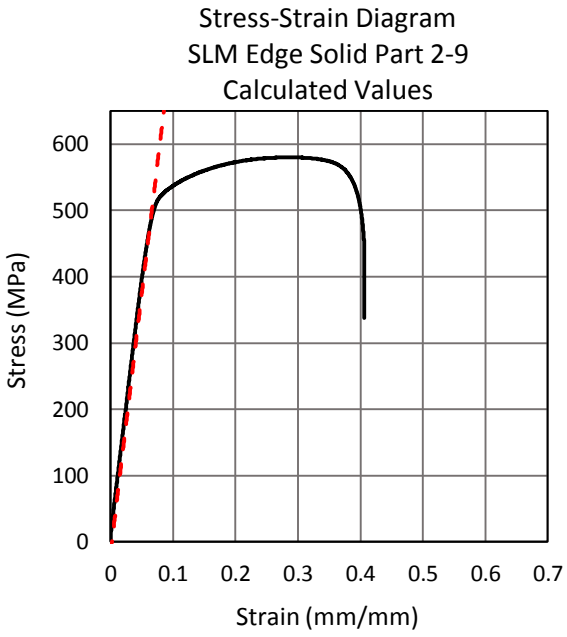
Stress-Strain Diagram
SLM Edge Solid Part 2-9
Calculated Values
Stress (MPa)
0
100
200
300
400
500
600
0
0.1
0.2
0.3
0.4
0.5
0.6
0.7
Strain (mm/mm)

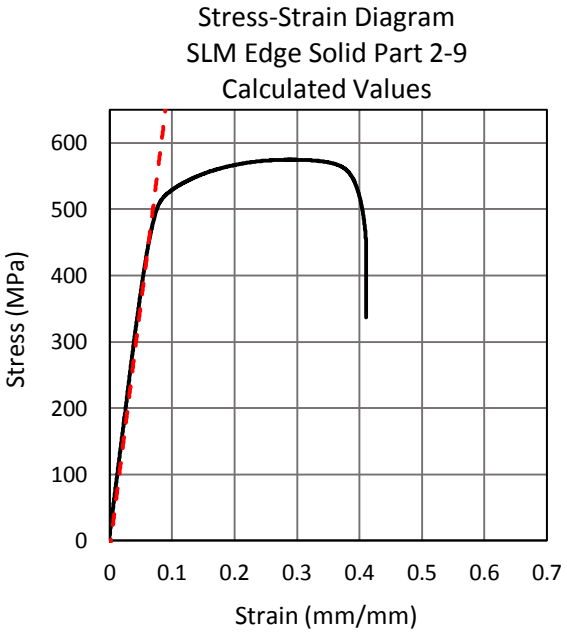
Stress-Strain Diagram
SLM Edge Solid Part 2-9
Calculated Values
Stress (MPa)
0
100
200
300
400
500
600
0
0.1
0.2
0.3
0.4
0.5
0.6
0.7
Strain (mm/mm)

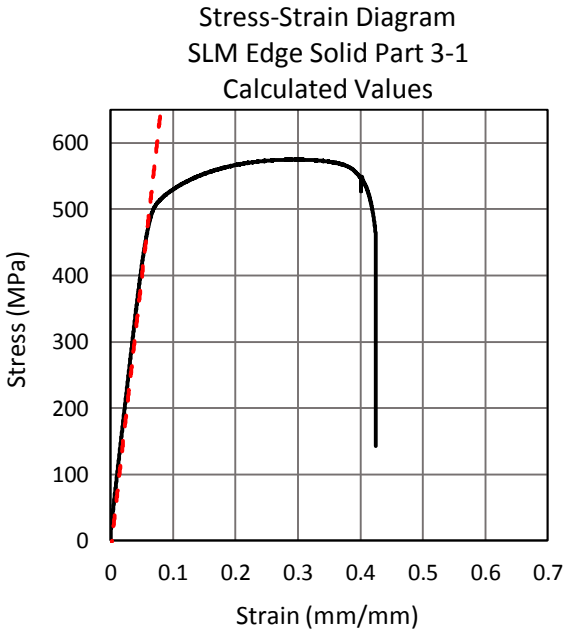
Stress-Strain Diagram
SLM Edge Solid Part 3-1
Calculated Values
Stress (MPa)
0
100
200
300
400
500
600
0
0.1
0.2
0.3
0.4
0.5
0.6
0.7
Strain (mm/mm)

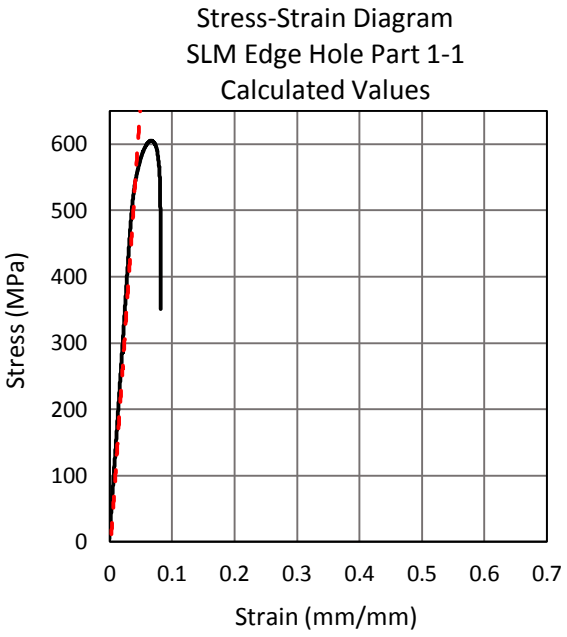
Stress-Strain Diagram
SLM Edge Hole Part 1-1
Calculated Values
Stress (MPa)
0
100
200
300
400
500
600
0
0.1
0.2
0.3
0.4
0.5
0.6
0.7
Strain (mm/mm)

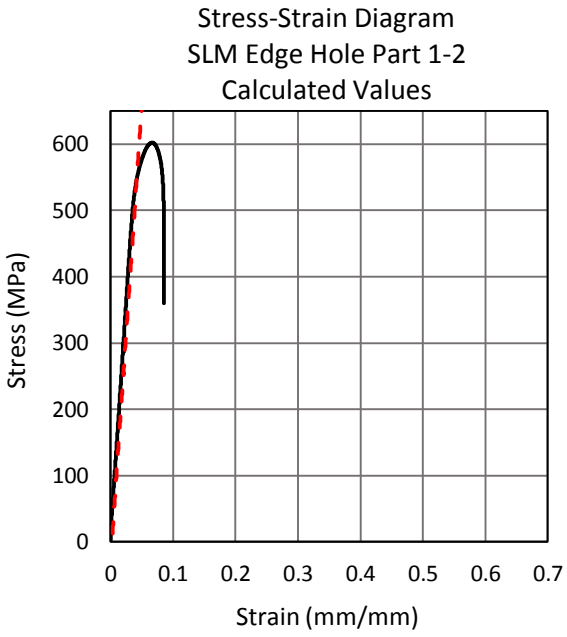
Stress-Strain Diagram
SLM Edge Hole Part 1-2
Calculated Values
Stress (MPa)
0
100
200
300
400
500
600
0
0.1
0.2
0.3
0.4
0.5
0.6
0.7
Strain (mm/mm)

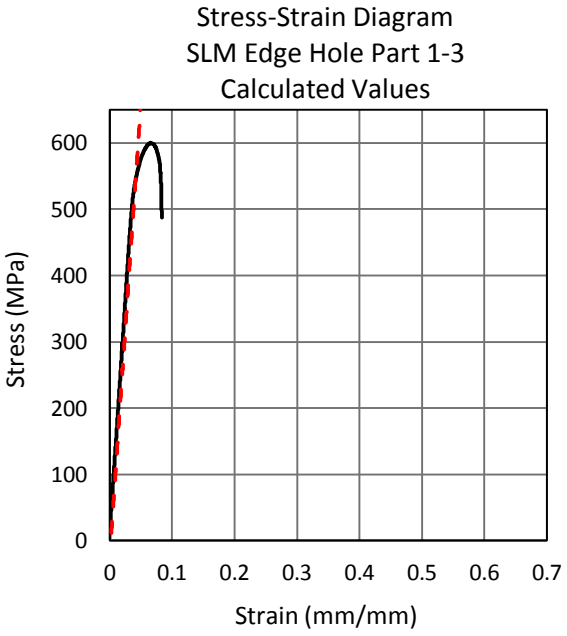
Stress-Strain Diagram
SLM Edge Hole Part 1-3
Calculated Values
Stress (MPa)
0
100
200
300
400
500
600
0
0.1
0.2
0.3
0.4
0.5
0.6
0.7
Strain (mm/mm)

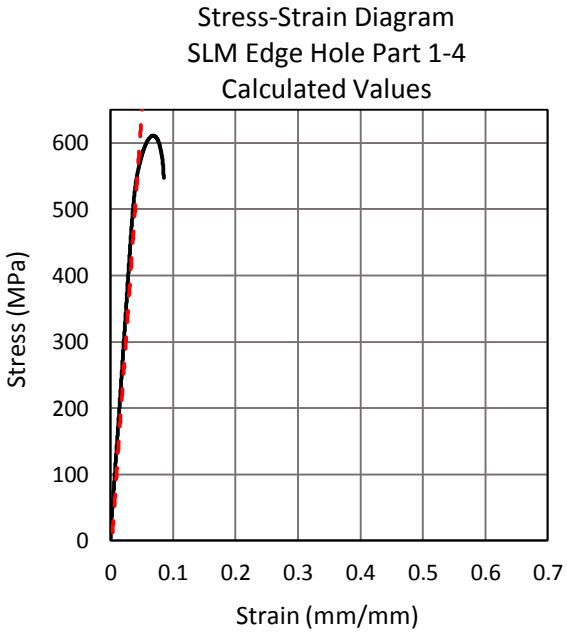
Stress-Strain Diagram
SLM Edge Hole Part 1-4
Calculated Values
Stress (MPa)
0
100
200
300
400
500
600
0
0.1
0.2
0.3
0.4
0.5
0.6
0.7
Strain (mm/mm)

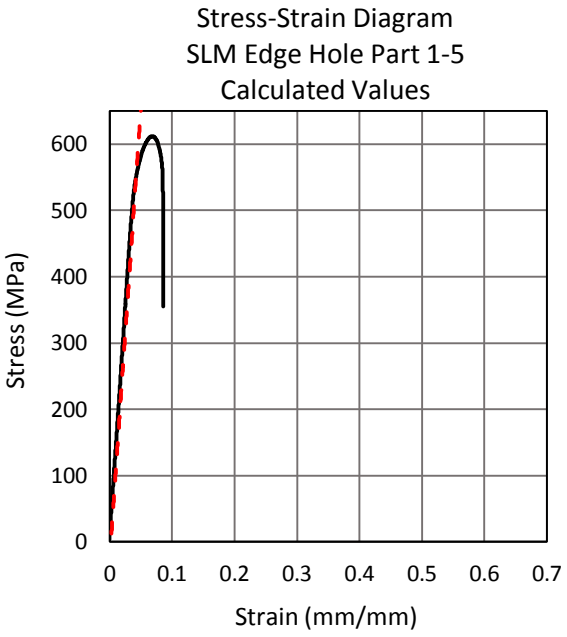
Stress-Strain Diagram
SLM Edge Hole Part 1-5
Calculated Values
Stress (MPa)
0
100
200
300
400
500
600
0
0.1
0.2
0.3
0.4
0.5
0.6
0.7
Strain (mm/mm)

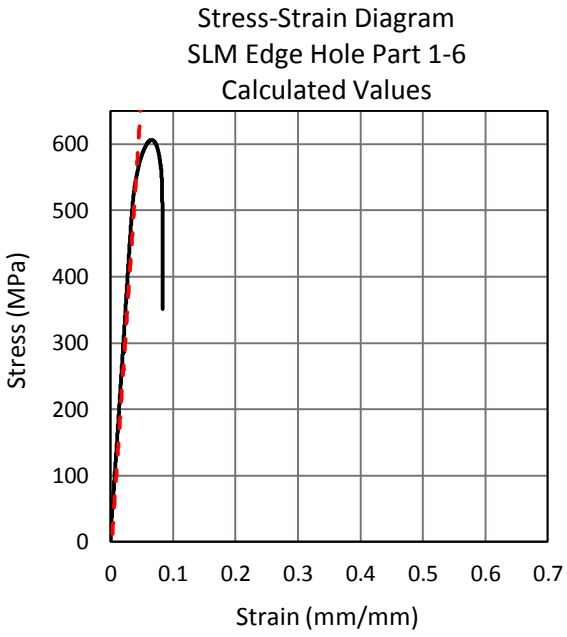
Stress-Strain Diagram
SLM Edge Hole Part 1-6
Calculated Values
Stress (MPa)
0
100
200
300
400
500
600
0
0.1
0.2
0.3
0.4
0.5
0.6
0.7
Strain (mm/mm)

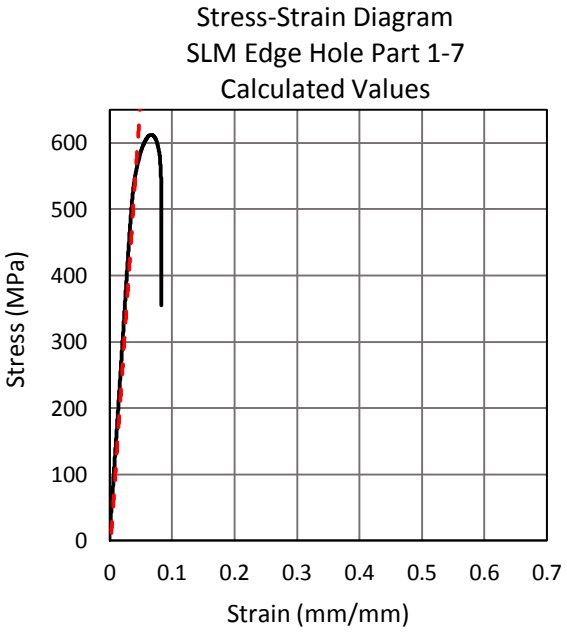
Stress-Strain Diagram
SLM Edge Hole Part 1-7
Calculated Values
Stress (MPa)
0
100
200
300
400
500
600
0
0.1
0.2
0.3
0.4
0.5
0.6
0.7
Strain (mm/mm)

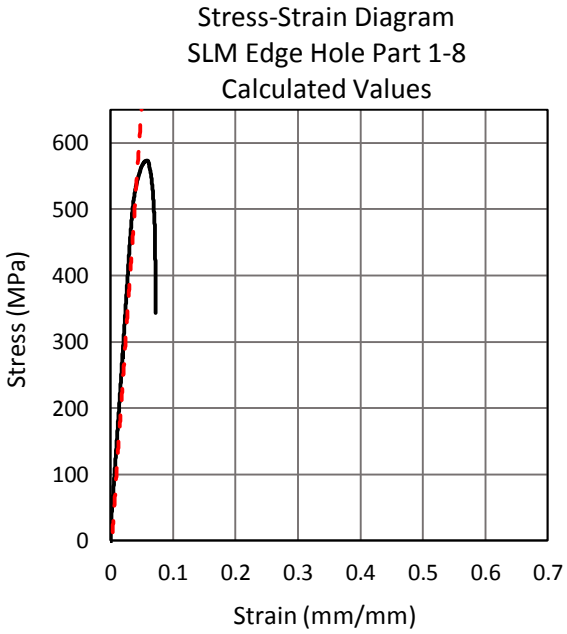
Stress-Strain Diagram
SLM Edge Hole Part 1-8
Calculated Values
Stress (MPa)
0
100
200
300
400
500
600
0
0.1
0.2
0.3
0.4
0.5
0.6
0.7
Strain (mm/mm)

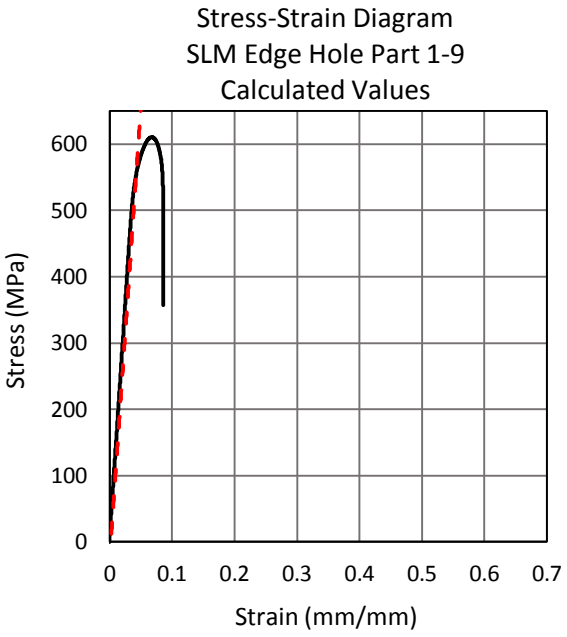
Stress-Strain Diagram
SLM Edge Hole Part 1-9
Calculated Values
Stress (MPa)
0
100
200
300
400
500
600
0
0.1
0.2
0.3
0.4
0.5
0.6
0.7
Strain (mm/mm)

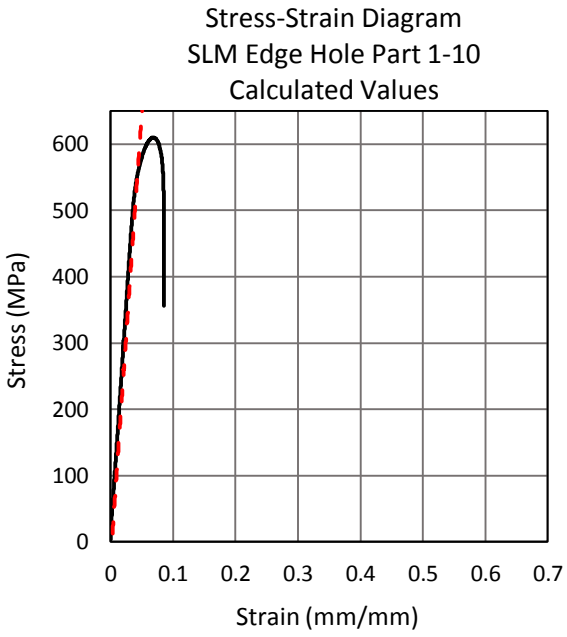
Stress-Strain Diagram
SLM Edge Hole Part 1-10
Calculated Values
Stress (MPa)
0
100
200
300
400
500
600
0
0.1
0.2
0.3
0.4
0.5
0.6
0.7
Strain (mm/mm)

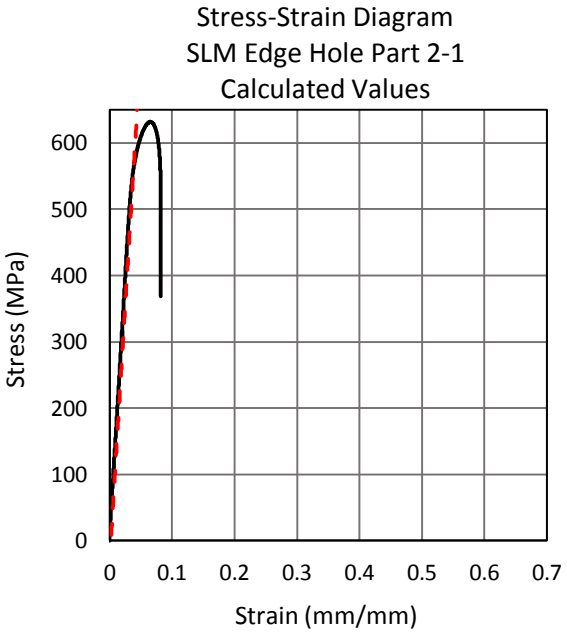
Stress-Strain Diagram
SLM Edge Hole Part 2-1
Calculated Values
Stress (MPa)
0
100
200
300
400
500
600
0
0.1
0.2
0.3
0.4
0.5
0.6
0.7
Strain (mm/mm)

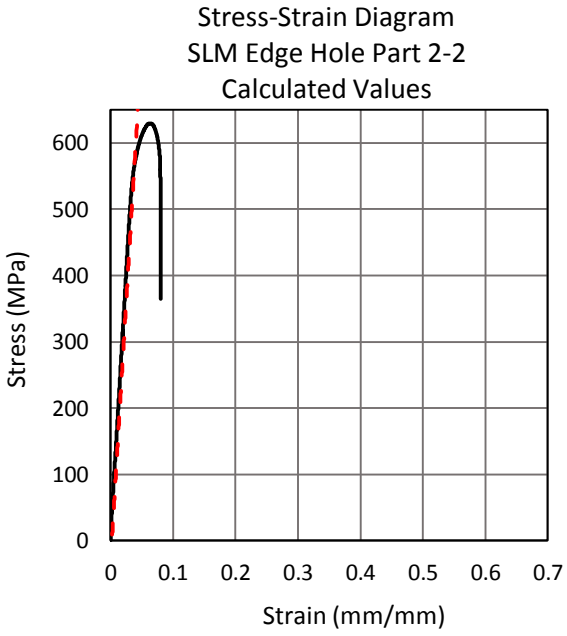
Stress-Strain Diagram
SLM Edge Hole Part 2-2
Calculated Values
Stress (MPa)
0
100
200
300
400
500
600
0
0.1
0.2
0.3
0.4
0.5
0.6
0.7
Strain (mm/mm)

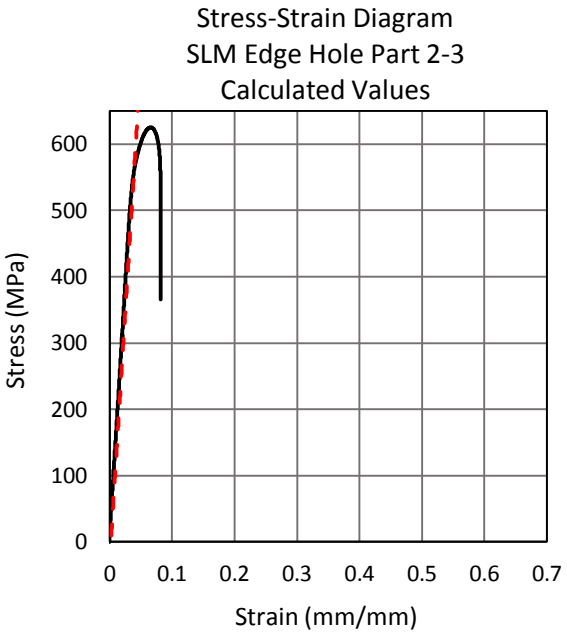
Stress-Strain Diagram
SLM Edge Hole Part 2-3
Calculated Values
Stress (MPa)
0
100
200
300
400
500
600
0
0.1
0.2
0.3
0.4
0.5
0.6
0.7
Strain (mm/mm)

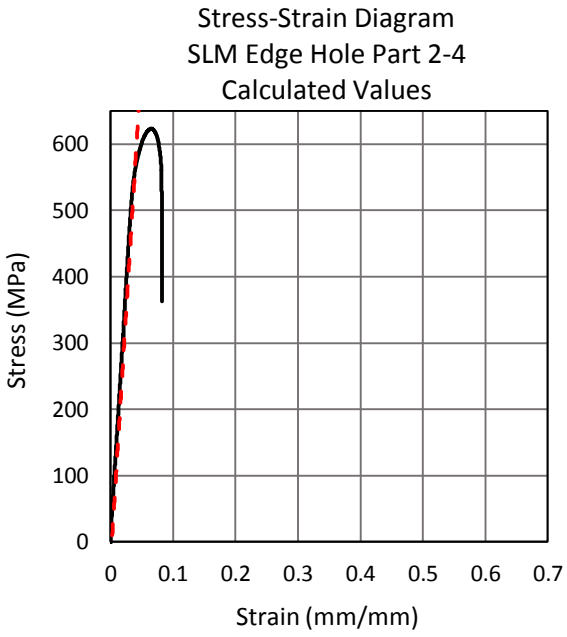
Stress-Strain Diagram
SLM Edge Hole Part 2-4
Calculated Values
Stress (MPa)
0
100
200
300
400
500
600
0
0.1
0.2
0.3
0.4
0.5
0.6
0.7
Strain (mm/mm)

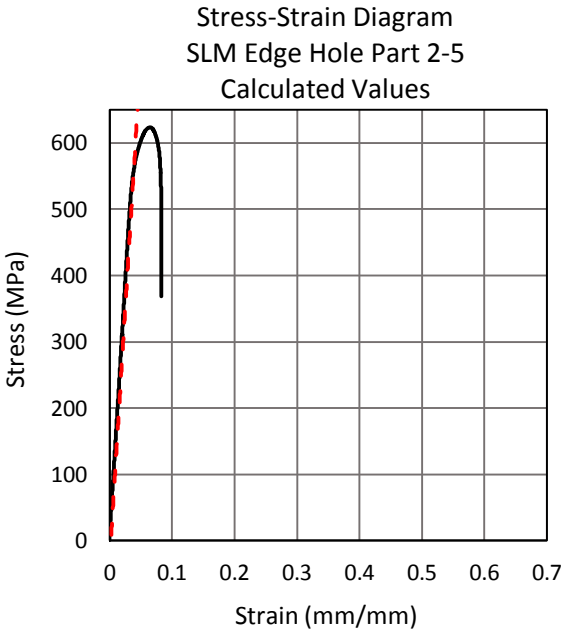
Stress-Strain Diagram
SLM Edge Hole Part 2-5
Calculated Values
Stress (MPa)
0
100
200
300
400
500
600
0
0.1
0.2
0.3
0.4
0.5
0.6
0.7
Strain (mm/mm)

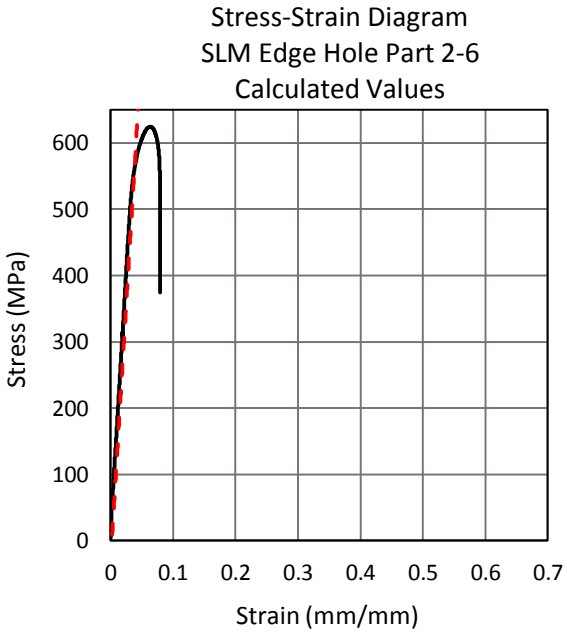
Stress-Strain Diagram
SLM Edge Hole Part 2-6
Calculated Values
Stress (MPa)
0
100
200
300
400
500
600
0
0.1
0.2
0.3
0.4
0.5
0.6
0.7
Strain (mm/mm)

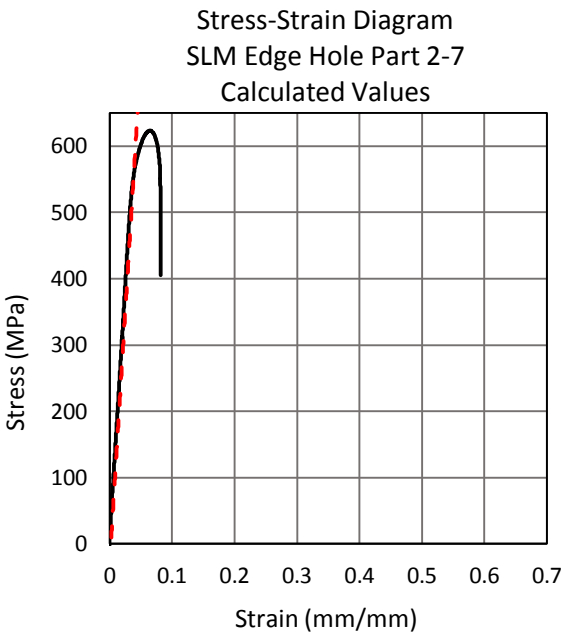
Stress-Strain Diagram
SLM Edge Hole Part 2-7
Calculated Values
Stress (MPa)
600
500
400
300
200
100
0
0
0.1
0.2
0.3
0.4
0.5
0.6
0.7
Strain (mm/mm)

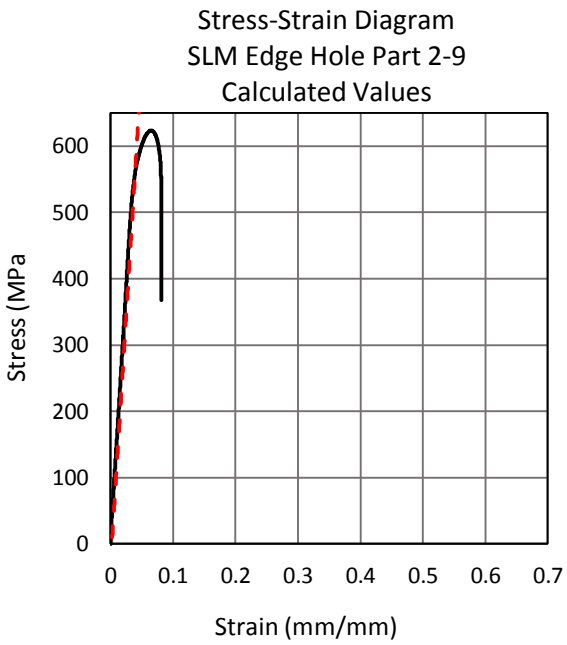
Stress-Strain Diagram
SLM Edge Hole Part 2-9
Calculated Values
Stress (MPa
600
500
400
300
200
100
0
0
0.1
0.2
0.3
0.4
0.5
0.6
0.7
Strain (mm/mm)

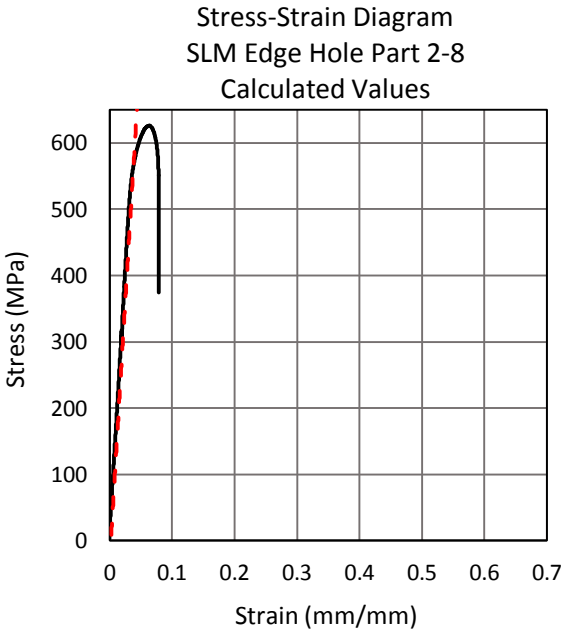
Stress-Strain Diagram
SLM Edge Hole Part 2-8
Calculated Values
Stress (MPa)
600
500
400
300
200
100
0
0
0.1
0.2
0.3
0.4
0.5
0.6
0.7
Strain (mm/mm)

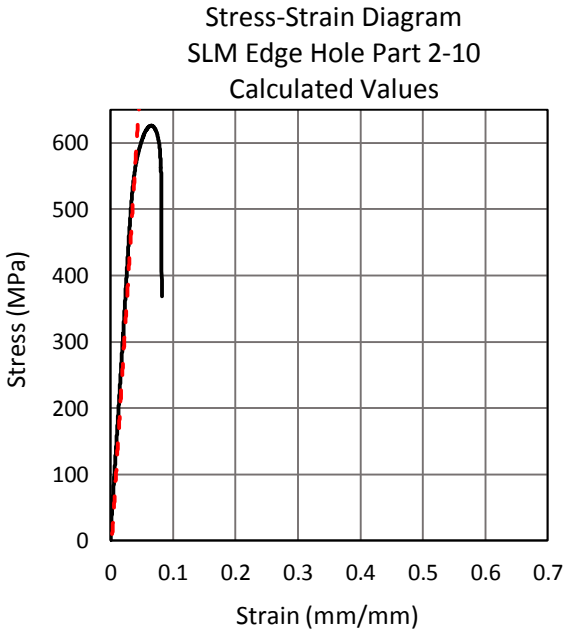
Stress-Strain Diagram
SLM Edge Hole Part 2-10
Calculated Values
Stress (MPa)
600
500
400
300
200
100
0
0
0.1
0.2
0.3
0.4
0.5
0.6
0.7
Strain (mm/mm)

Stress – Strain Graphs of SLM Flat Parts

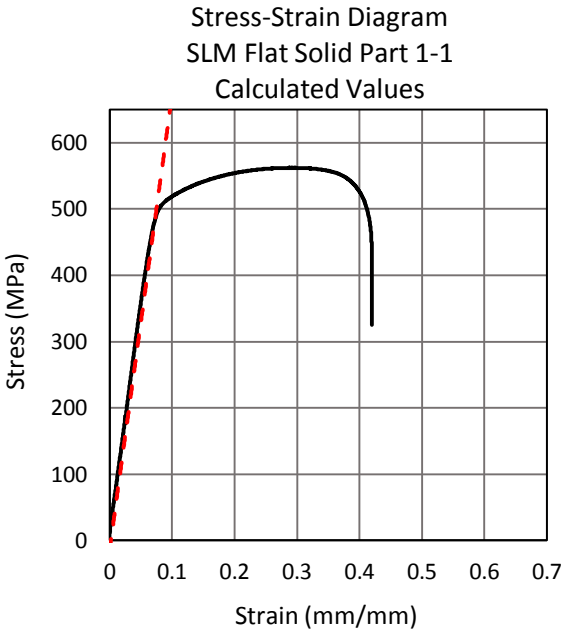

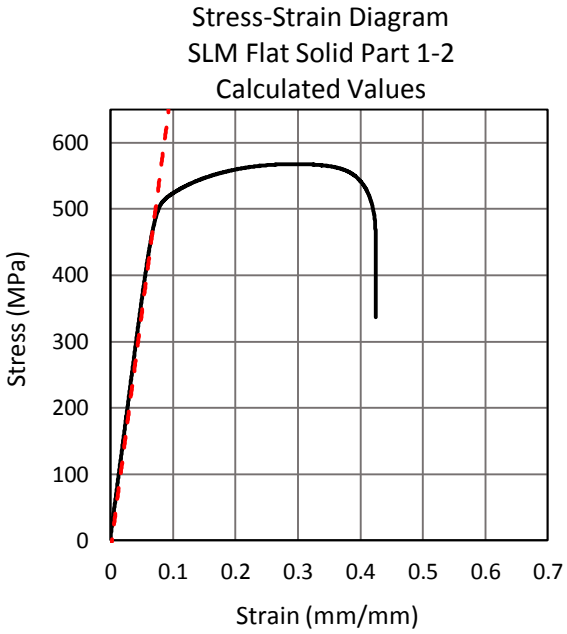

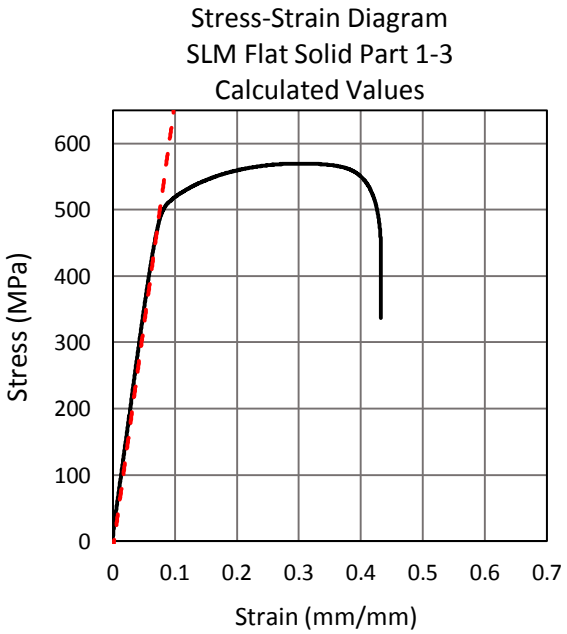

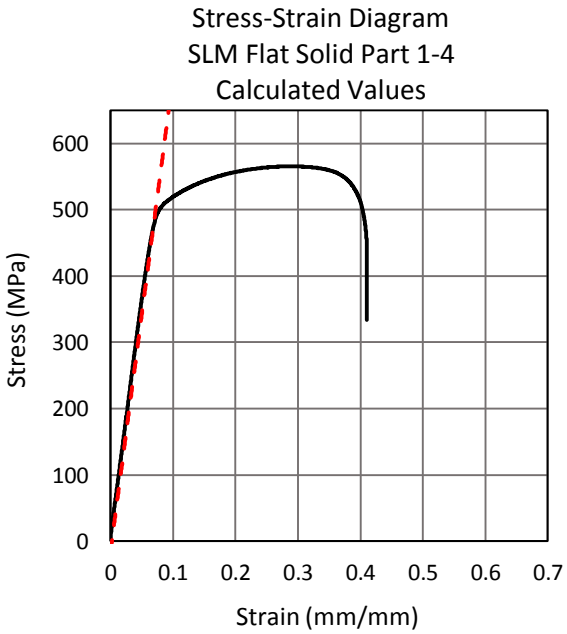

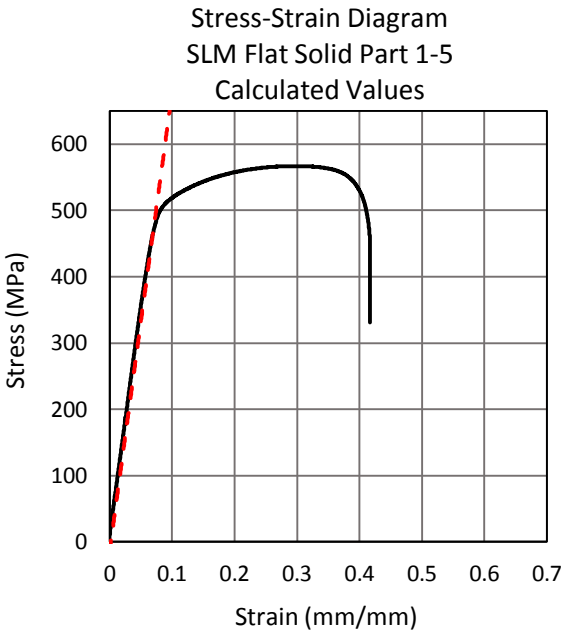
Stress-Strain Diagram
SLM Flat Solid Part 1-5
Calculated Values
Stress (MPa)
0
100
200
300
400
500
600
0
0.1
0.2
0.3
0.4
0.5
0.6
0.7
Strain (mm/mm)

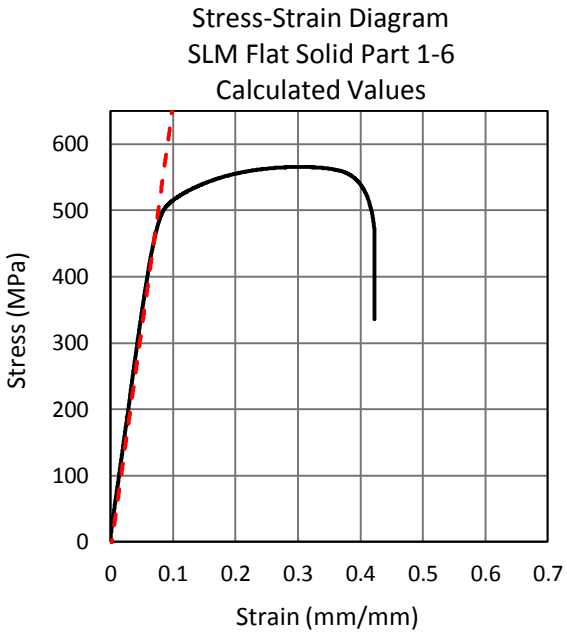
Stress-Strain Diagram
SLM Flat Solid Part 1-6
Calculated Values
Stress (MPa)
0
100
200
300
400
500
600
0
0.1
0.2
0.3
0.4
0.5
0.6
0.7
Strain (mm/mm)

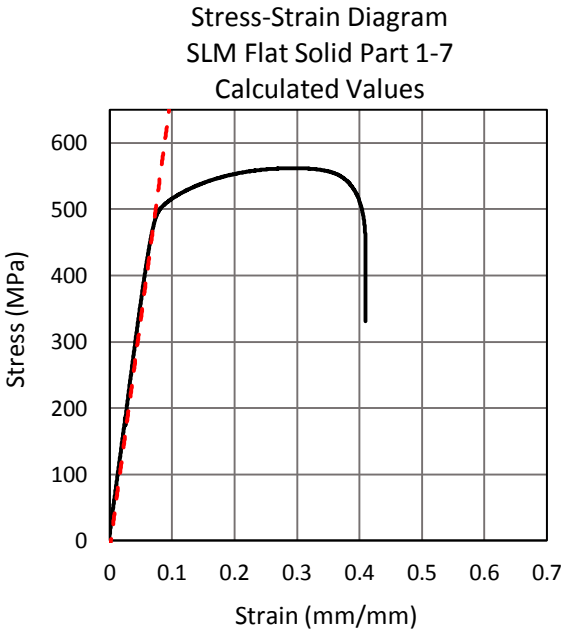
Stress-Strain Diagram
SLM Flat Solid Part 1-7
Calculated Values
Stress (MPa)
0
100
200
300
400
500
600
0
0.1
0.2
0.3
0.4
0.5
0.6
0.7
Strain (mm/mm)

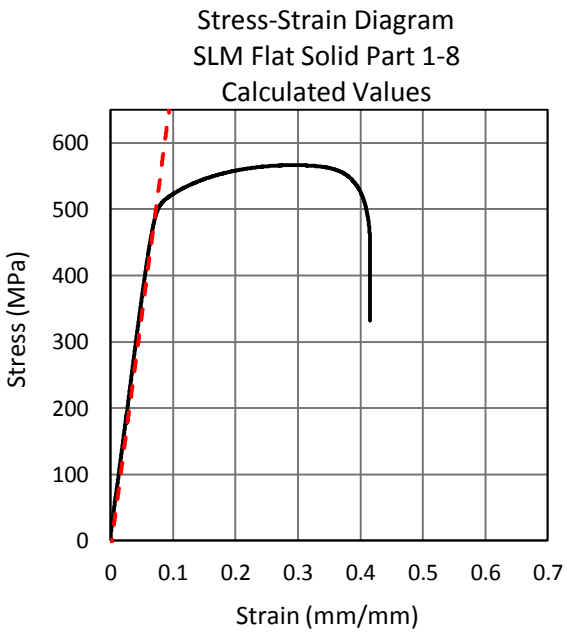
Stress-Strain Diagram
SLM Flat Solid Part 1-8
Calculated Values
Stress (MPa)
0
100
200
300
400
500
600
0
0.1
0.2
0.3
0.4
0.5
0.6
0.7
Strain (mm/mm)

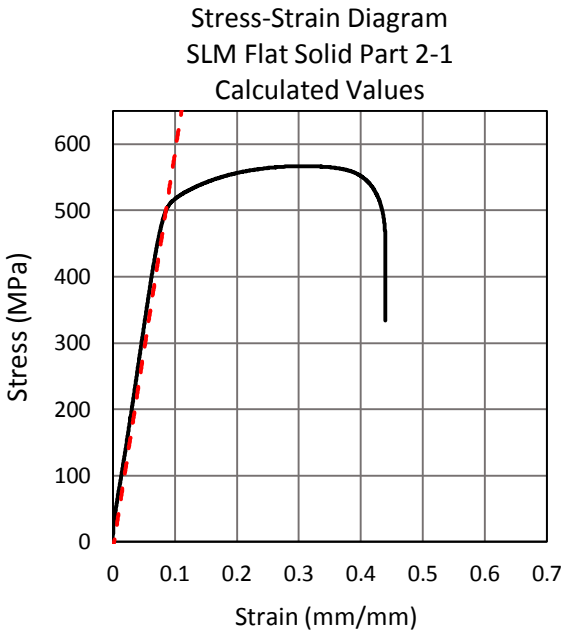
Stress-Strain Diagram
SLM Flat Solid Part 2-1
Calculated Values
Stress (MPa)
0
100
200
300
400
500
600
0
0.1
0.2
0.3
0.4
0.5
0.6
0.7
Strain (mm/mm)

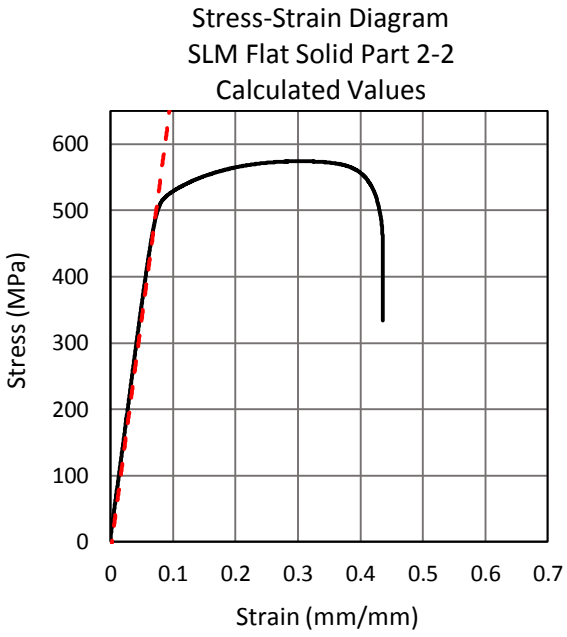
Stress-Strain Diagram
SLM Flat Solid Part 2-2
Calculated Values
Stress (MPa)
0
100
200
300
400
500
600
0
0.1
0.2
0.3
0.4
0.5
0.6
0.7
Strain (mm/mm)

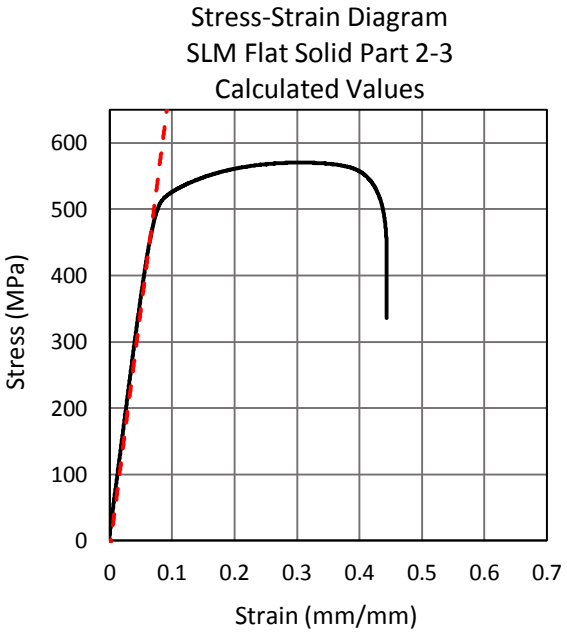
Stress-Strain Diagram
SLM Flat Solid Part 2-3
Calculated Values
Stress (MPa)
0
100
200
300
400
500
600
0
0.1
0.2
0.3
0.4
0.5
0.6
0.7
Strain (mm/mm)

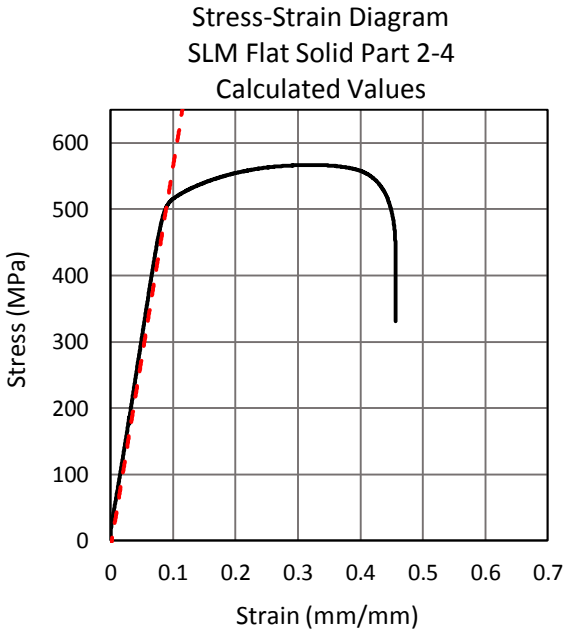
Stress-Strain Diagram
SLM Flat Solid Part 2-4
Calculated Values
Stress (MPa)
0
100
200
300
400
500
600
0
0.1
0.2
0.3
0.4
0.5
0.6
0.7
Strain (mm/mm)

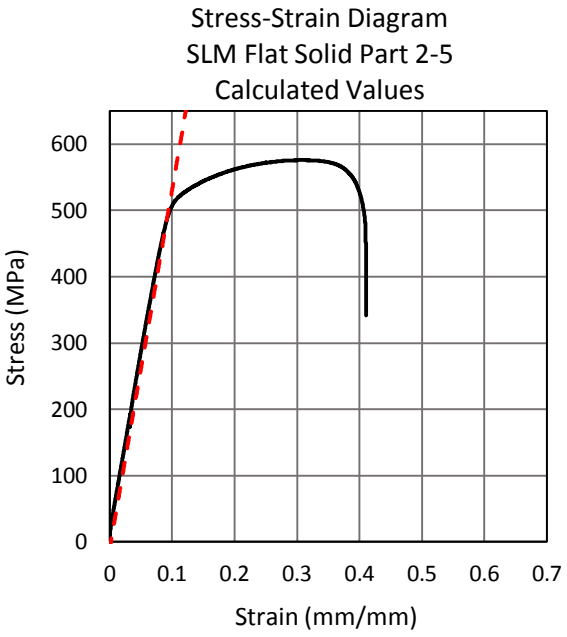
Stress-Strain Diagram
SLM Flat Solid Part 2-5
Calculated Values
Stress (MPa)
0
100
200
300
400
500
600
0
0.1
0.2
0.3
0.4
0.5
0.6
0.7
Strain (mm/mm)

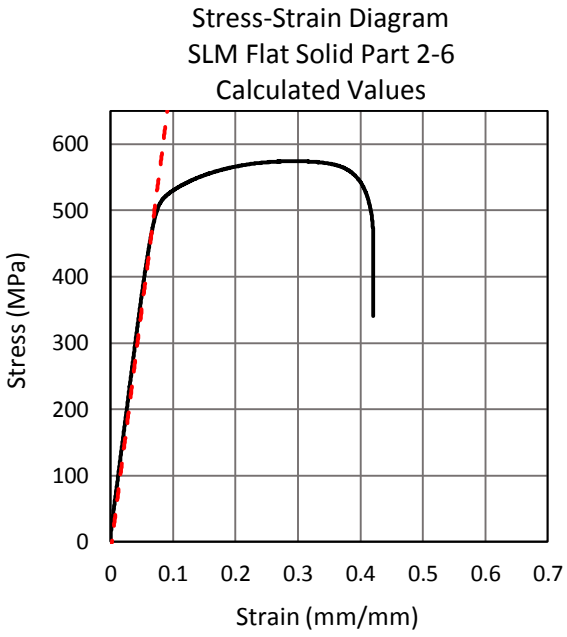
Stress-Strain Diagram
SLM Flat Solid Part 2-6
Calculated Values
Stress (MPa)
0
100
200
300
400
500
600
0
0.1
0.2
0.3
0.4
0.5
0.6
0.7
Strain (mm/mm)

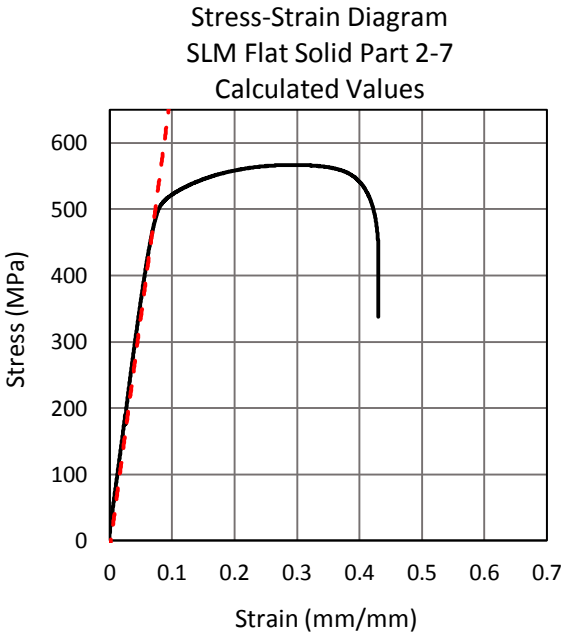
Stress-Strain Diagram
SLM Flat Solid Part 2-7
Calculated Values
Stress (MPa)
0
100
200
300
400
500
600
0
0.1
0.2
0.3
0.4
0.5
0.6
0.7
Strain (mm/mm)

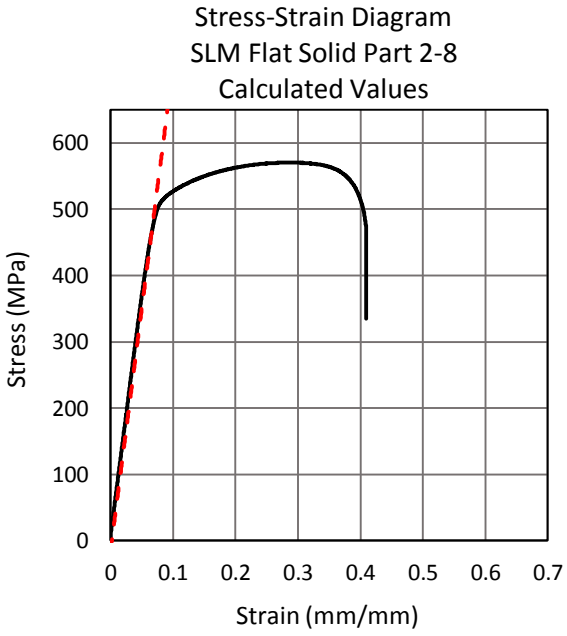
Stress-Strain Diagram
SLM Flat Solid Part 2-8
Calculated Values
Stress (MPa)
0
100
200
300
400
500
600
0
0.1
0.2
0.3
0.4
0.5
0.6
0.7
Strain (mm/mm)

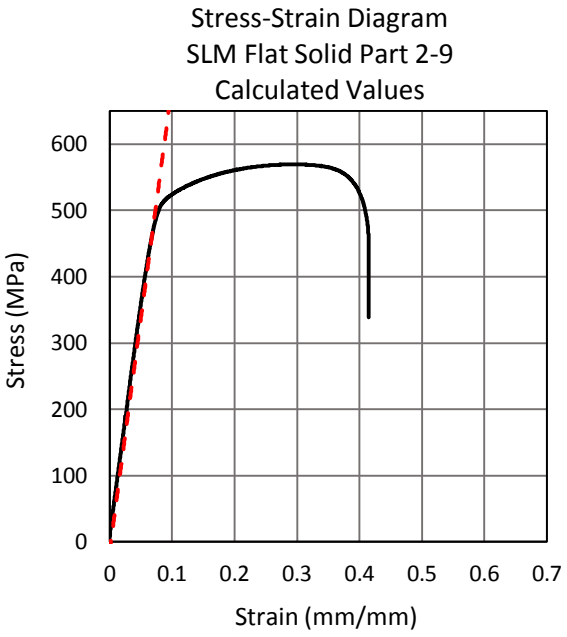
Stress-Strain Diagram
SLM Flat Solid Part 2-9
Calculated Values
Stress (MPa)
0
100
200
300
400
500
600
0
0.1
0.2
0.3
0.4
0.5
0.6
0.7
Strain (mm/mm)

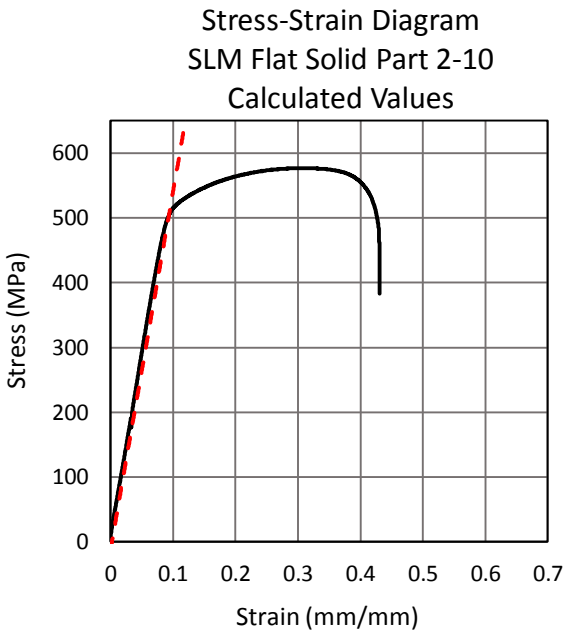
Stress-Strain Diagram
SLM Flat Solid Part 2-10
Calculated Values
Stress (MPa)
0
100
200
300
400
500
600
0
0.1
0.2
0.3
0.4
0.5
0.6
0.7
Strain (mm/mm)

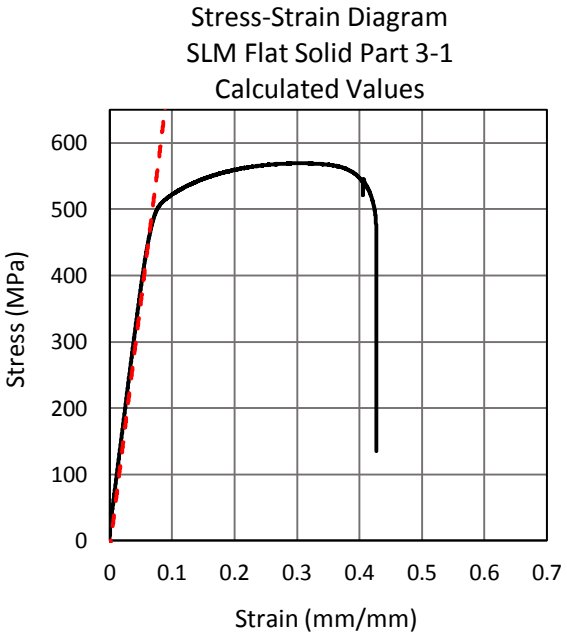
Stress-Strain Diagram
SLM Flat Solid Part 3-1
Calculated Values
Stress (MPa)
0
100
200
300
400
500
600
0
0.1
0.2
0.3
0.4
0.5
0.6
0.7
Strain (mm/mm)

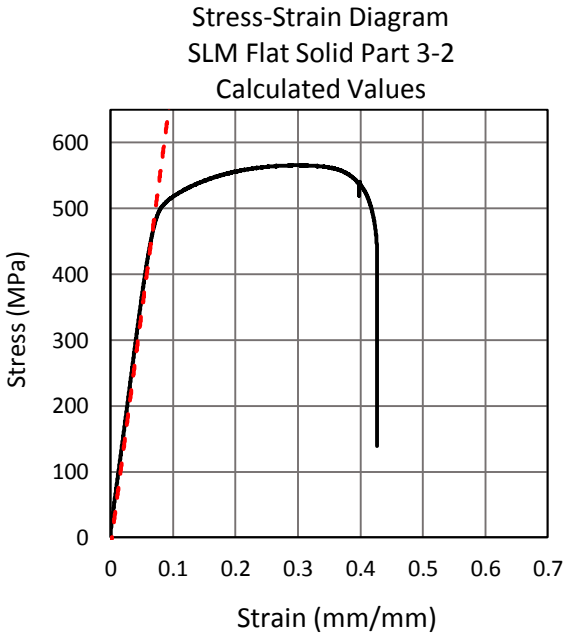
Stress-Strain Diagram
SLM Flat Solid Part 3-2
Calculated Values
Stress (MPa)
0
100
200
300
400
500
600
0
0.1
0.2
0.3
0.4
0.5
0.6
0.7
Strain (mm/mm)

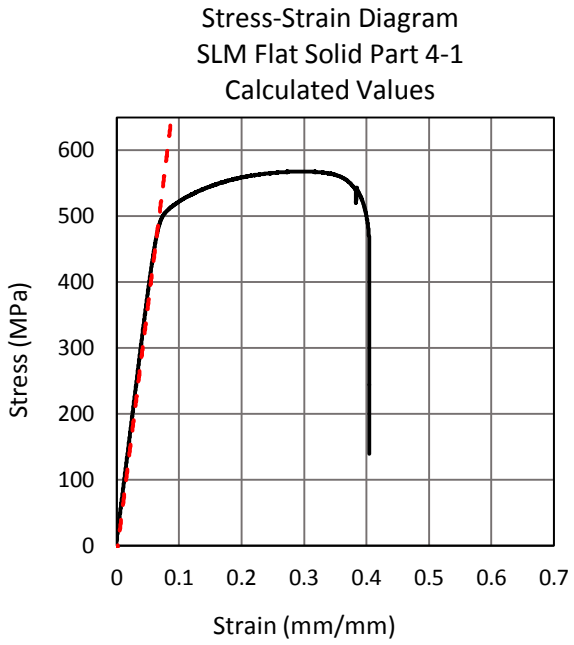
Stress-Strain Diagram
SLM Flat Solid Part 4-1
Calculated Values
Stress (MPa)
0
100
200
300
400
500
600
0
0.1
0.2
0.3
0.4
0.5
0.6
0.7
Strain (mm/mm)

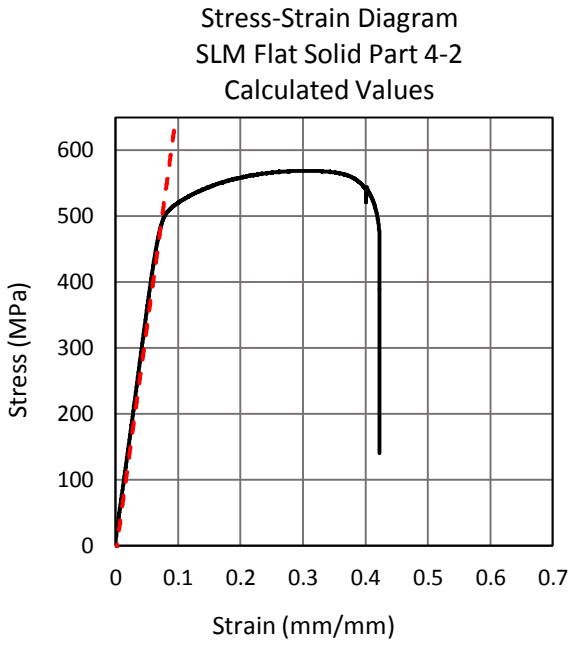
Stress-Strain Diagram
SLM Flat Solid Part 4-2
Calculated Values
Stress (MPa)
0
100
200
300
400
500
600
0
0.1
0.2
0.3
0.4
0.5
0.6
0.7
Strain (mm/mm)

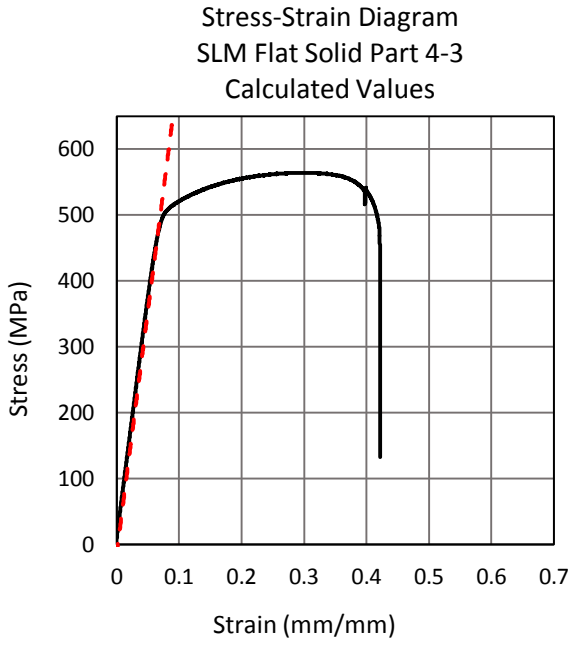
Stress-Strain Diagram
SLM Flat Solid Part 4-3
Calculated Values
Stress (MPa)
0
100
200
300
400
500
600
0
0.1
0.2
0.3
0.4
0.5
0.6
0.7
Strain (mm/mm)

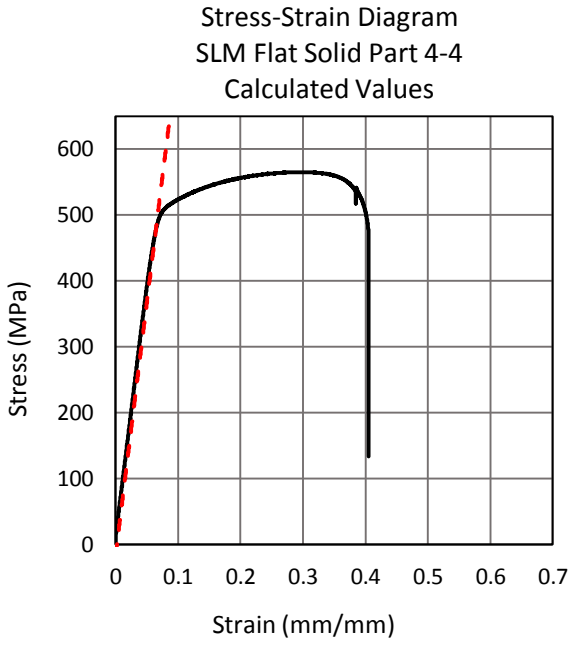
Stress-Strain Diagram
SLM Flat Solid Part 4-4
Calculated Values
Stress (MPa)
0
100
200
300
400
500
600
0
0.1
0.2
0.3
0.4
0.5
0.6
0.7
Strain (mm/mm)

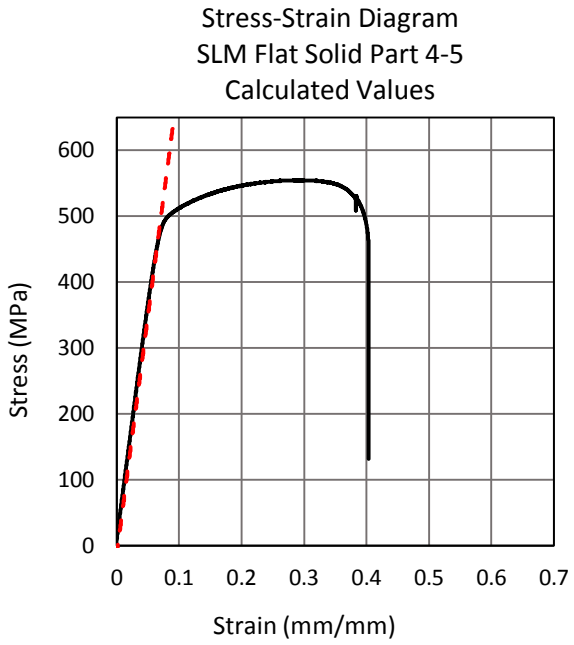
Stress-Strain Diagram
SLM Flat Solid Part 4-5
Calculated Values
Stress (MPa)
600
500
400
300
200
100
0
0
0.1
0.2
0.3
0.4
0.5
0.6
0.7
Strain (mm/mm)

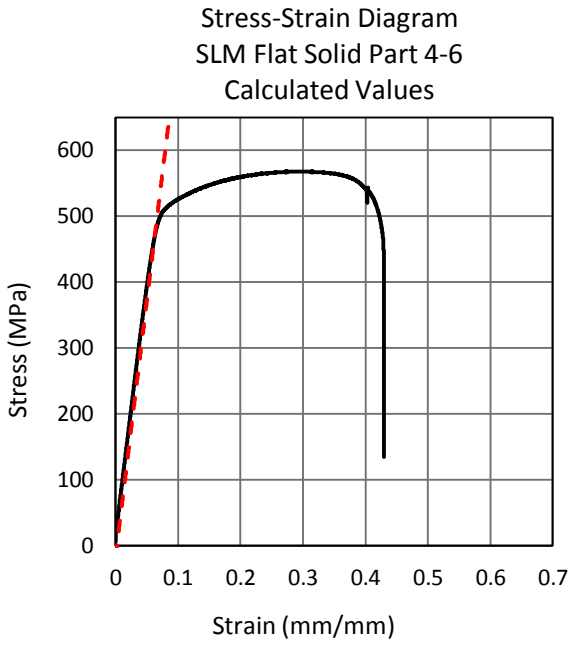
Stress-Strain Diagram
SLM Flat Solid Part 4-6
Calculated Values
Stress (MPa)
600
500
400
300
200
100
0
0
0.1
0.2
0.3
0.4
0.5
0.6
0.7
Strain (mm/mm)

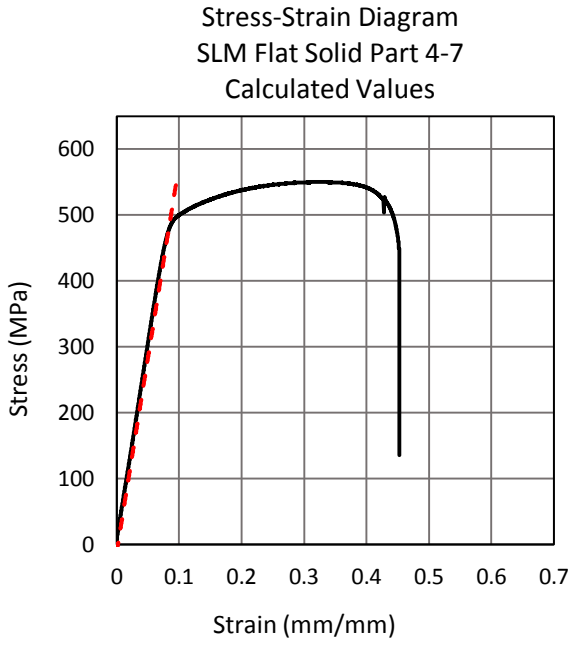
Stress-Strain Diagram
SLM Flat Solid Part 4-7
Calculated Values
Stress (MPa)
600
500
400
300
200
100
0
0
0.1
0.2
0.3
0.4
0.5
0.6
0.7
Strain (mm/mm)

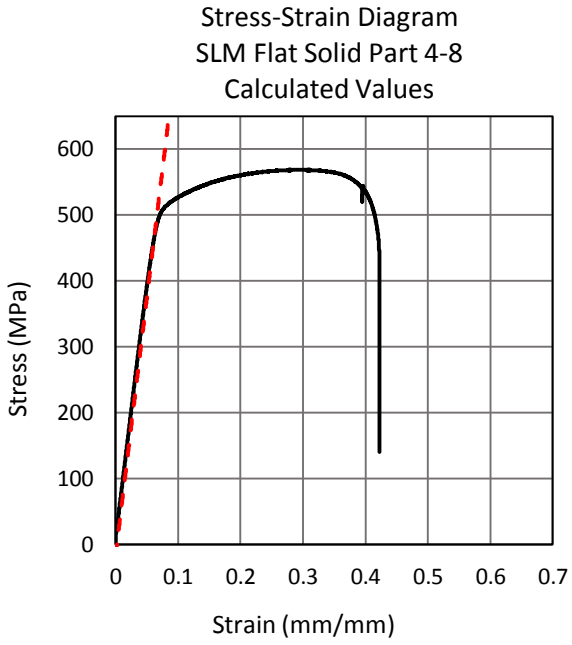
Stress-Strain Diagram
SLM Flat Solid Part 4-8
Calculated Values
Stress (MPa)
600
500
400
300
200
100
0
0
0.1
0.2
0.3
0.4
0.5
0.6
0.7
Strain (mm/mm)

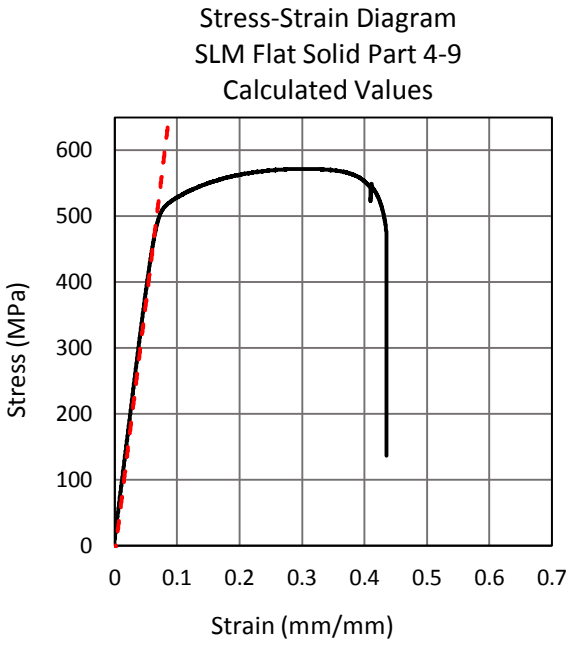
Stress-Strain Diagram
SLM Flat Solid Part 4-9
Calculated Values
Stress (MPa)
0
100
200
300
400
500
600
0
0.1
0.2
0.3
0.4
0.5
0.6
0.7
Strain (mm/mm)

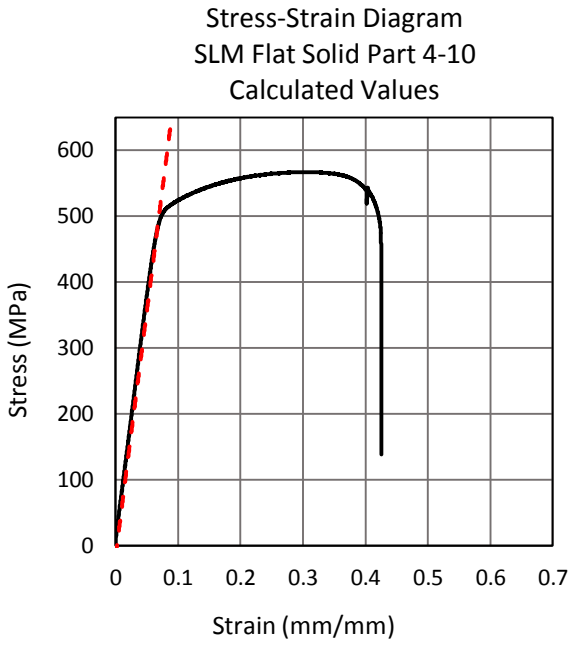
Stress-Strain Diagram
SLM Flat Solid Part 4-10
Calculated Values
Stress (MPa)
0
100
200
300
400
500
600
0
0.1
0.2
0.3
0.4
0.5
0.6
0.7
Strain (mm/mm)

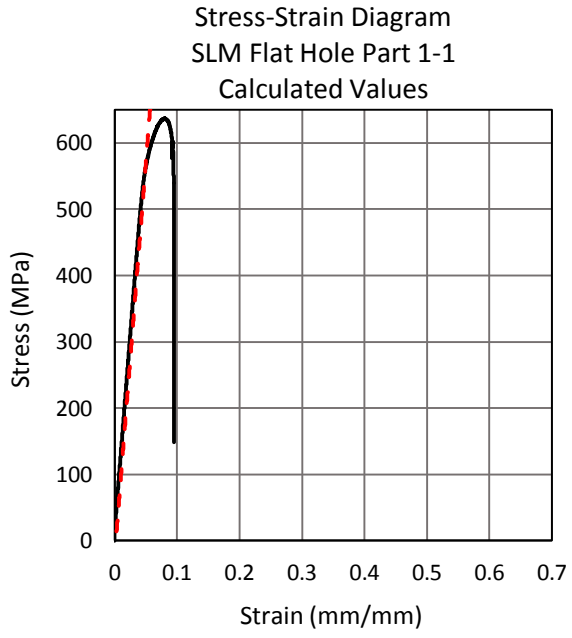
Stress-Strain Diagram
SLM Flat Hole Part 1-1
Calculated Values
Stress (MPa)
0
100
200
300
400
500
600
0
0.1
0.2
0.3
0.4
0.5
0.6
0.7
Strain (mm/mm)

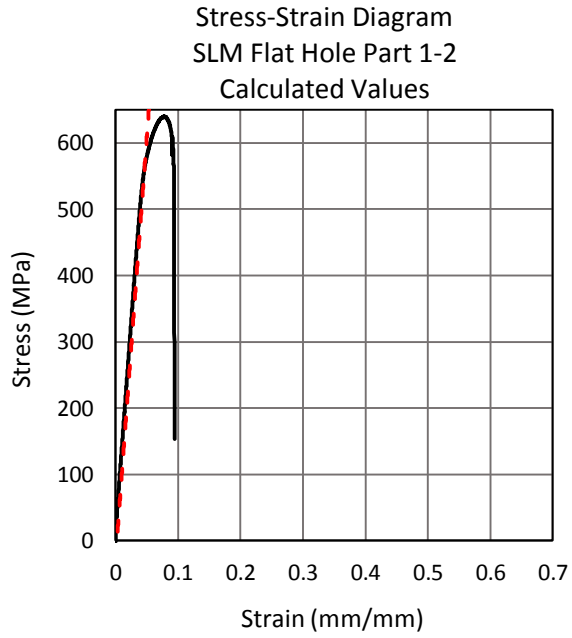
Stress-Strain Diagram
SLM Flat Hole Part 1-2
Calculated Values
Stress (MPa)
0
100
200
300
400
500
600
0
0.1
0.2
0.3
0.4
0.5
0.6
0.7
Strain (mm/mm)

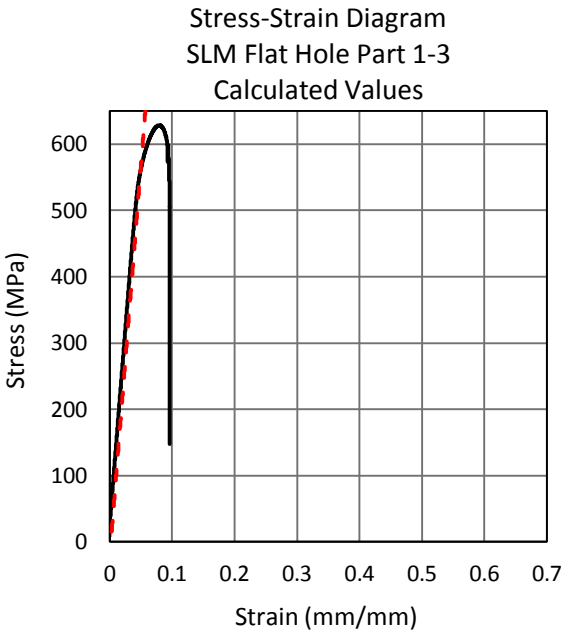
Stress-Strain Diagram
SLM Flat Hole Part 1-3
Calculated Values
Stress (MPa)
600
500
400
300
200
100
0
0
0.1
0.2
0.3
0.4
0.5
0.6
0.7
Strain (mm/mm)

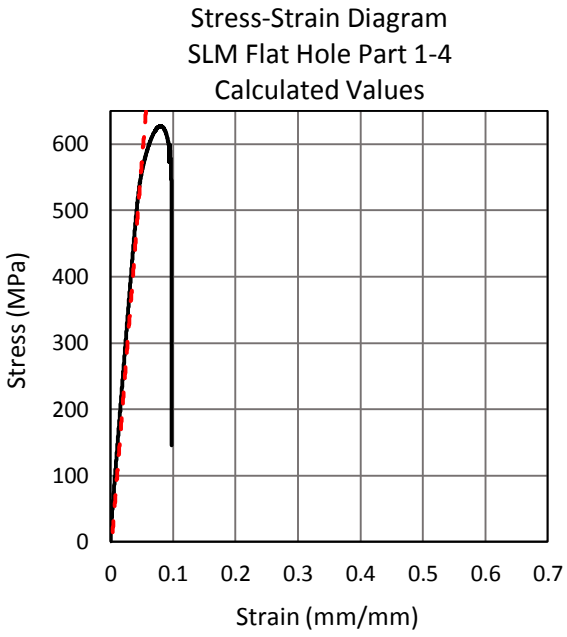
Stress-Strain Diagram
SLM Flat Hole Part 1-4
Calculated Values
Stress (MPa)
600
500
400
300
200
100
0
0
0.1
0.2
0.3
0.4
0.5
0.6
0.7
Strain (mm/mm)

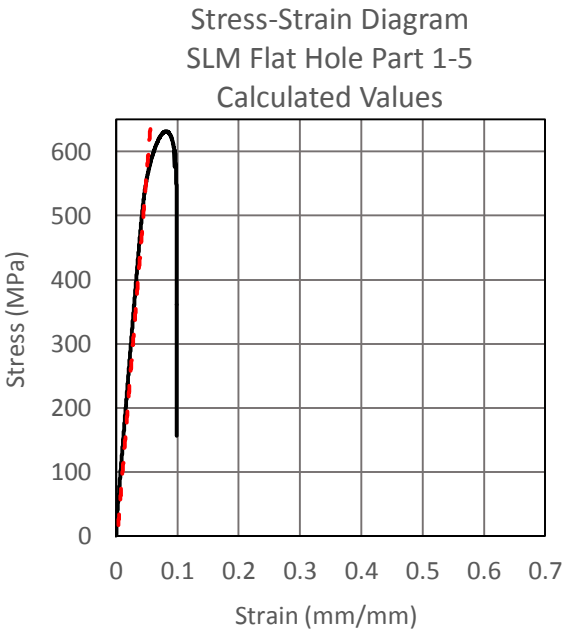
Stress-Strain Diagram
SLM Flat Hole Part 1-5
Calculated Values
Stress (MPa)
600
500
400
300
200
100
0
0
0.1
0.2
0.3
0.4
0.5
0.6
0.7
Strain (mm/mm)

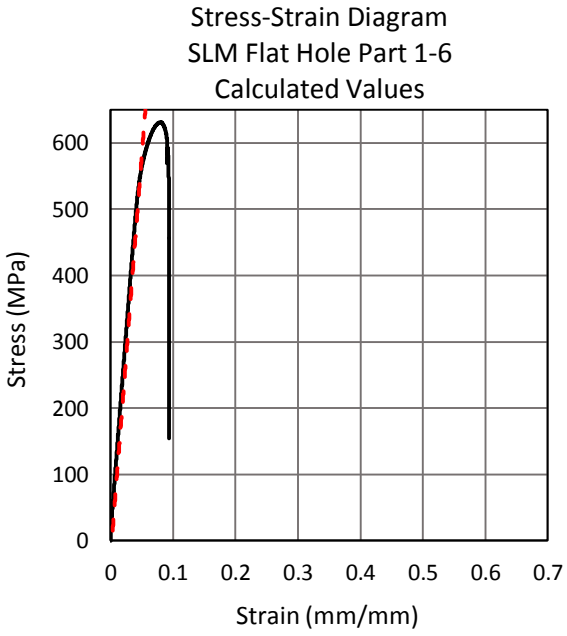
Stress-Strain Diagram
SLM Flat Hole Part 1-6
Calculated Values
Stress (MPa)
600
500
400
300
200
100
0
0
0.1
0.2
0.3
0.4
0.5
0.6
0.7
Strain (mm/mm)

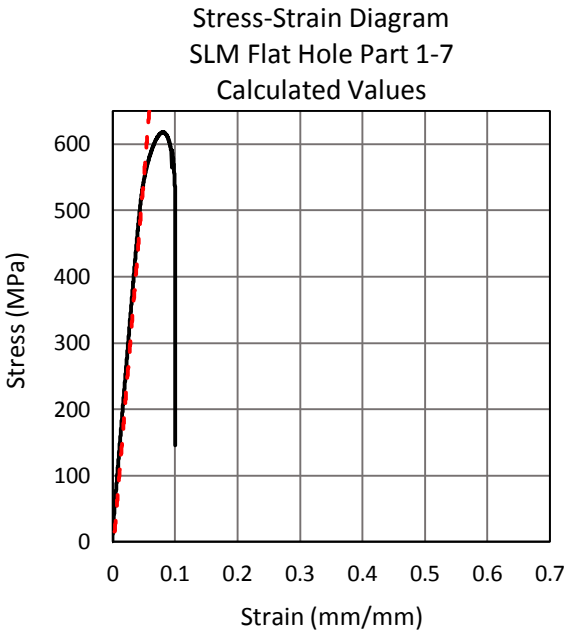
Stress-Strain Diagram
SLM Flat Hole Part 1-7
Calculated Values
Stress (MPa)
0
100
200
300
400
500
600
0
0.1
0.2
0.3
0.4
0.5
0.6
0.7
Strain (mm/mm)

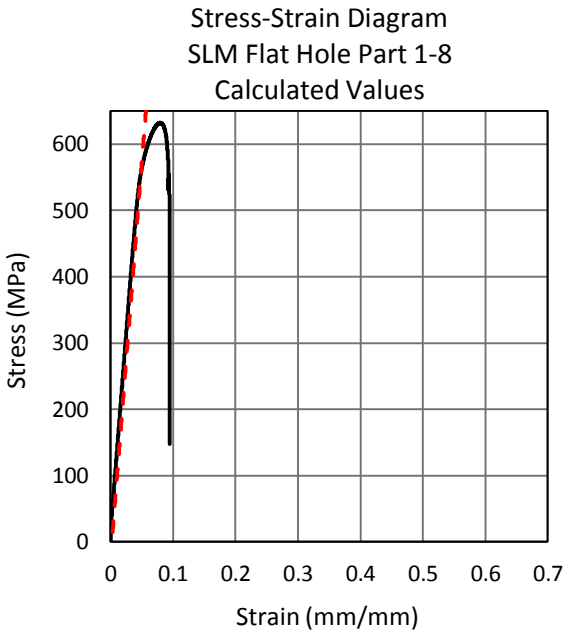
Stress-Strain Diagram
SLM Flat Hole Part 1-8
Calculated Values
Stress (MPa)
0
100
200
300
400
500
600
0
0.1
0.2
0.3
0.4
0.5
0.6
0.7
Strain (mm/mm)

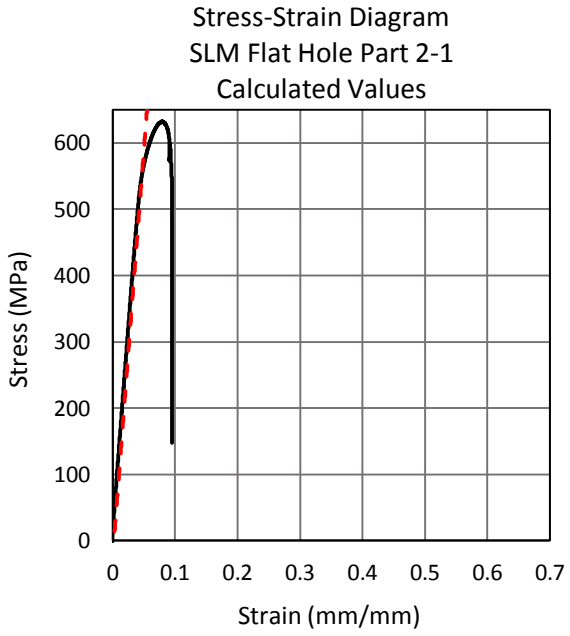
Stress-Strain Diagram
SLM Flat Hole Part 2-1
Calculated Values
Stress (MPa)
0
100
200
300
400
500
600
0
0.1
0.2
0.3
0.4
0.5
0.6
0.7
Strain (mm/mm)

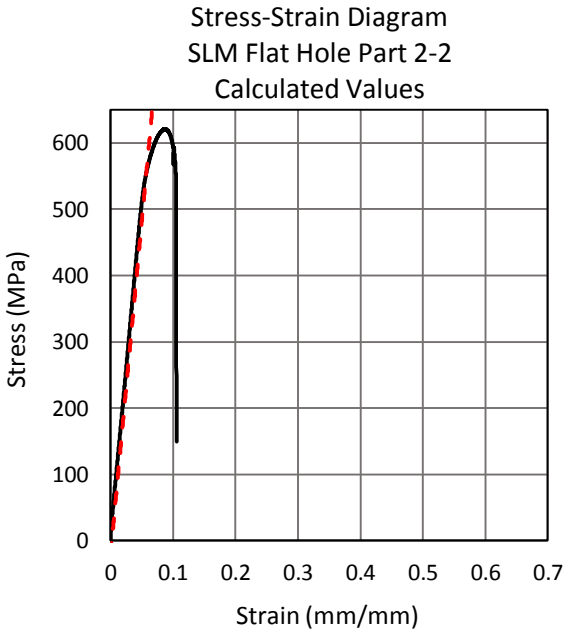
Stress-Strain Diagram
SLM Flat Hole Part 2-2
Calculated Values
Stress (MPa)
0
100
200
300
400
500
600
0
0.1
0.2
0.3
0.4
0.5
0.6
0.7
Strain (mm/mm)

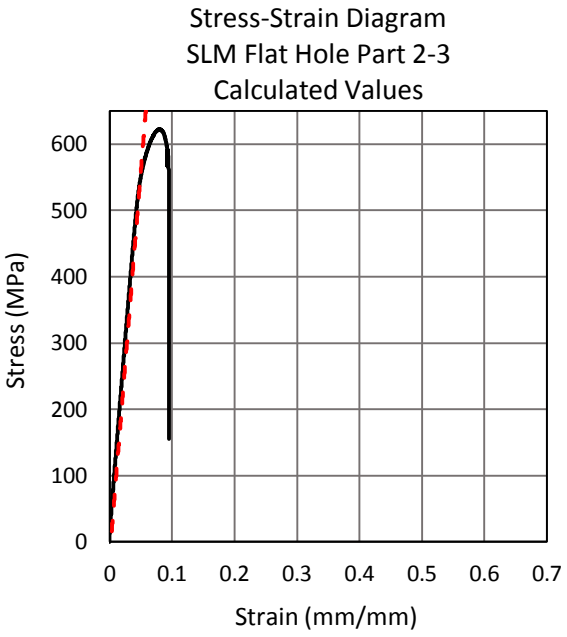
Stress-Strain Diagram
SLM Flat Hole Part 2-3
Calculated Values
Stress (MPa)
0
100
200
300
400
500
600
0
0.1
0.2
0.3
0.4
0.5
0.6
0.7
Strain (mm/mm)

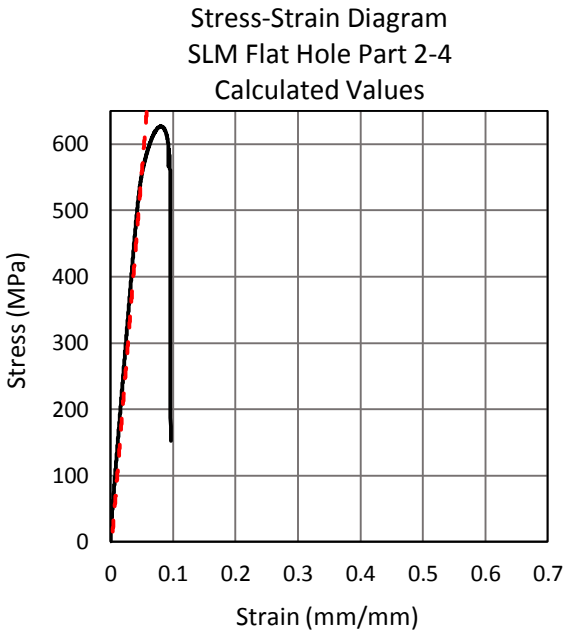
Stress-Strain Diagram
SLM Flat Hole Part 2-4
Calculated Values
Stress (MPa)
0
100
200
300
400
500
600
0
0.1
0.2
0.3
0.4
0.5
0.6
0.7
Strain (mm/mm)

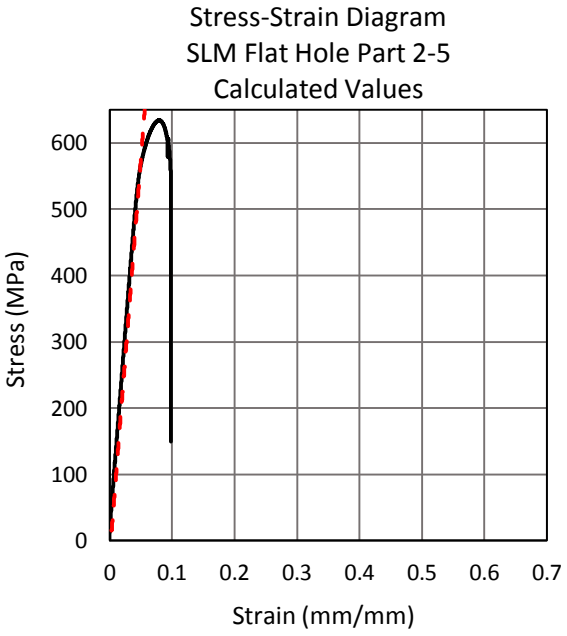
Stress-Strain Diagram
SLM Flat Hole Part 2-5
Calculated Values
Stress (MPa)
0
100
200
300
400
500
600
0
0.1
0.2
0.3
0.4
0.5
0.6
0.7
Strain (mm/mm)

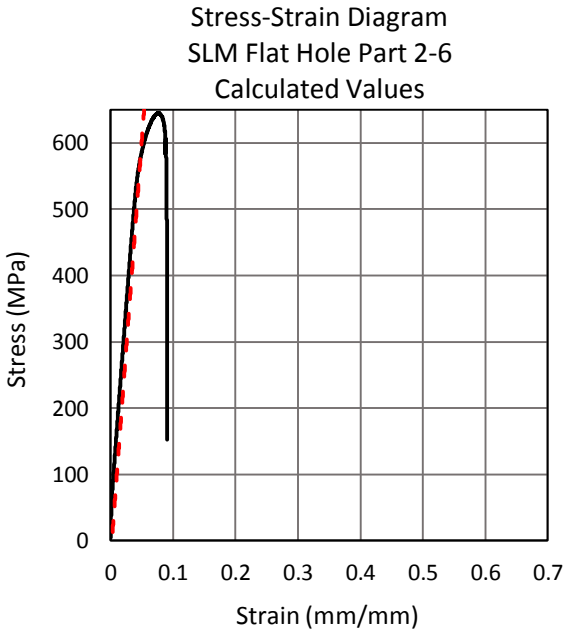
Stress-Strain Diagram
SLM Flat Hole Part 2-6
Calculated Values
Stress (MPa)
0
100
200
300
400
500
600
0
0.1
0.2
0.3
0.4
0.5
0.6
0.7
Strain (mm/mm)

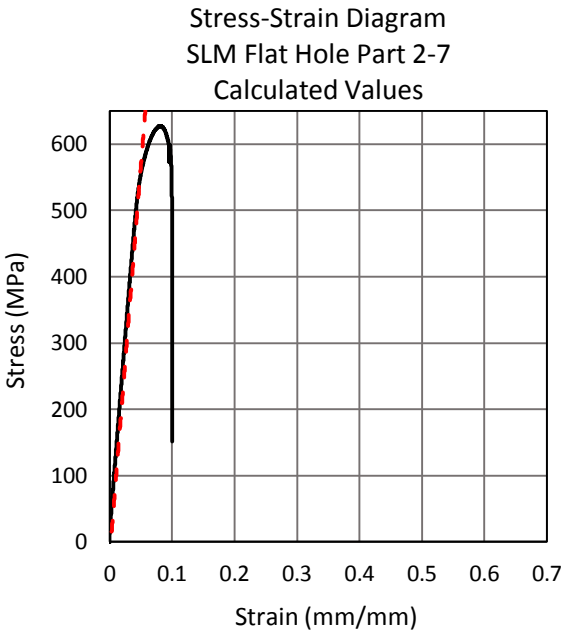
Stress-Strain Diagram
SLM Flat Hole Part 2-7
Calculated Values
Stress (MPa)
0
100
200
300
400
500
600
0
0.1
0.2
0.3
0.4
0.5
0.6
0.7
Strain (mm/mm)

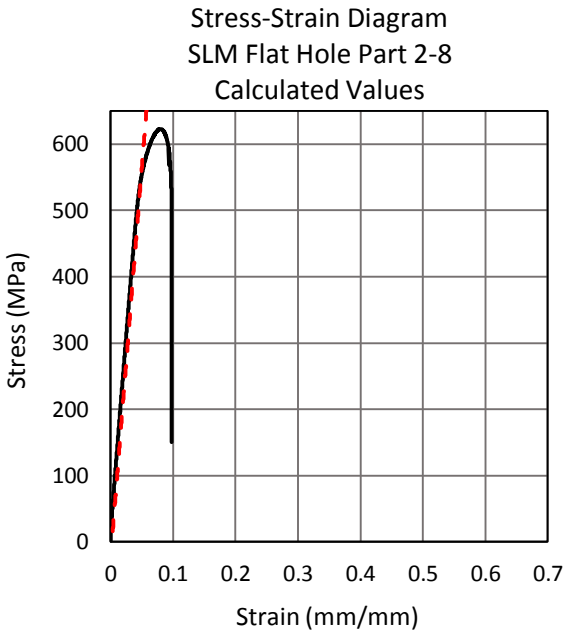
Stress-Strain Diagram
SLM Flat Hole Part 2-8
Calculated Values
Stress (MPa)
0
100
200
300
400
500
600
0
0.1
0.2
0.3
0.4
0.5
0.6
0.7
Strain (mm/mm)

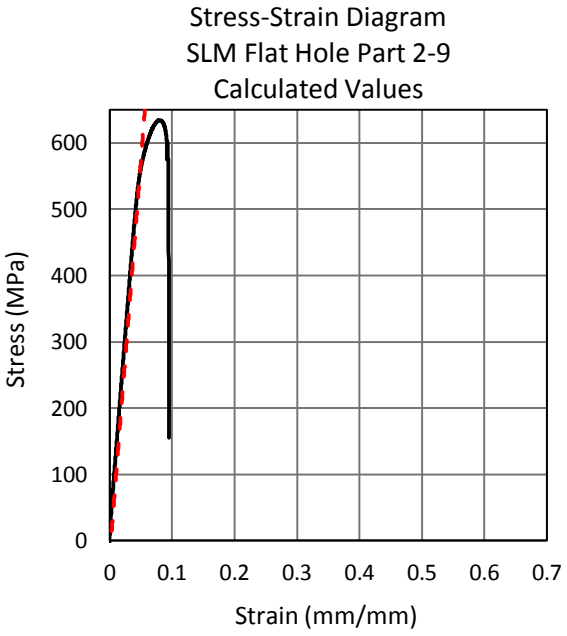
Stress-Strain Diagram
SLM Flat Hole Part 2-9
Calculated Values
Stress (MPa)
0
100
200
300
400
500
600
0
0.1
0.2
0.3
0.4
0.5
0.6
0.7
Strain (mm/mm)

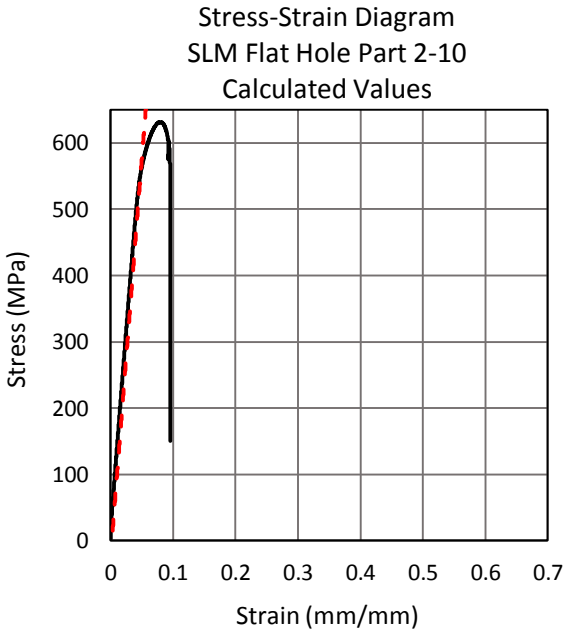
Stress-Strain Diagram
SLM Flat Hole Part 2-10
Calculated Values
Stress (MPa)
0
100
200
300
400
500
600
0
0.1
0.2
0.3
0.4
0.5
0.6
0.7
Strain (mm/mm)

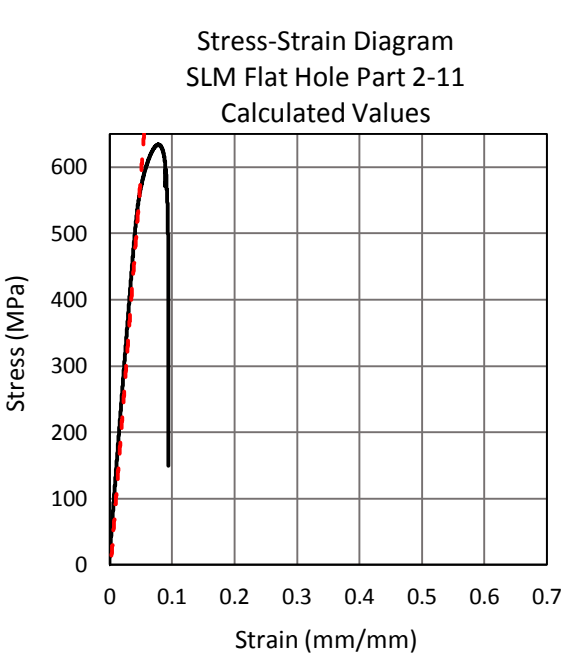
Stress-Strain Diagram
SLM Flat Hole Part 2-11
Calculated Values
Stress (MPa)
600
500
400
300
200
100
0
0
0.1
0.2
0.3
0.4
0.5
0.6
0.7
Strain (mm/mm)

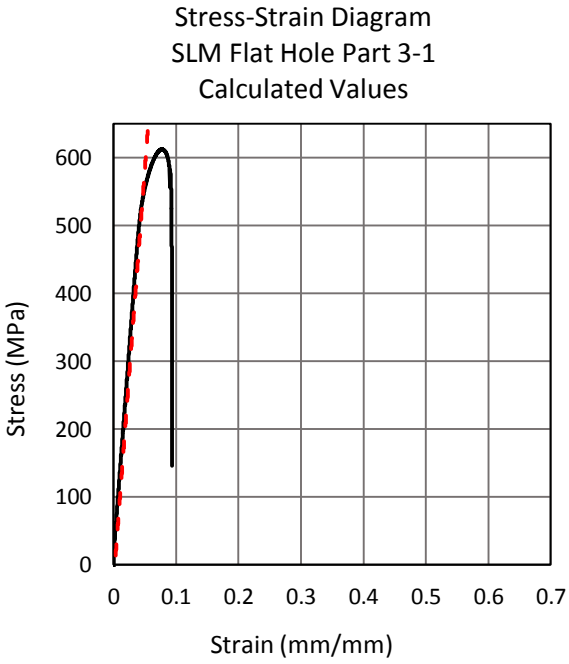
Stress-Strain Diagram
SLM Flat Hole Part 3-1
Calculated Values
Stress (MPa)
600
500
400
300
200
100
0
0
0.1
0.2
0.3
0.4
0.5
0.6
0.7
Strain (mm/mm)

Stress – Strain Graphs of Purchased Parts

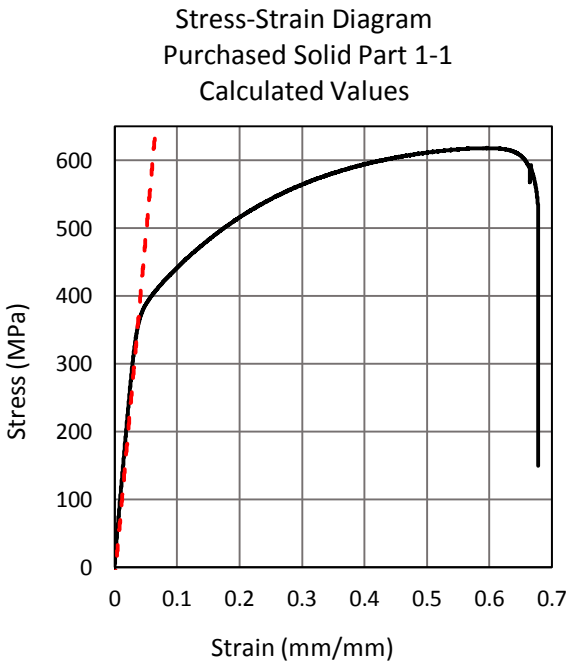

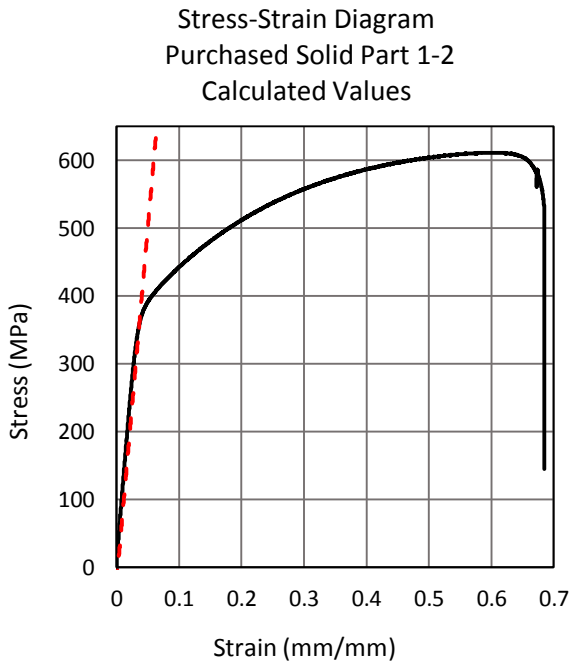

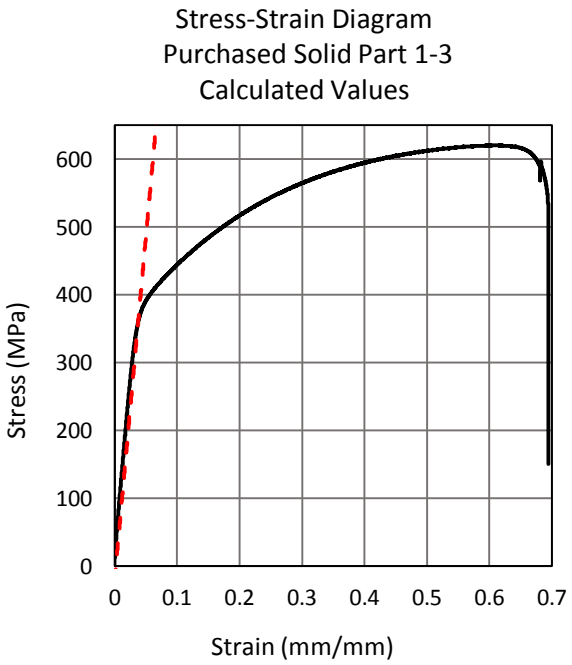

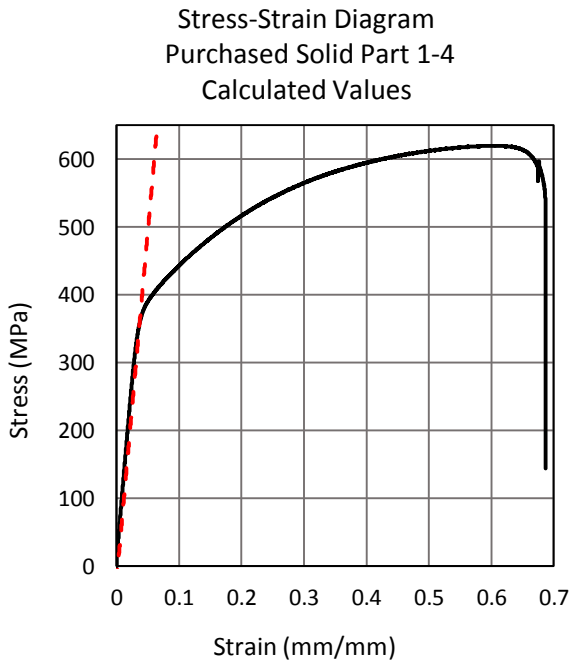

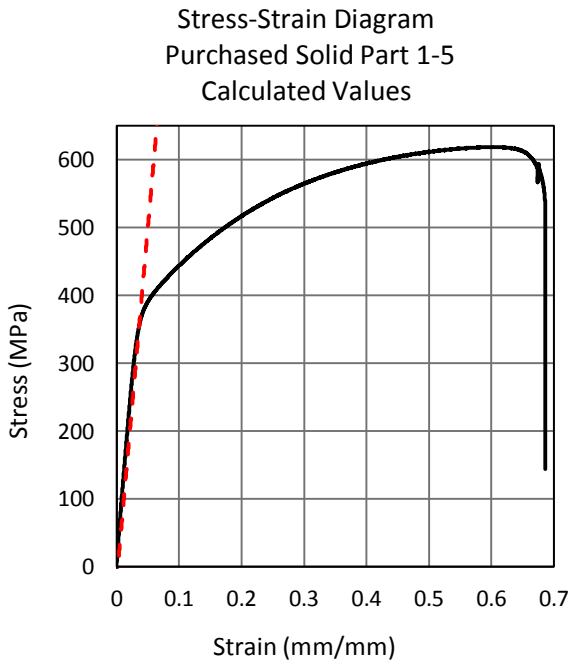
Stress-Strain Diagram
Purchased Solid Part 1-5
Calculated Values
Stress (MPa)
0
100
200
300
400
500
600
0
0.1
0.2
0.3
0.4
0.5
0.6
0.7
Strain (mm/mm)

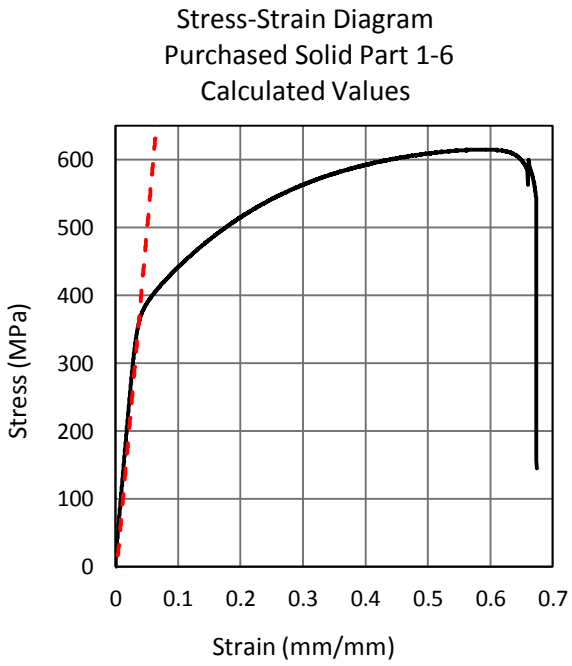
Stress-Strain Diagram
Purchased Solid Part 1-6
Calculated Values
Stress (MPa)
0
100
200
300
400
500
600
0
0.1
0.2
0.3
0.4
0.5
0.6
0.7
Strain (mm/mm)

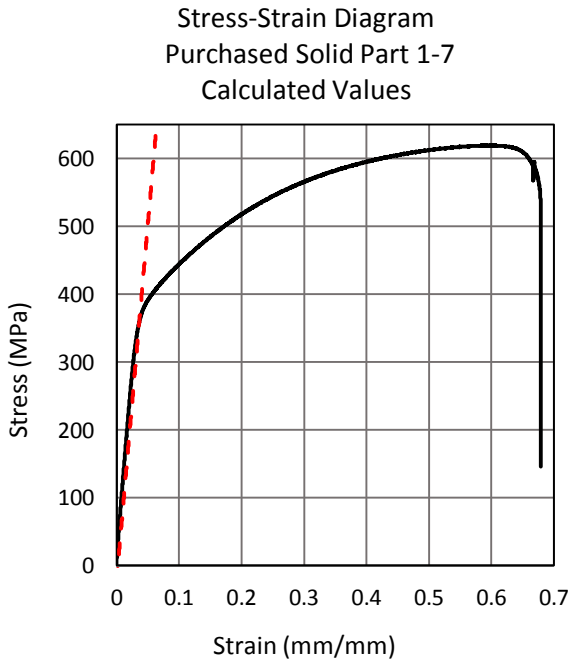
Stress-Strain Diagram
Purchased Solid Part 1-7
Calculated Values
Stress (MPa)
0
100
200
300
400
500
600
0
0.1
0.2
0.3
0.4
0.5
0.6
0.7
Strain (mm/mm)

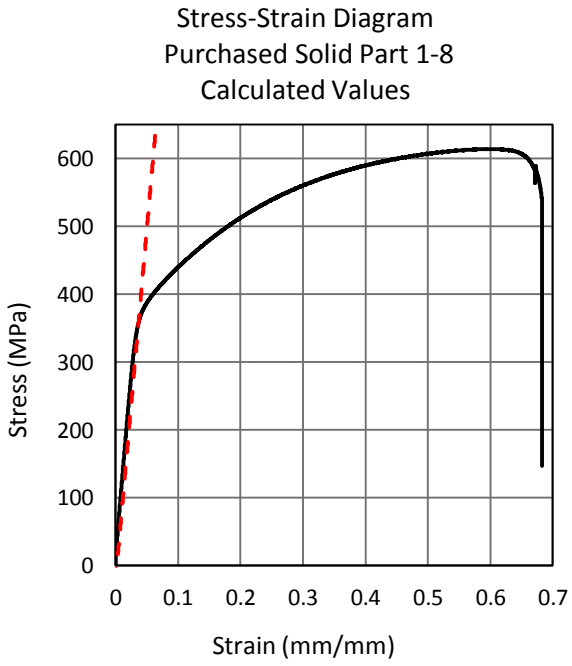
Stress-Strain Diagram
Purchased Solid Part 1-8
Calculated Values
Stress (MPa)
0
100
200
300
400
500
600
0
0.1
0.2
0.3
0.4
0.5
0.6
0.7
Strain (mm/mm)

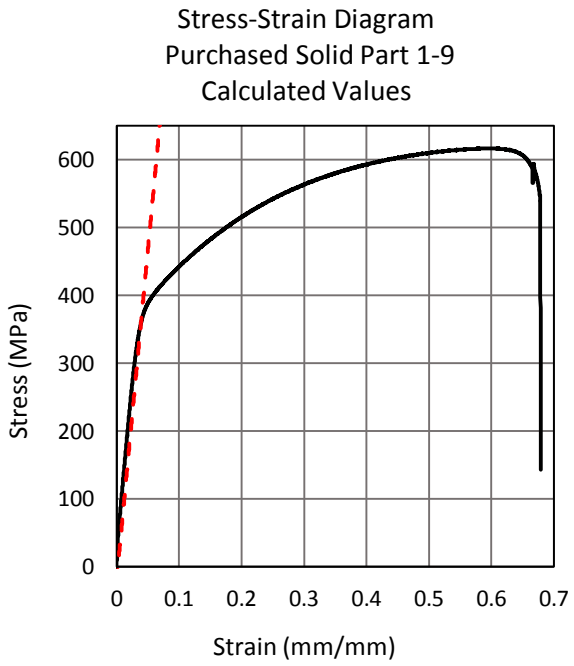
Stress-Strain Diagram
Purchased Solid Part 1-9
Calculated Values
Stress (MPa)
0
100
200
300
400
500
600
0
0.1
0.2
0.3
0.4
0.5
0.6
0.7
Strain (mm/mm)

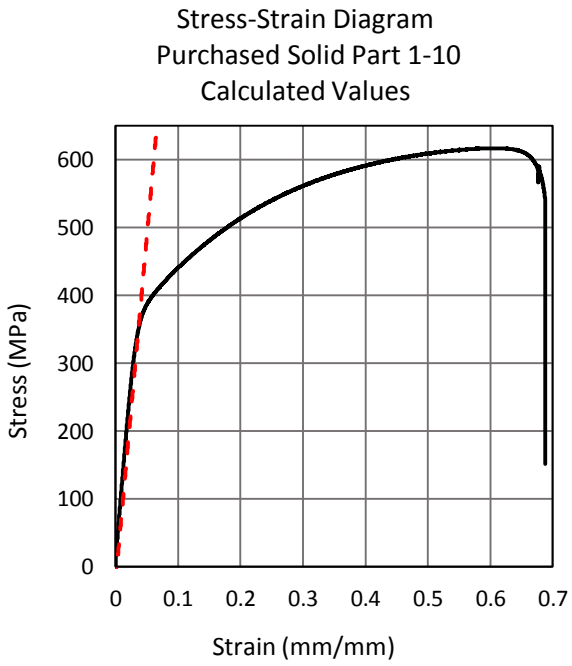
Stress-Strain Diagram
Purchased Solid Part 1-10
Calculated Values
Stress (MPa)
0
100
200
300
400
500
600
0
0.1
0.2
0.3
0.4
0.5
0.6
0.7
Strain (mm/mm)

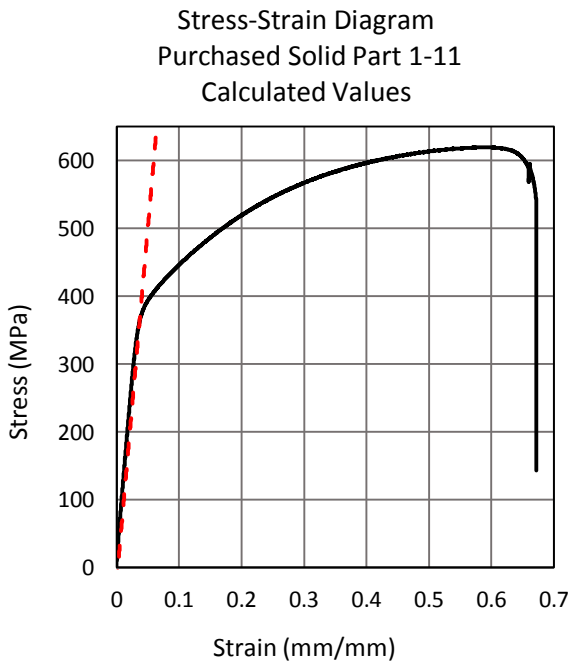
Stress-Strain Diagram
Purchased Solid Part 1-11
Calculated Values
Stress (MPa)
0
100
200
300
400
500
600
0
0.1
0.2
0.3
0.4
0.5
0.6
0.7
Strain (mm/mm)

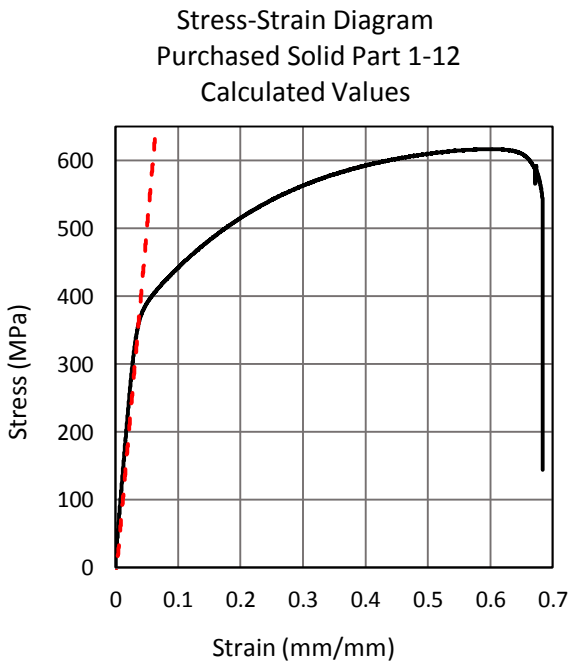
Stress-Strain Diagram
Purchased Solid Part 1-12
Calculated Values
Stress (MPa)
0
100
200
300
400
500
600
0
0.1
0.2
0.3
0.4
0.5
0.6
0.7
Strain (mm/mm)

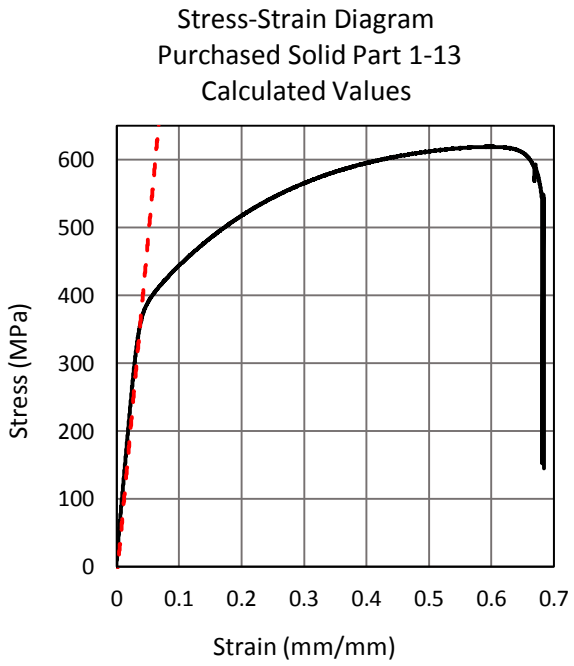
Stress-Strain Diagram
Purchased Solid Part 1-13
Calculated Values
Stress (MPa)
0
100
200
300
400
500
600
0
0.1
0.2
0.3
0.4
0.5
0.6
0.7
Strain (mm/mm)

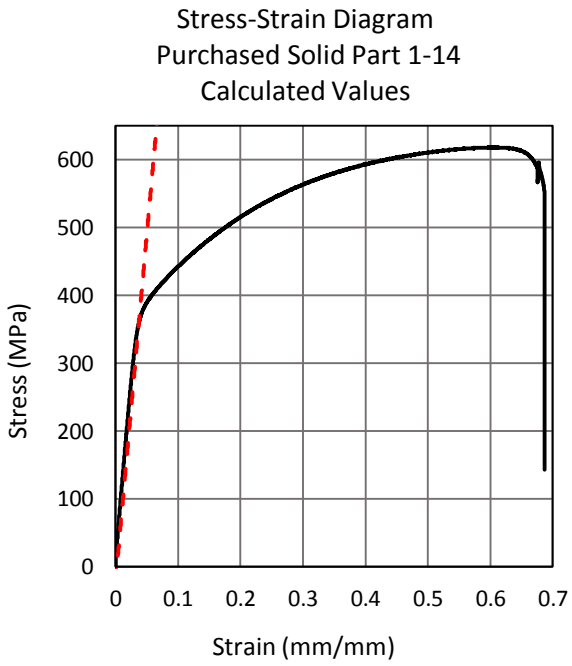
Stress-Strain Diagram
Purchased Solid Part 1-14
Calculated Values
Stress (MPa)
0
100
200
300
400
500
600
0
0.1
0.2
0.3
0.4
0.5
0.6
0.7
Strain (mm/mm)

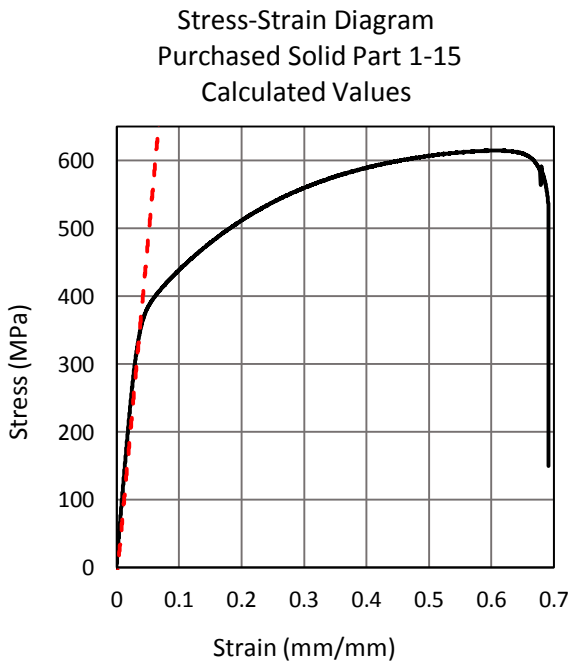
Stress-Strain Diagram
Purchased Solid Part 1-15
Calculated Values
Stress (MPa)
0
100
200
300
400
500
600
0
0.1
0.2
0.3
0.4
0.5
0.6
0.7
Strain (mm/mm)

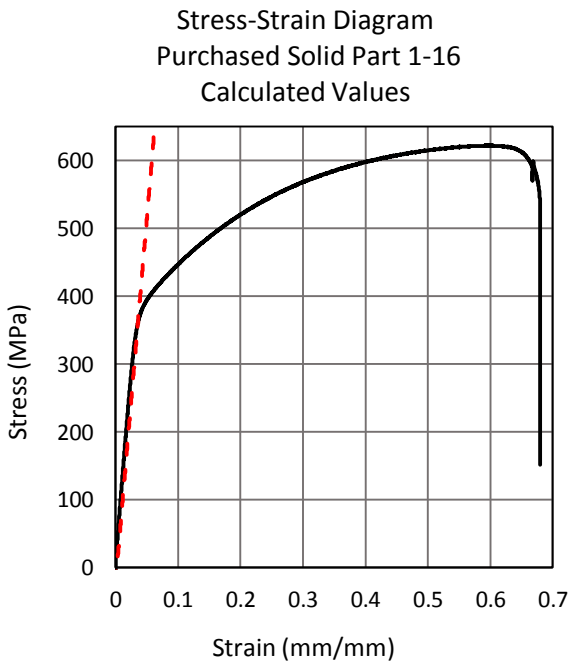
Stress-Strain Diagram
Purchased Solid Part 1-16
Calculated Values
Stress (MPa)
0
100
200
300
400
500
600
0
0.1
0.2
0.3
0.4
0.5
0.6
0.7
Strain (mm/mm)

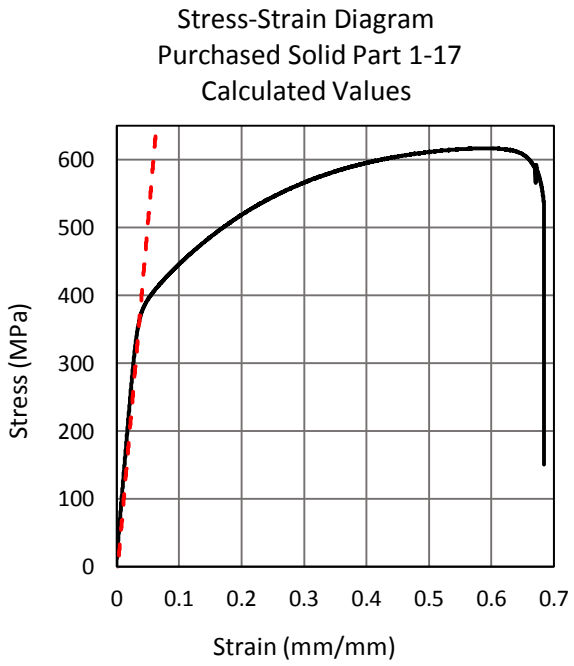
Stress-Strain Diagram
Purchased Solid Part 1-17
Calculated Values
Stress (MPa)
0
100
200
300
400
500
600
0
0.1
0.2
0.3
0.4
0.5
0.6
0.7
Strain (mm/mm)

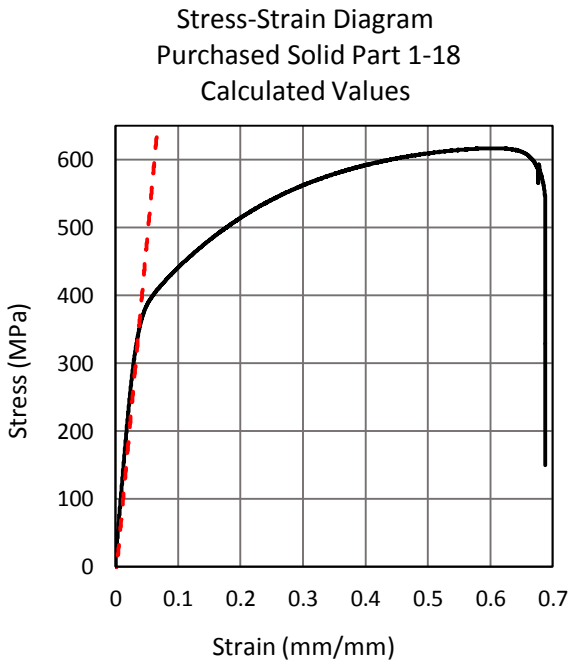
Stress-Strain Diagram
Purchased Solid Part 1-18
Calculated Values
Stress (MPa)
0
100
200
300
400
500
600
0
0.1
0.2
0.3
0.4
0.5
0.6
0.7
Strain (mm/mm)

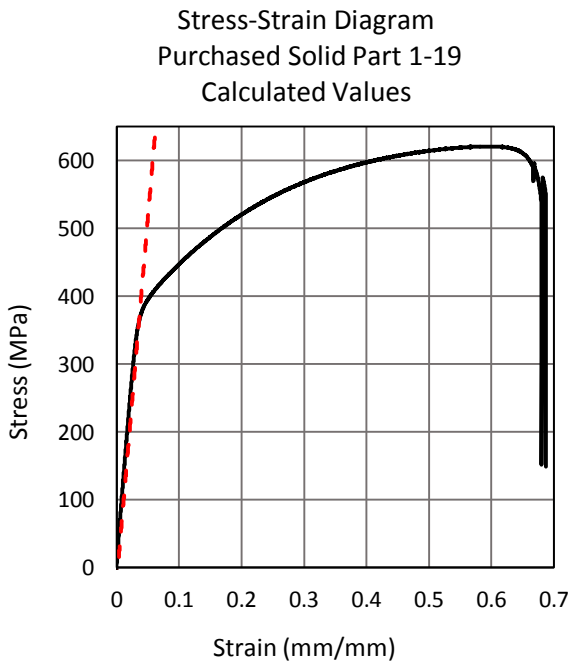
Stress-Strain Diagram
Purchased Solid Part 1-19
Calculated Values
Stress (MPa)
0
100
200
300
400
500
600
0
0.1
0.2
0.3
0.4
0.5
0.6
0.7
Strain (mm/mm)

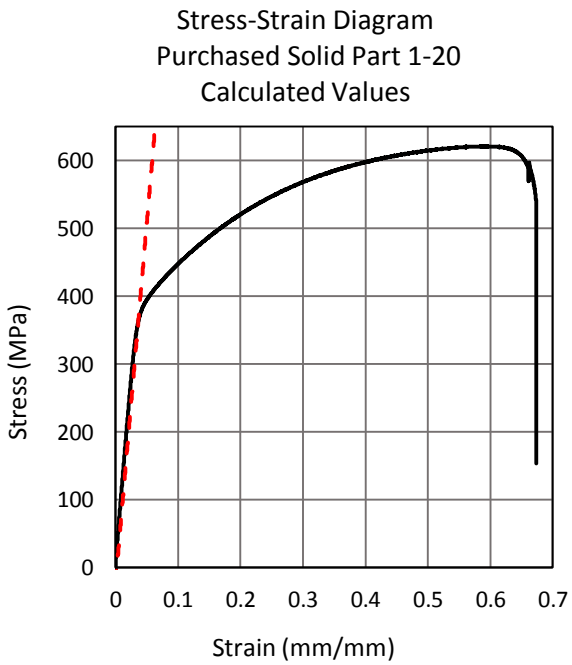
Stress-Strain Diagram
Purchased Solid Part 1-20
Calculated Values
Stress (MPa)
0
100
200
300
400
500
600
0
0.1
0.2
0.3
0.4
0.5
0.6
0.7
Strain (mm/mm)

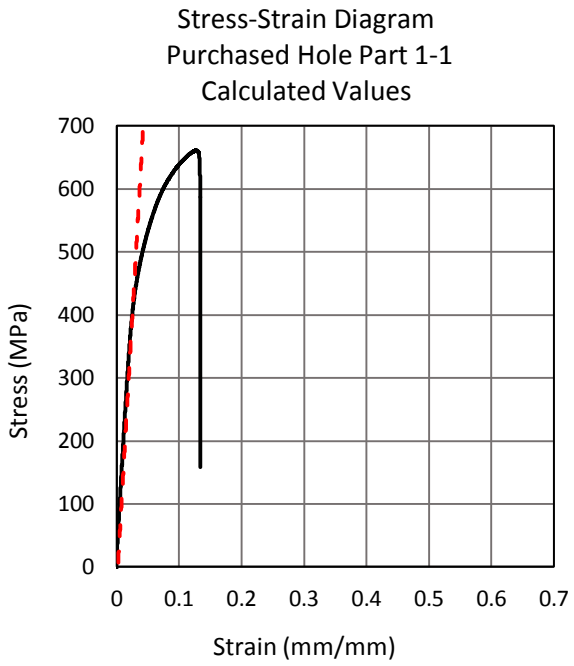
Stress-Strain Diagram
Purchased Hole Part 1-1
Calculated Values
Stress (MPa)
700
600
500
400
300
200
100
0
0
0.1
0.2
0.3
0.4
0.5
0.6
0.7
Strain (mm/mm)

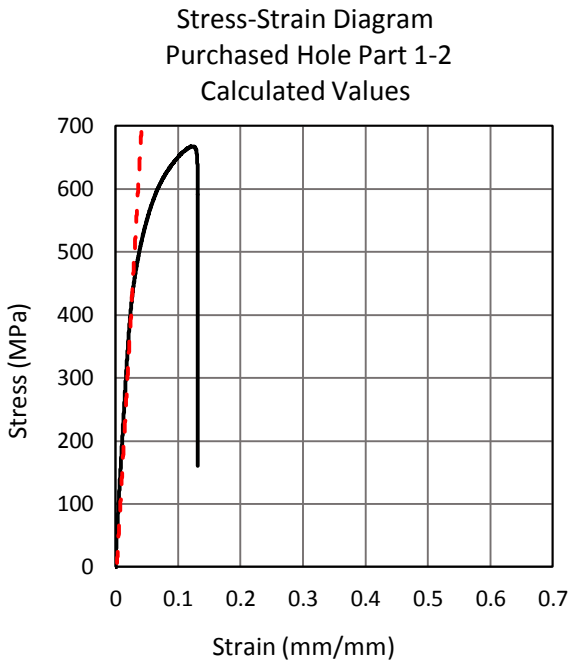
Stress-Strain Diagram
Purchased Hole Part 1-2
Calculated Values
Stress (MPa)
700
600
500
400
300
200
100
0
0
0.1
0.2
0.3
0.4
0.5
0.6
0.7
Strain (mm/mm)

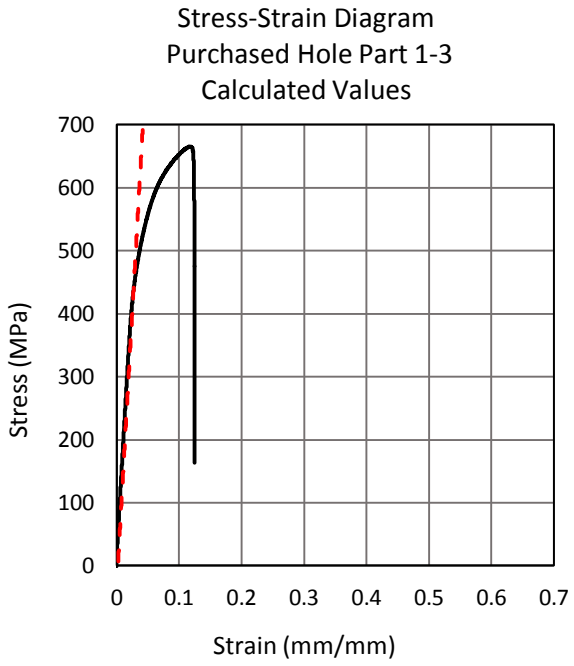
Stress-Strain Diagram
Purchased Hole Part 1-3
Calculated Values
Stress (MPa)
700
600
500
400
300
200
100
0
0
0.1
0.2
0.3
0.4
0.5
0.6
0.7
Strain (mm/mm)

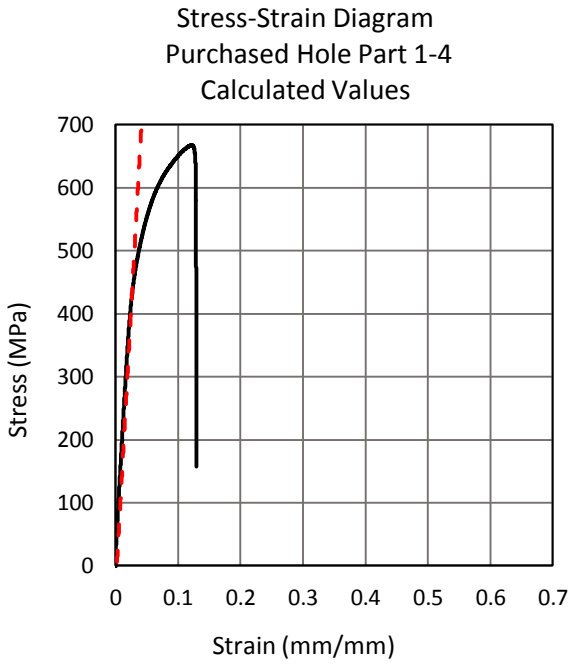
Stress-Strain Diagram
Purchased Hole Part 1-4
Calculated Values
Stress (MPa)
700
600
500
400
300
200
100
0
0
0.1
0.2
0.3
0.4
0.5
0.6
0.7
Strain (mm/mm)

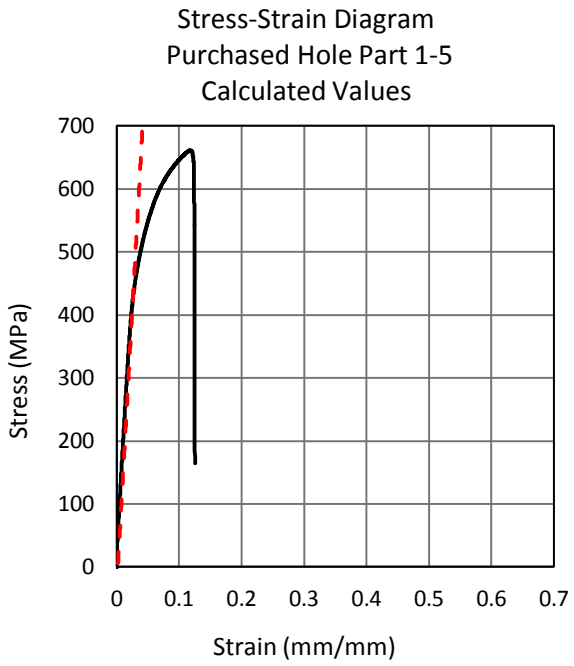
Stress-Strain Diagram
Purchased Hole Part 1-5
Calculated Values
Stress (MPa)
700
600
500
400
300
200
100
0
0
0.1
0.2
0.3
0.4
0.5
0.6
0.7
Strain (mm/mm)

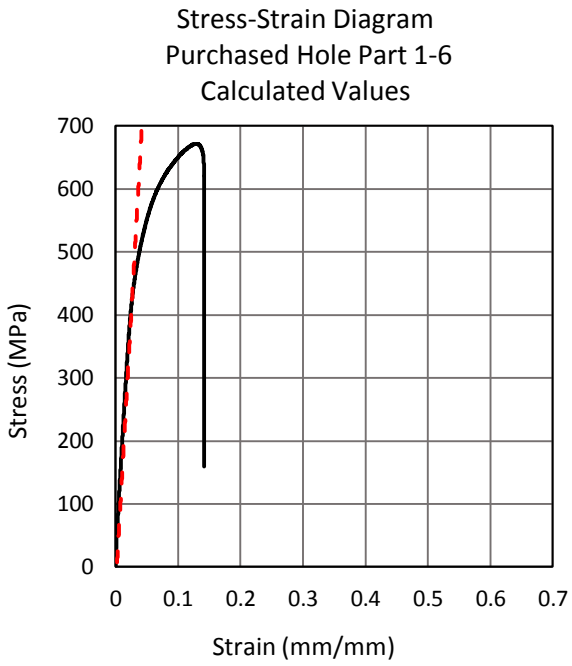
Stress-Strain Diagram
Purchased Hole Part 1-6
Calculated Values
Stress (MPa)
700
600
500
400
300
200
100
0
0
0.1
0.2
0.3
0.4
0.5
0.6
0.7
Strain (mm/mm)

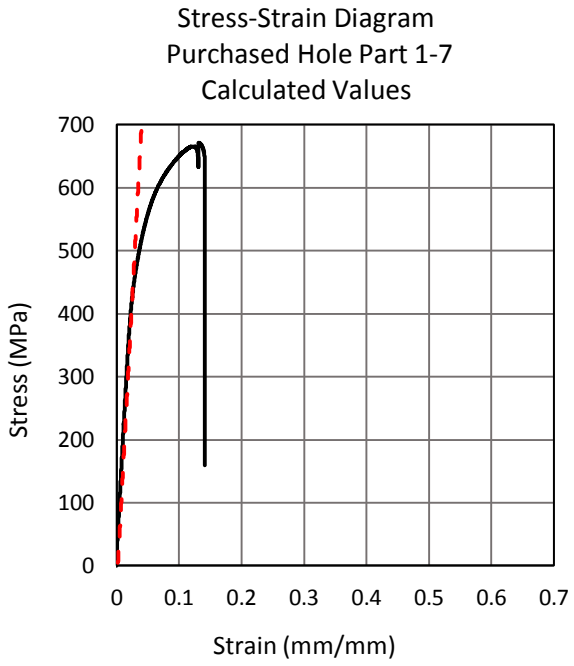
Stress-Strain Diagram
Purchased Hole Part 1-7
Calculated Values
Stress (MPa)
700
600
500
400
300
200
100
0
0
0.1
0.2
0.3
0.4
0.5
0.6
0.7
Strain (mm/mm)

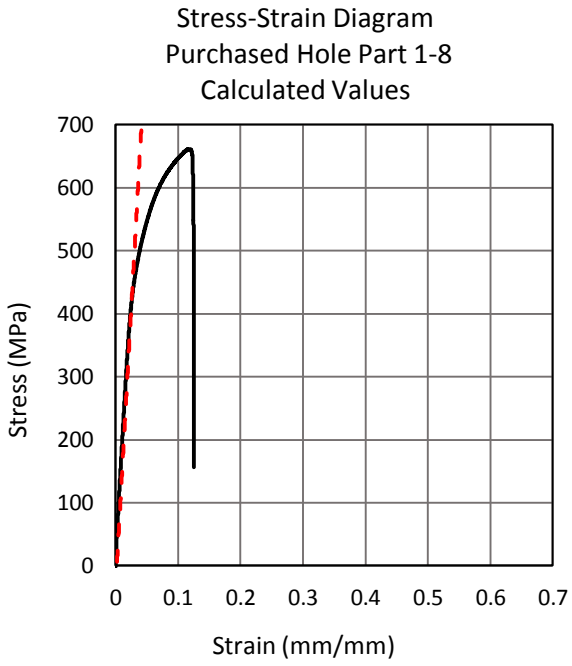
Stress-Strain Diagram
Purchased Hole Part 1-8
Calculated Values
Stress (MPa)
700
600
500
400
300
200
100
0
0
0.1
0.2
0.3
0.4
0.5
0.6
0.7
Strain (mm/mm)

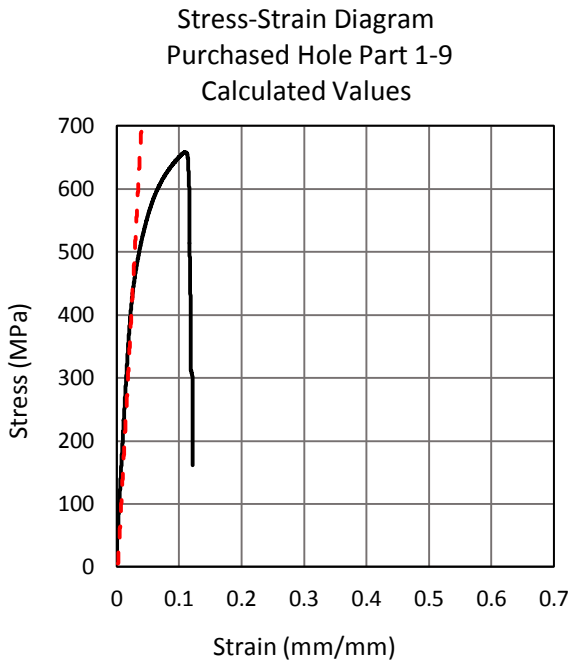
Stress-Strain Diagram
Purchased Hole Part 1-9
Calculated Values
Stress (MPa)
700
600
500
400
300
200
100
0
0
0.1
0.2
0.3
0.4
0.5
0.6
0.7
Strain (mm/mm)

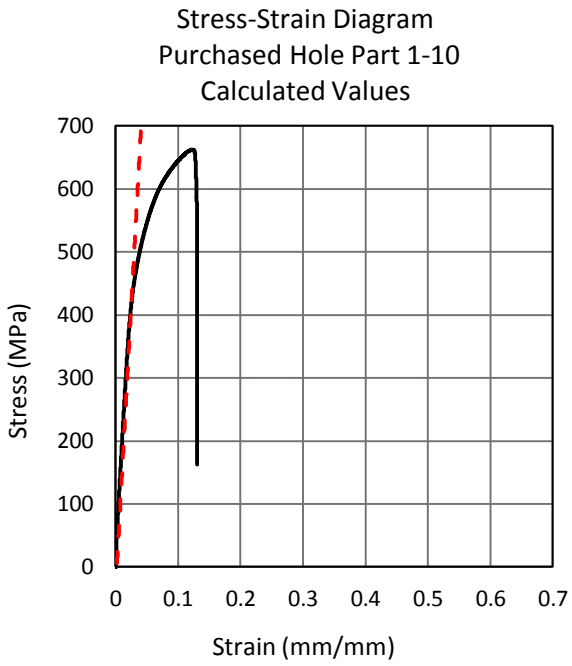
Stress-Strain Diagram
Purchased Hole Part 1-10
Calculated Values
Stress (MPa)
700
600
500
400
300
200
100
0
0
0.1
0.2
0.3
0.4
0.5
0.6
0.7
Strain (mm/mm)

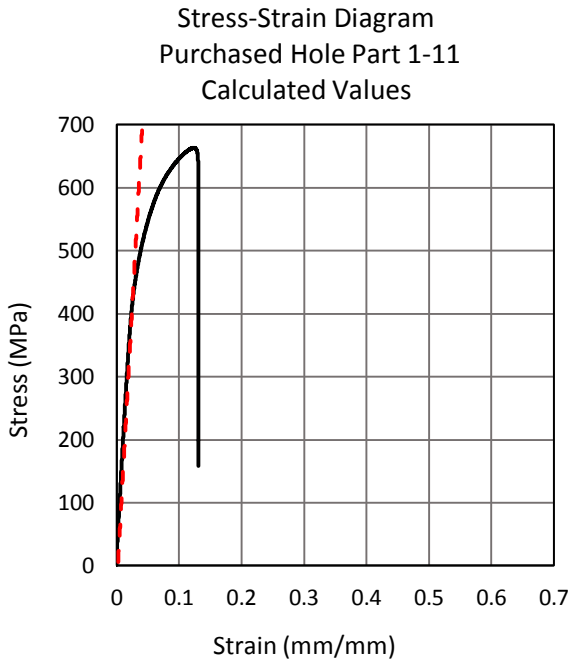
Stress-Strain Diagram
Purchased Hole Part 1-11
Calculated Values
Stress (MPa)
700
600
500
400
300
200
100
0
0
0.1
0.2
0.3
0.4
0.5
0.6
0.7
Strain (mm/mm)

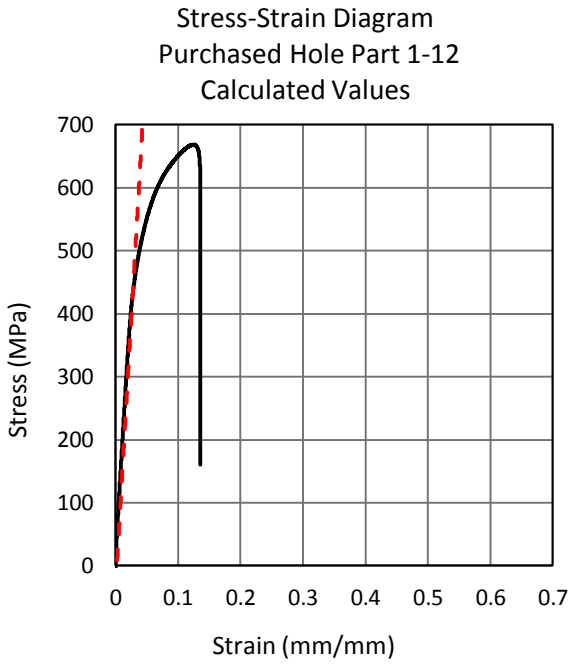
Stress-Strain Diagram
Purchased Hole Part 1-12
Calculated Values
Stress (MPa)
700
600
500
400
300
200
100
0
0
0.1
0.2
0.3
0.4
0.5
0.6
0.7
Strain (mm/mm)

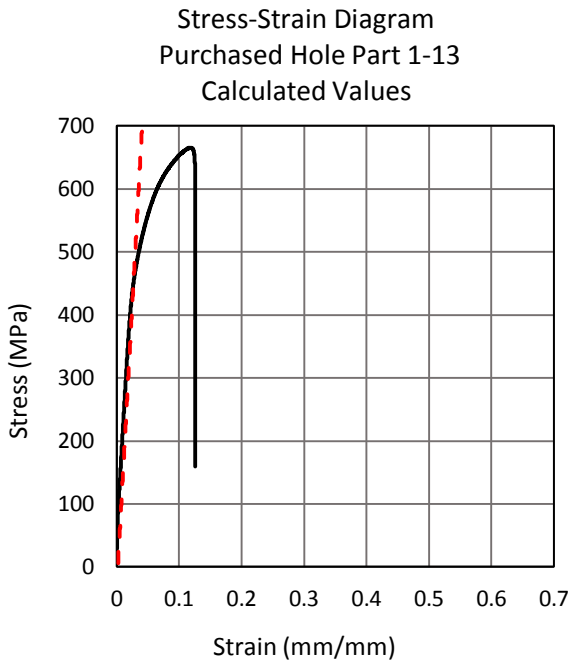
Stress-Strain Diagram
Purchased Hole Part 1-13
Calculated Values
Stress (MPa)
Strain (mm/mm)
0
100
200
300
400
500
600
700
0
0.1
0.2
0.3
0.4
0.5
0.6
0.7

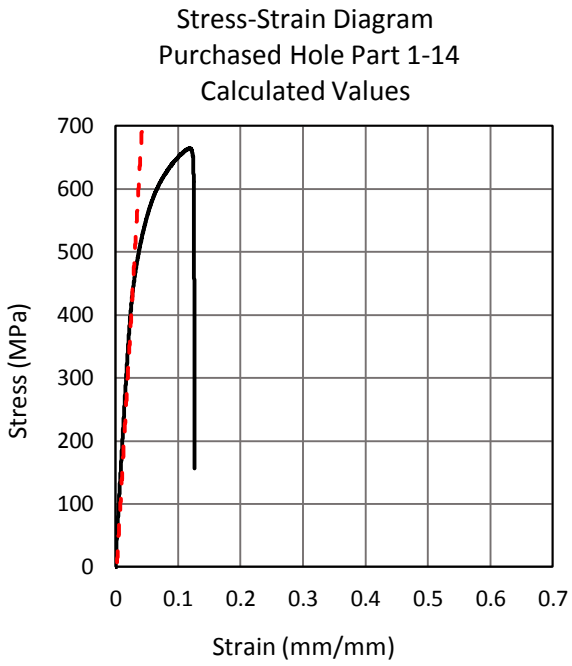
Stress-Strain Diagram
Purchased Hole Part 1-14
Calculated Values
Stress (MPa)
Strain (mm/mm)
0
100
200
300
400
500
600
700
0
0.1
0.2
0.3
0.4
0.5
0.6
0.7

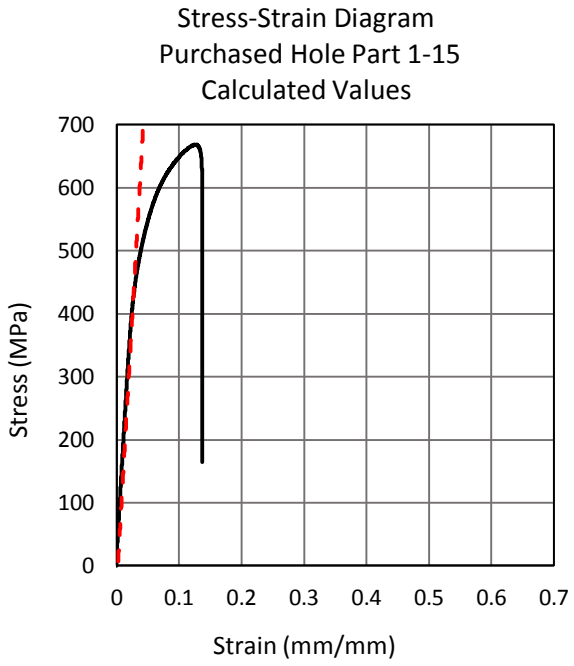
Stress-Strain Diagram
Purchased Hole Part 1-15
Calculated Values
Stress (MPa)
Strain (mm/mm)
0
100
200
300
400
500
600
700
0
0.1
0.2
0.3
0.4
0.5
0.6
0.7

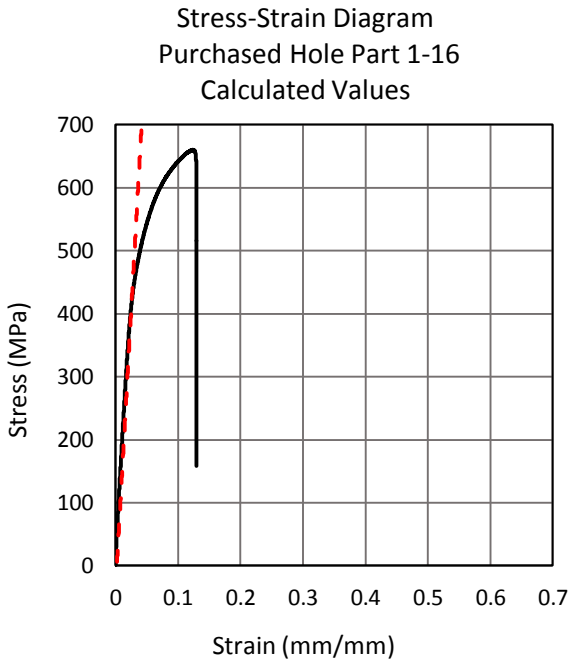
Stress-Strain Diagram
Purchased Hole Part 1-16
Calculated Values
Stress (MPa)
Strain (mm/mm)
0
100
200
300
400
500
600
700
0
0.1
0.2
0.3
0.4
0.5
0.6
0.7

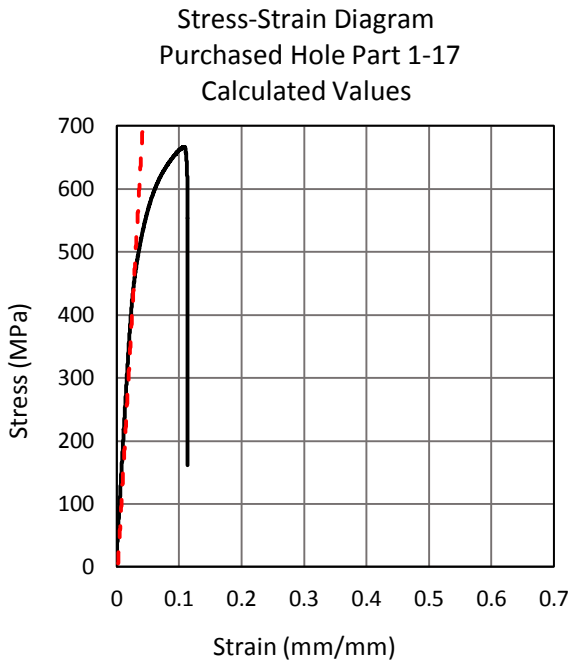
Stress-Strain Diagram
Purchased Hole Part 1-17
Calculated Values
Stress (MPa)
700
600
500
400
300
200
100
0
0
0.1
0.2
0.3
0.4
0.5
0.6
0.7
Strain (mm/mm)

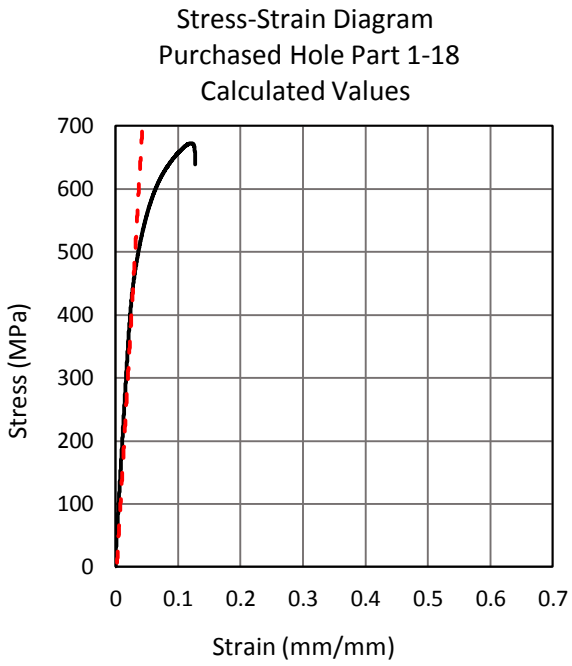
Stress-Strain Diagram
Purchased Hole Part 1-18
Calculated Values
Stress (MPa)
700
600
500
400
300
200
100
0
0
0.1
0.2
0.3
0.4
0.5
0.6
0.7
Strain (mm/mm)

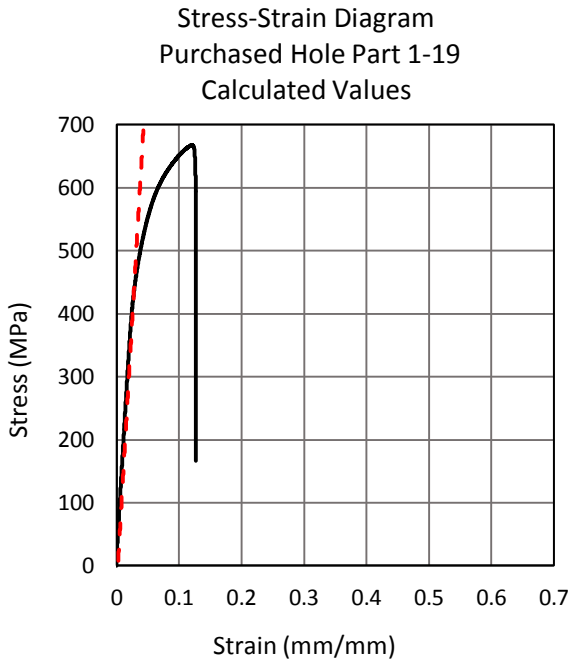
Stress-Strain Diagram
Purchased Hole Part 1-19
Calculated Values
Stress (MPa)
700
600
500
400
300
200
100
0
0
0.1
0.2
0.3
0.4
0.5
0.6
0.7
Strain (mm/mm)

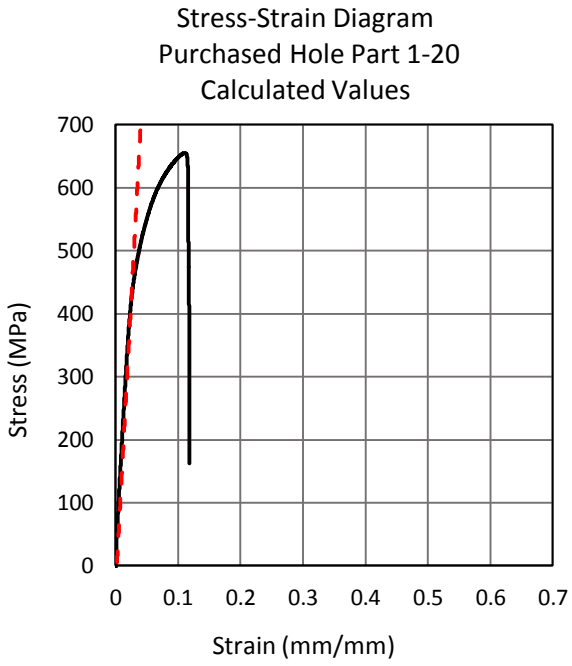
Stress-Strain Diagram
Purchased Hole Part 1-20
Calculated Values
Stress (MPa)
700
600
500
400
300
200
100
0
0
0.1
0.2
0.3
0.4
0.5
0.6
0.7
Strain (mm/mm)

APPENDIX E: BOXPLOTS OF MECHANICAL PROPERTIES

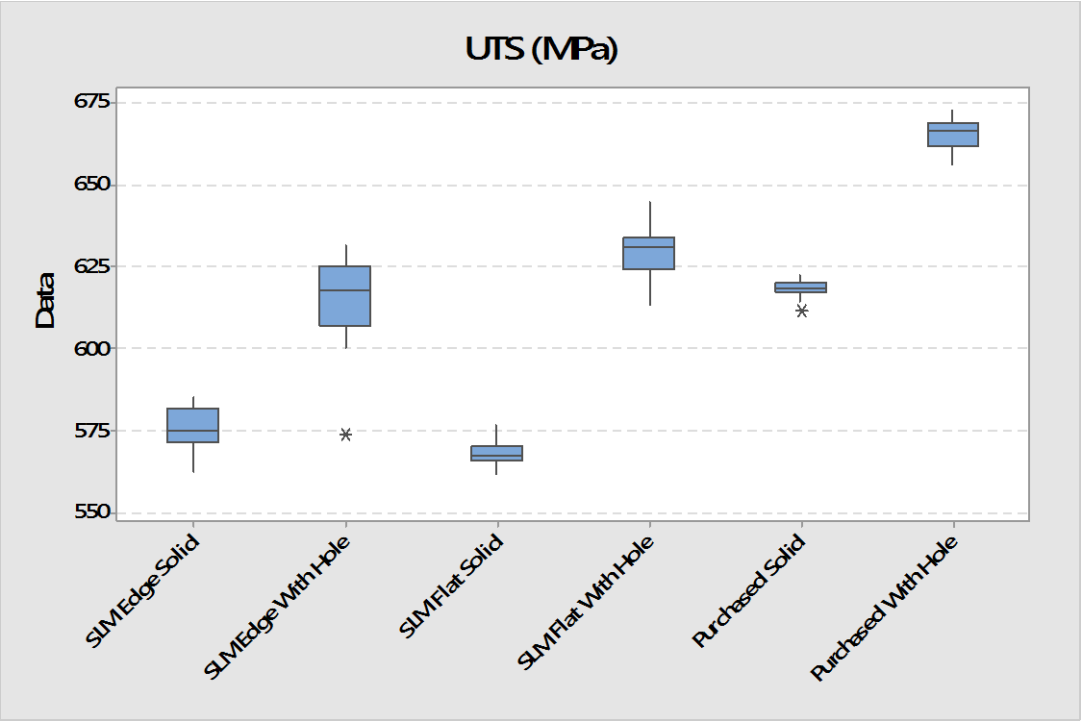

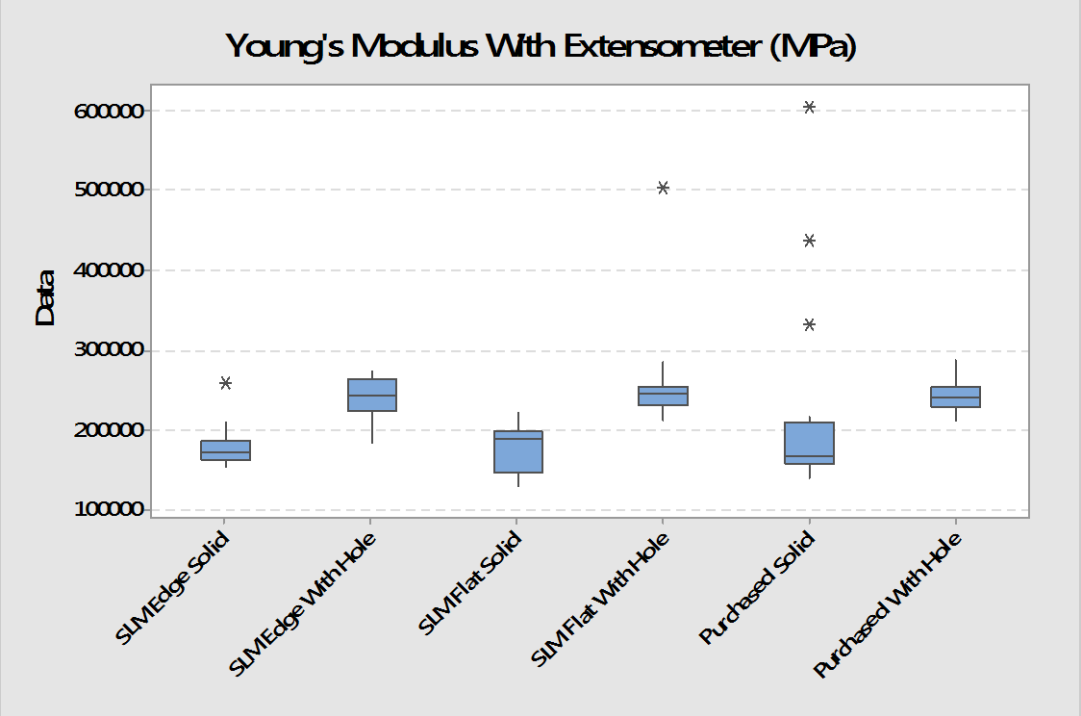

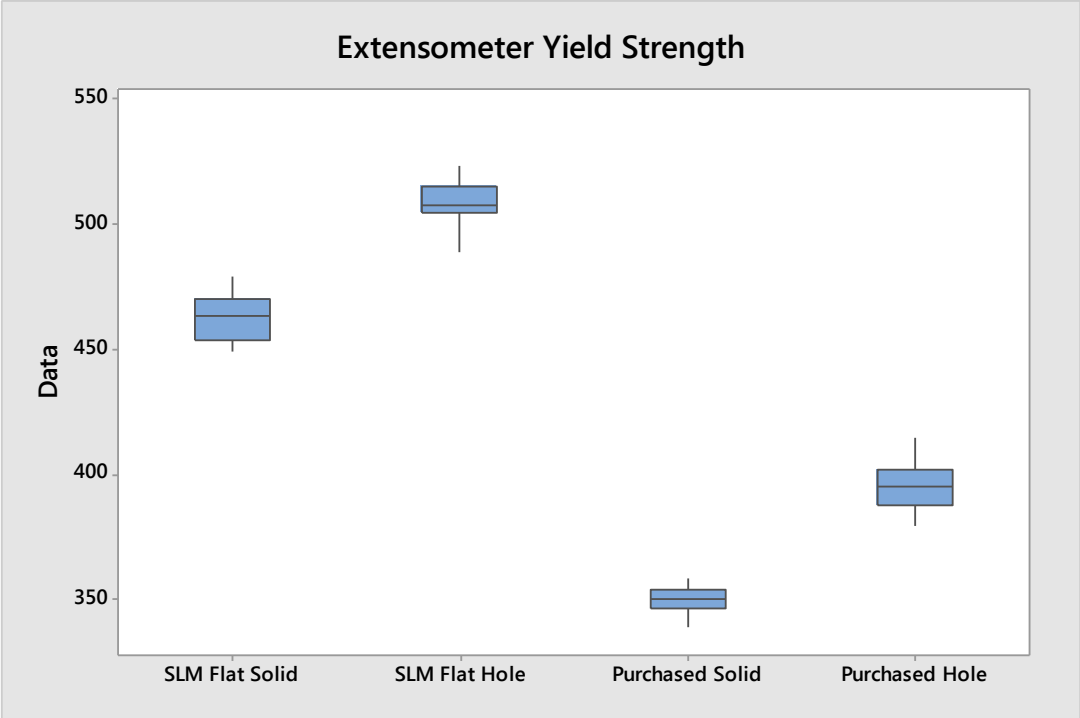
Extensometer Yield Strength
Data
550
500
450
400
350
SLM Flat Solid
SLM Flat Hole
Purchased Solid
Purchased Hole

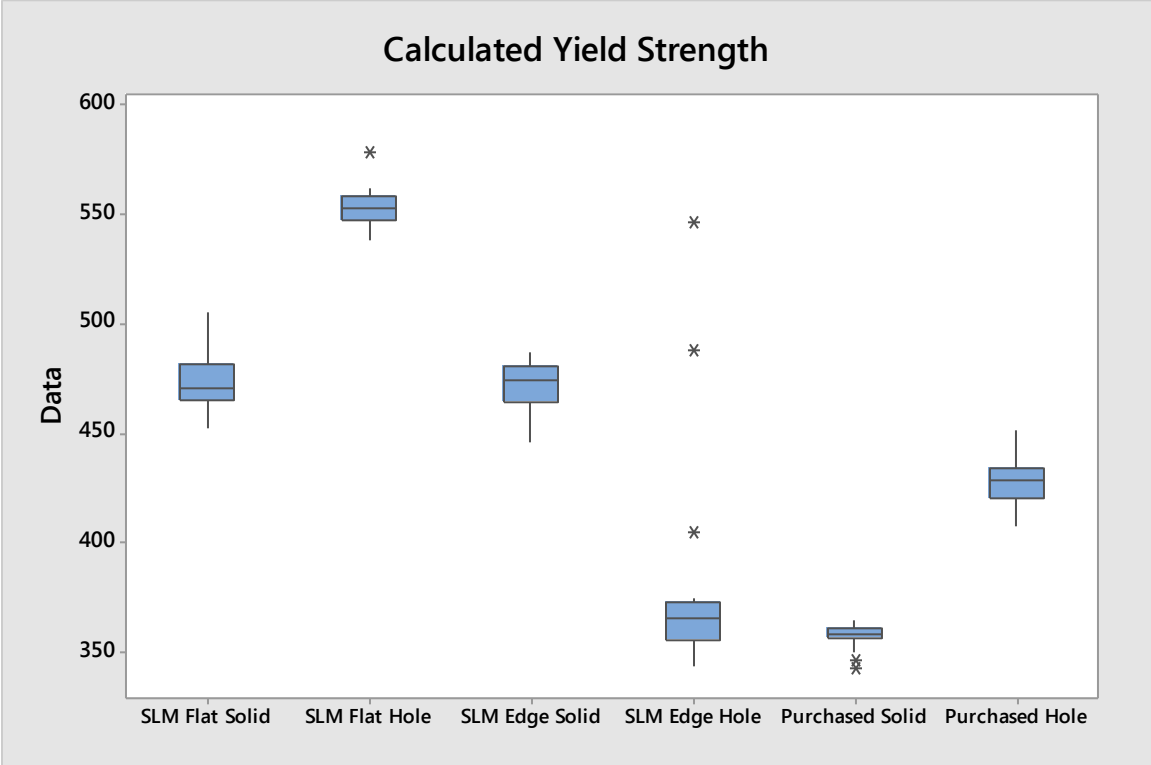
Calculated Yield Strength
Data
600
550
500
450
400
350
SLM Flat Solid
SLM Flat Hole
SLM Edge Solid
SLM Edge Hole
Purchased Solid
Purchased Hole

APPENDIX F: NORMAL PROBABILITY PLOTS OF MECHANICAL PROPERTIES

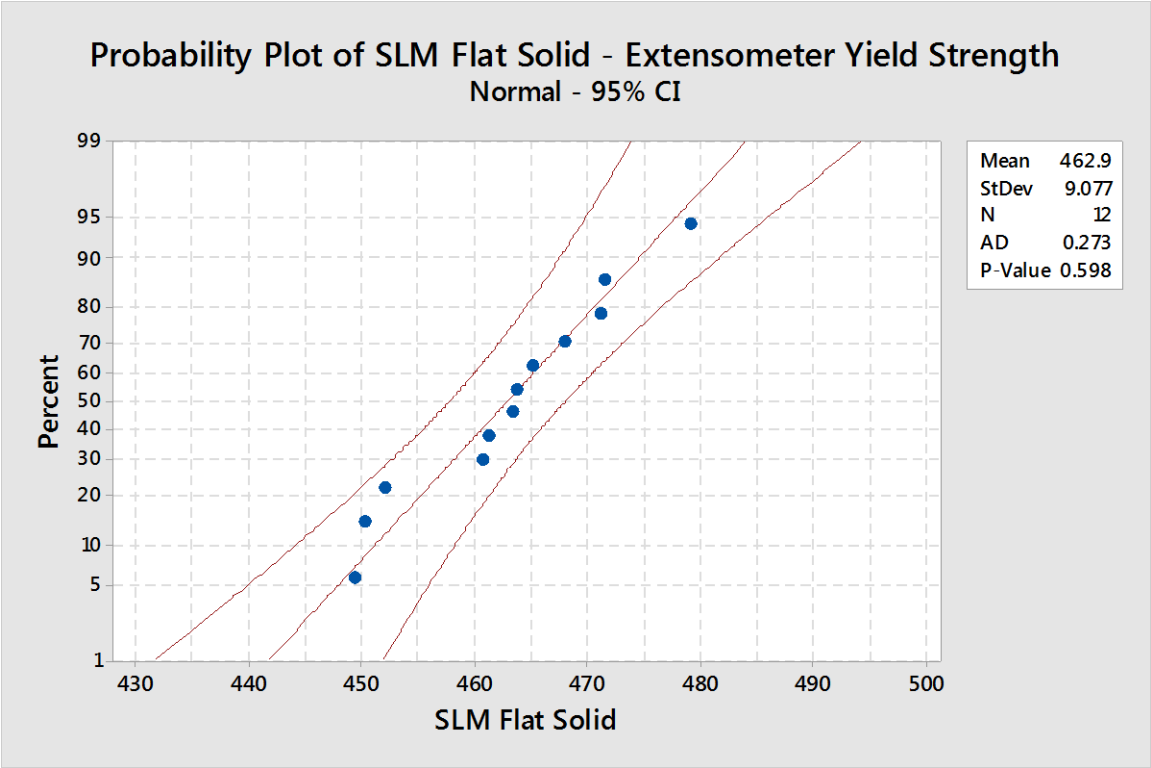

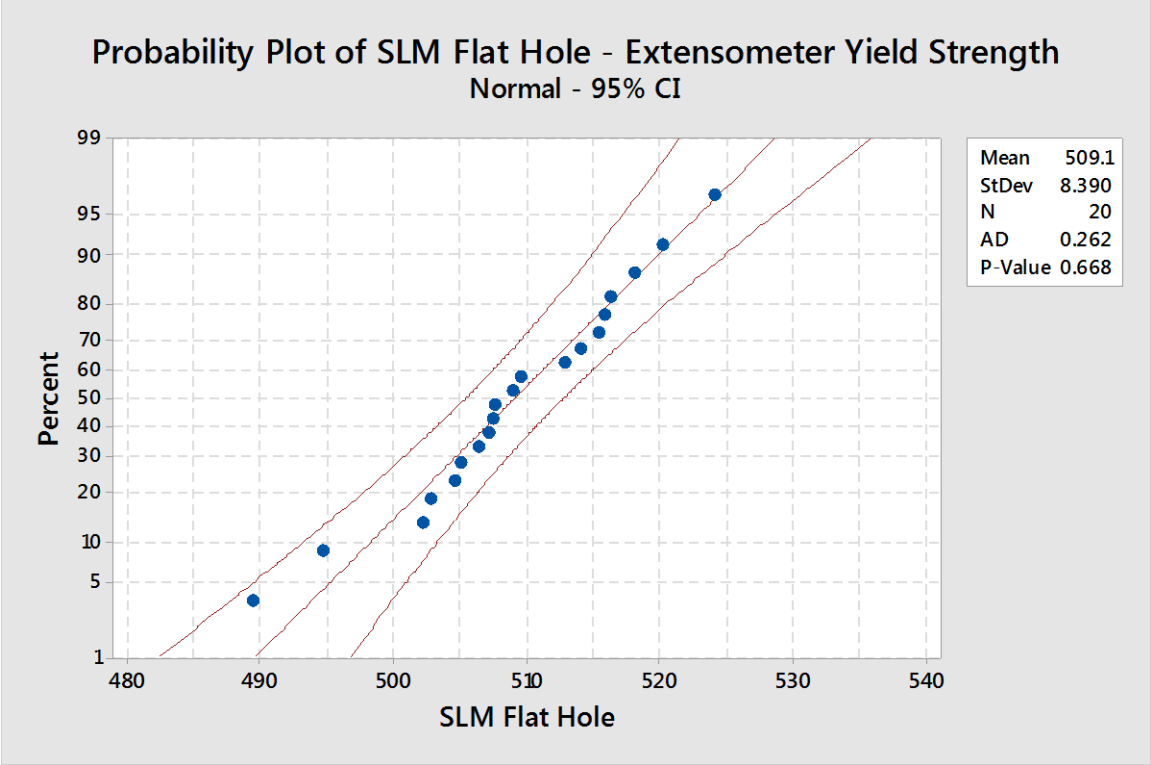

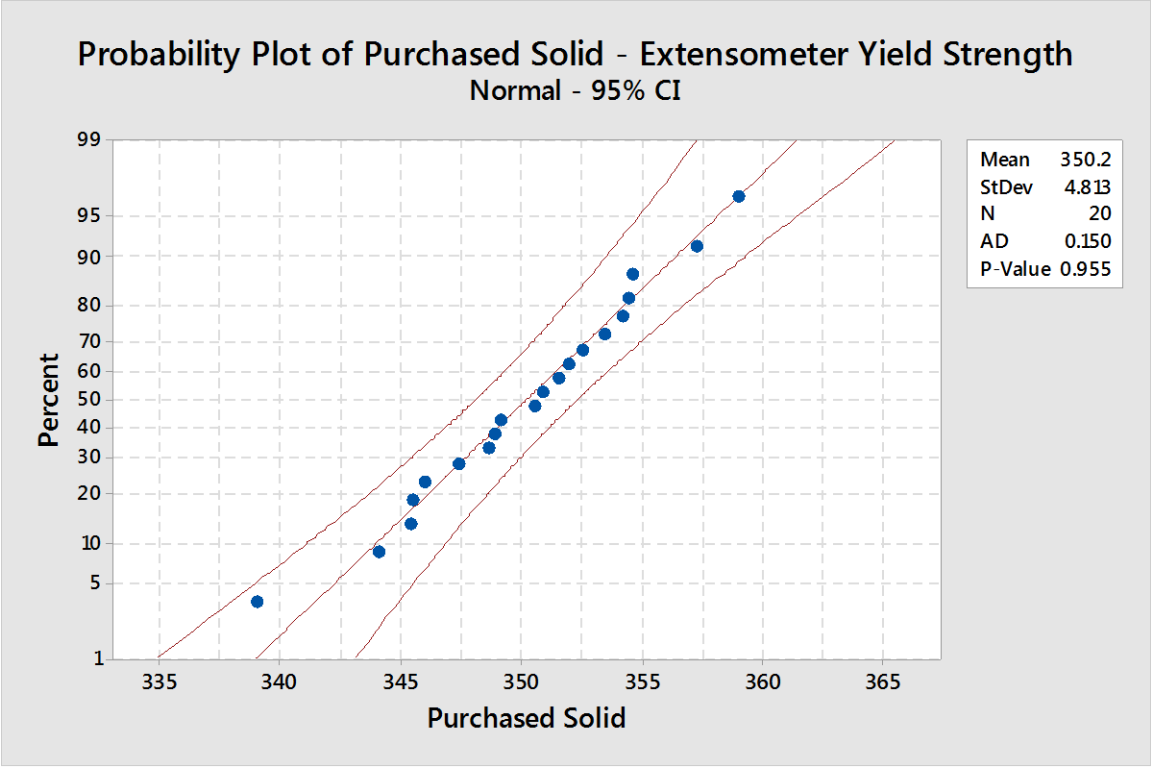
Probability Plot of Purchased Solid - Extensometer Yield Strength
Normal - 95% CI
Mean 350.2
StDev 4.813
N 20
AD 0.150
P-Value 0.955
Percent
Purchased Solid
99
95
90
80
70
60
50
40
30
20
10
5
1
335
340
345
350
355
360
365

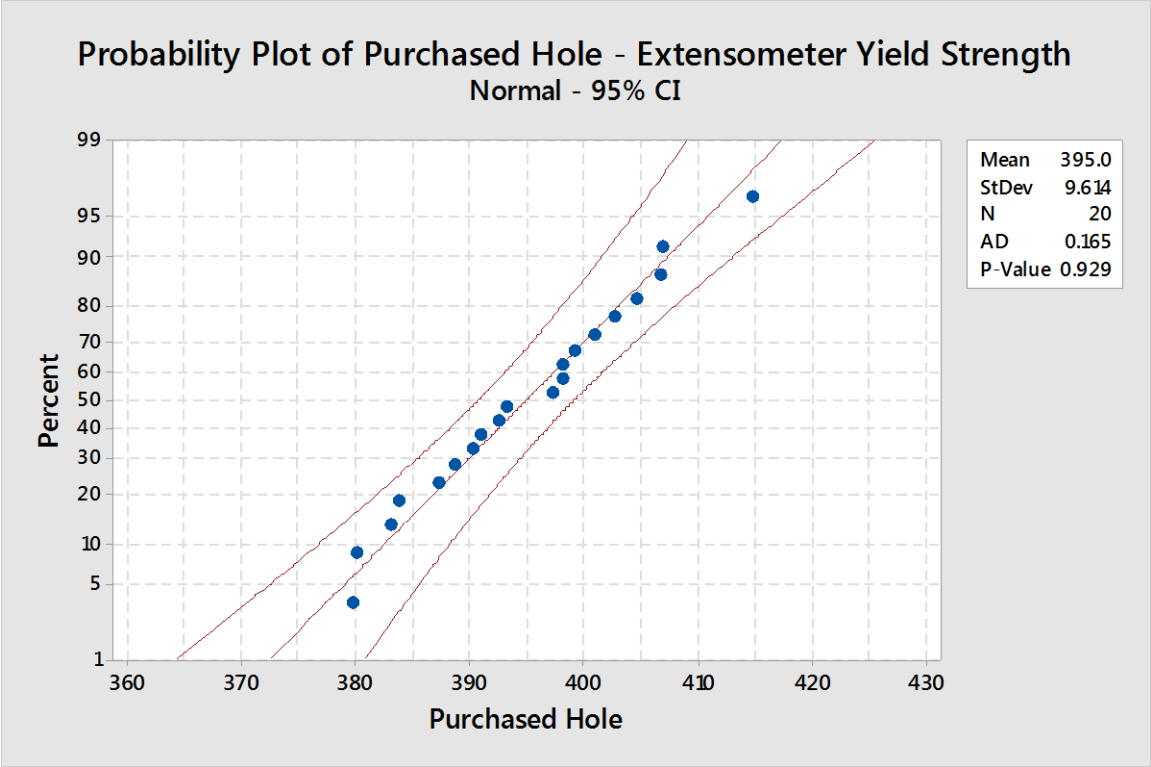
Probability Plot of Purchased Hole - Extensometer Yield Strength
Normal - 95% CI
Mean 395.0
StDev 9.614
N 20
AD 0.165
P-Value 0.929
Percent
Purchased Hole
99
95
90
80
70
60
50
40
30
20
10
5
1
360
370
380
390
400
410
420
430

APPENDIX G: MINITAB STATISTICAL ANALYSIS RESULTS

Minitab GLM Results

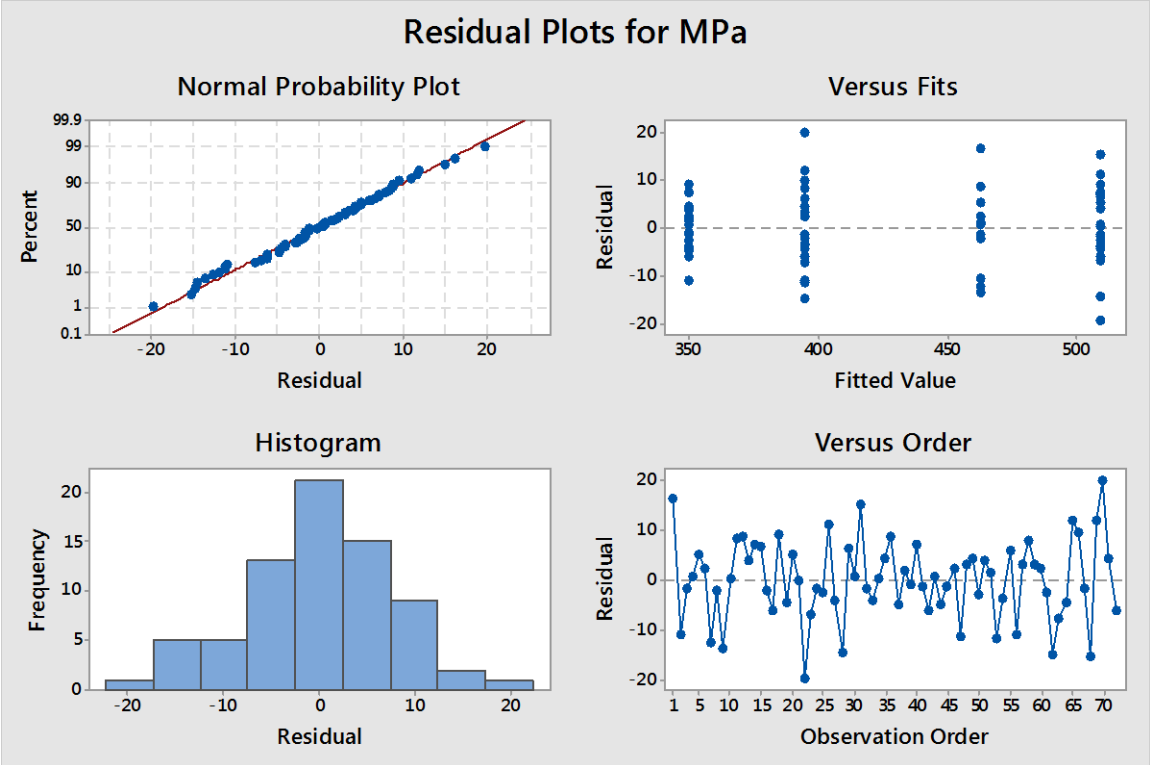

General Linear Model: MPa versus Cats

```
Method

Factor coding  (1, 0)


Factor Information

Factor  Type   Levels  Values
Cats    Fixed       4  Purchased Hole, Purchased Solid, SLM Flat
Hole, SLM Flat Solid


Analysis of Variance

Source  DF  Adj SS   Adj MS  F-Value  P-Value
```

```
  Cats   3  288724  96241.4  1473.95    0.000
Error   68    4440     65.3
Total   71  293164
```

Model Summary

```
      S    R-sq  R-sq(adj)  R-sq(pred)
8.08051  98.49%     98.42%      98.30%
```

Coefficients

```
Term                 Coef  SE Coef  T-Value  P-Value   VIF
Constant           394.98     1.81   218.60    0.000
Cats
  Purchased Solid  -44.77     2.56   -17.52    0.000  1.44
  SLM Flat Hole    114.15     2.56    44.67    0.000  1.44
  SLM Flat Solid    67.97     2.95    23.03    0.000  1.33
```

Regression Equation

```
MPa = 394.98 + 0.0 Cats_Purchased Hole - 44.77 Cats_Purchased
Solid + 114.15 Cats_SLM Flat
      Hole + 67.97 Cats_SLM Flat Solid
```

Fits and Diagnostics for Unusual Observations

```
Obs     MPa     Fit   Resid  Std Resid
  1  479.11  462.94   16.16       2.09  R
 32  489.40  509.13  -19.73      -2.51  R
 53  414.79  394.98   19.81       2.52  R

R  Large residual
```

Minitab One-Way ANOVA Results

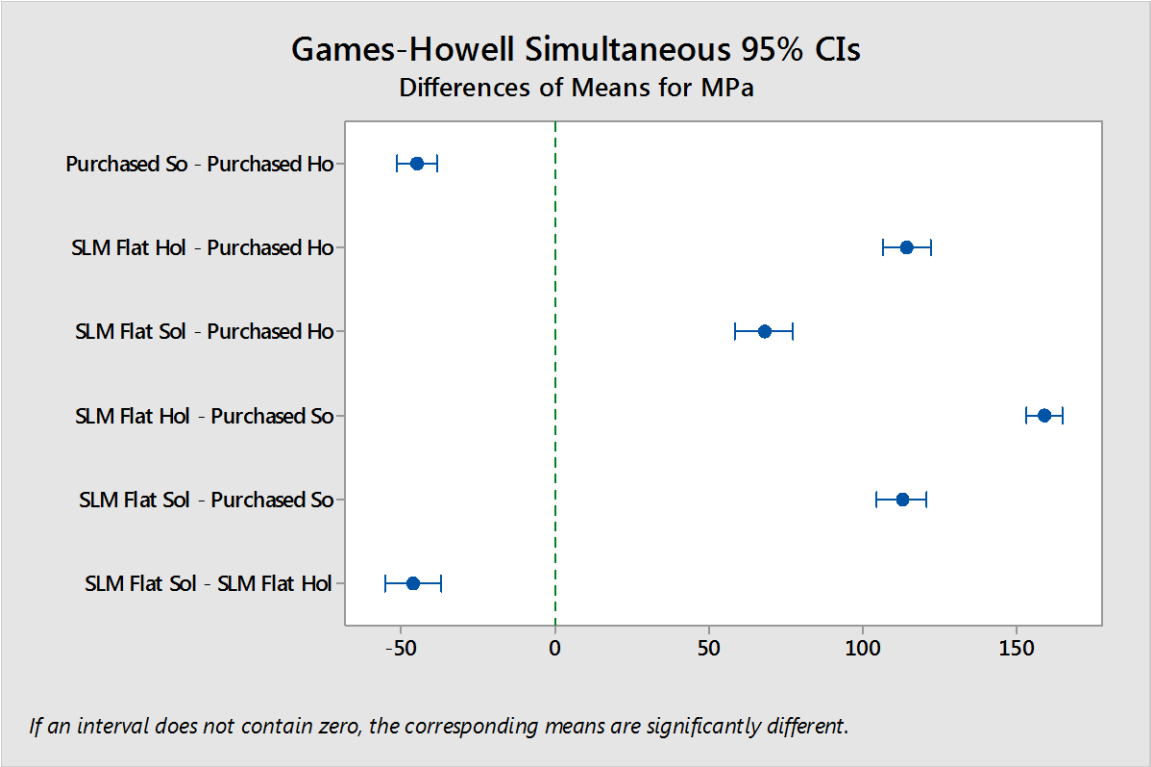

One-way ANOVA: MPa versus Cats

Method

Null hypothesis	All means are equal
Alternative hypothesis	At least one mean is different
Significance level	α = 0.05

Equal variances were not assumed for the analysis.

Factor Information

Factor	Levels	Values
Cats	4	Purchased Hole, Purchased Solid, SLM Flat Hole, SLM Flat Solid

Welch's Test

Source	DF Num	DF Den	F-Value	P-Value
Cats	3	31.8142	1950.58	0.000

Model Summary

R-sq	R-sq(adj)	PRESS	R-sq(pred)
98.49%	98.42%	4994.08	98.30%

Means

Cats	N	Mean	StDev	95% CI
Purchased Hole	20	394.98	9.61	(390.48, 399.48)
Purchased Solid	20	350.21	4.81	(347.96, 352.46)
SLM Flat Hole	20	509.13	8.39	(505.21, 513.06)
SLM Flat Solid	12	462.94	9.08	(457.18, 468.71)

Games-Howell Pairwise Comparisons

Grouping Information Using the Games-Howell Method and 95% Confidence

Cats	N	Mean	Grouping
SLM Flat Hole	20	509.13	A
SLM Flat Solid	12	462.94	B
Purchased Hole	20	394.98	C
Purchased Solid	20	350.21	D

Means that do not share a letter are significantly different.

Games-Howell Simultaneous Tests for Differences of Means

Difference of Levels	Difference of Means	SE of Difference	95% CI	Adjusted T-Value	P-Value
Purchased So - Purchased Ho	-44.77	2.40	(-51.33, -38.21)	-18.62	0.000
SLM Flat Hol - Purchased Ho	114.15	2.85	(106.49, 121.82)	40.01	0.000
SLM Flat Sol - Purchased Ho	67.97	3.39	(58.62, 77.31)	20.05	0.000
SLM Flat Hol - Purchased So	158.93	2.16	(153.05, 164.80)	73.48	0.000
SLM Flat Sol - Purchased So	112.74	2.83	(104.56, 120.91)	39.80	0.000
SLM Flat Sol - SLM Flat Hol	-46.19	3.22	(-55.15, -37.23)	-14.33	0.000